UNIVERSITA' DEGLI STUDI DI PADOVA

Dipartimento di Ingegneria Industriale DII

Corso di Laurea Magistrale in Ingegneria dei Materiali

Tesi di Laurea Magistrale in Ingegneria dei Materiali

PEEK FUNCTIONALIZATION WITH BIOACTIVE PEPTIDES FOR BONE TISSUE ENGINEERING

Relatore: Prof.ssa Monica Dettin

Correlatori: Dott.ssa Annj Zamuner

Dott. Leonardo Cassari

Laureanda: Ilaria Vignato

Anno Accademico 2021/2022

Abstract

Polyetheretherketone (PEEK) is a thermoplastic polymer that has been recently employed for bone tissue engineering, thanks to its mechanical properties close to human bones, as well as to its biocompatibility. However, PEEK is a bio-inert material, that is, once implanted, it does not interact with the receiver's tissues, causing difficulties in the process of implant integration. To overcome this issue, in this work PEEK was functionalized with several bioactive peptide sequences, namely the (351-359) sequence of human vitronectin (HVP), the fragment (48-69) of BMP2 protein (GBMP1α), and a self-assembling peptide (EAK). Peptides were synthetized with Solid State Peptide Synthesis (SPPS), purified and characterized with Reverse Phase-High Performance Liquid Chromatography (RP-HPLC) and mass analysis, and, finally, anchored to the polymer surface through covalent bonds through oxime chemistry.

The scaffolds prepared in this work were characterized by surface and mechanical tests. X-ray Photoelectron Spectroscopy (XPS) analysis confirmed the peptide presence, while Water Contact Angle (WCA) and Atomic Force Microscopy (AFM) measurements showed the modification of PEEK with the peptide sequences.

Furthermore, a biological characterization was performed with immortalized human osteoblast cells. The presence of bioactive sequences on PEEK surface allowed the design of a "smart" implant able to promote proliferation and differentiation of osteoblasts, hence the formation of new bone tissue in close contact with the implant.

Abstract

Il polietereterchetone (PEEK) è un polimero termoplastico che recentemente ha conosciuto un sempre maggior impiego negli impianti per la sostituzione del tessuto osseo grazie alle sue proprietà meccaniche affini a quelle dell'osso umano, oltre che alla sua biocompatibilità. Il PEEK, tuttavia, è un biomateriale inerte, cioè non interagisce con il tessuto del ricevente una volta impiantato, causando difficoltà nell'osteointegrazione. Per ovviare al problema, in questo lavoro di tesi il PEEK è stato funzionalizzato con diverse sequenze peptidiche bioattive, in particolare la sequenza (351-359) della Vitronectina umana (HVP), il frammento (48-69) della proteina BMP2 (GBMP1α) e, inoltre, con un peptide autoassemblante (EAK). I peptidi sono stati preparati mediante sintesi peptidica su fase solida, purificati e caratterizzati con cromatografia liquida ad alte prestazioni a fase inversa e analisi di massa e, infine, ancorati covalentemente alla superficie del polimero tramite coniugazione selettiva via ossima.

Gli *scaffold* così realizzati sono stati caratterizzati: l'analisi di spettrometria fotoelettronica a raggi X ha confermato la presenza di peptide, mentre le misure dell'angolo di contatto e di microscopia a forza atomica hanno fornito la bagnabilità in acqua e il modulo di Young delle superfici.

Oltre a ciò, sono stati realizzati alcuni saggi biologici con osteoblasti umani immortalizzati. La presenza di sequenze bioattive sulla superficie del PEEK ha consentito la progettazione di un impianto "*smart*", capace di promuovere l'adesione, la proliferazione e la differenziazione degli osteoblasti, e dunque la formazione di nuovo tessuto osseo a stretto contatto con l'impianto.

Contents

Chapter 1

Introduction

1.1 Bone-tissue engineering

Tissue engineering can be defined as "an interdisciplinary field of research that applies the principles of engineering and the life sciences towards the development of biological substitutes that restore, maintain, or improve tissue function" [1] . In contrast to classic biomaterial approach, it aims to create living tissues-like structures rather than just to implant new spare parts. This goal is archived by integrating knowledge from physics, chemistry, materials science, engineering, biology, and medicine in an interdisciplinary approach [2].

One of the main objectives of tissue engineering is bone regeneration, as bone tissue is fundamental for structural support of the body, mineral reservoir, muscular contraction support and protection of internal organs, and major alterations of it can severely deteriorate the quality of life.

Established treatment of bone defects involves the use of bone grafts. These can be divided into three categories:

- Autologous bone grafting, which was the gold standard of bone replacement for many years, consists in taking bone tissue from the patient itself. The main drawbacks of this technique are the limited availability of autograft and donor site morbidity.
- Allogenic bone grafting refers to bone tissue taken from another person's body. Limitations of this approach are the lack of osteogenicity and the immune response of the host.
- Xenografting, where the source of the graft is a different species than the human one. The main drawback is the immune response, that requires tissue treating to minimize rejection.

An alternative to grafts is metals and ceramics. However, metals do not integrate well with the tissue and expose it to the risk of infection or failing due to fatigue loading, and ceramics are very brittle.

Tissue engineering provides a solution to the limitations mentioned. Independently from the type of tissue considered, there are three fundamental "ingredients" in tissue engineering (Figure 1.1):

- Cells: they can be stem cells, thus able to self-renew and differentiate, or differentiated adult cells.
- Scaffolds: an artificial support that provides a microenvironment similar to the physiological extracellular matrix (ECM), that promotes cell attachment, proliferation, and differentiation for the repairing of damaged tissue.
- Biochemical signals: molecules usually of protein nature that promote adhesion, proliferation, and differentiation of cells. They include growth and differentiation factors.

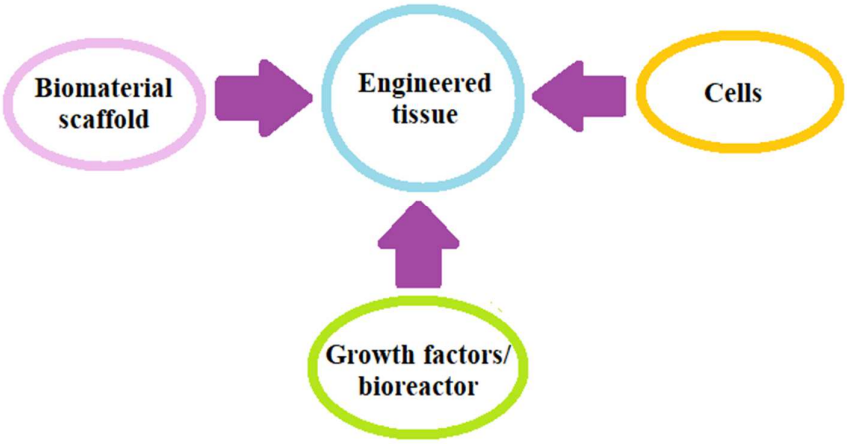

Figure 1.1 *- The triad of tissue engineering*

1.2 Biomaterials

The introduction of nonbiological materials into the human body can be traced back to prehistory. Starting from thousands of years ago, various materials, such as seashells, linen, wood, catgut, metals and many more have been used for dental implants, sutures, prostheses, and, in general, for partial or total replacement of damaged tissues and organs [3]. However, the term "biomaterial" is quite recent, as just about 70 years ago it did not exist. In recent years, many definitions have been given to this term. They are reported in The Williams Dictionary of Biomaterials [4]:

1. A non-viable material used in a medical device, intended to interact with biological systems (Consensus Conference on Definitions in Biomaterials Science, European Society of Biomaterials, 1986)

2. A material intended to interface with biological systems to evaluate, treat, augment or replace any tissue, organ or function of the body (Consensus Conference II, European Society for Biomaterials, 1999). This definition shows a shift from a traditional bioinert material to a bioactive material.
3. Synthetic, natural or modified natural material intended to be in contact and interact with the biological system.
4. Any substance (other than a drug), synthetic or natural, that can be used as a system or part of a system that treats, augments, or replaces any tissue, organ, or function of the body (Consensus Conference on the Clinical Application of Biomaterials, National Health Institute, 1984).

Regardless of the definition considered, it is clear that biomaterials are considered on the basis of their applications, not of their physical properties. These materials are applied as scaffolds for tissue engineering.

Biomaterials can be classified according to their different nature. This divides biomaterials in:

- Polymeric materials: their structure is made by a large number of repeating units called monomers. They can be further divided into natural (collagen, elastin, silk, polysaccharides, polynucleotides etc.) and synthetic (polyetheretherketone, polylactic acid, polyglycolic acid, polycaprolactone etc.).
- Metal materials: made by one or more elements bound together by a metallic bond. If one of the elements is not a metal, the material is called an alloy. They can be ferrous (example: iron) or nonferrous (example: titanium, magnesium etc.).
- Ceramic materials: inorganic solid compounds made by metallic and nonmetallic elements bound together with ionic or covalent bonds. One important example is calcium phosphate ceramics, which have been widely studied for bone tissue repair [5].
- Composite materials: made by a combination of the aforementioned classes.

Table 1 shows different properties and applications of biomaterials according to their nature.

Material	Advantages	Disadvantages	Applications
Metals and metallic alloys (Stainless steel, cobalt-chromium molybdenum alloy, titanium and titanium alloys)	Excellent thermal and electrical conductivity, good mechanical properties, corrosion resistance	High mass density, release of potentially toxic debris	Load-bearing implants
Ceramics (alumina, zirconia, pyrolytic carbon, bioglasses)	Strength, stiffness, resistance to corrosion and wear, high resistance to compression loads, low density	Brittleness, sensitivity to the presence of cracks or other defects, difficulty in manufacturing	Dental prostheses, hip prostheses, medical sensors
Polymers (silicone rubbers, polyesters, polyethylene acrylates)	Good biocompatibility, flexibility, lightweight, wide variety of compositions, easy manufacturing	Low mechanical resistance, low durability	Prostheses, sutures, cardiac valves, bone cements, contact and intraocular lenses, drug delivery
Composites	Wide variety of unusual properties and characteristics	Low cohesion between components, processing difficulty	Cardiovascular stents, peacemakers, dental implants, artificial cartilage, joint prostheses

Table 1 *– Biomaterials according to their different nature*

The interaction between a biomaterial and the biological system is a two-way relationship: the living organism produces an effect on the biomaterial, and, on the other hand, the organism is affected by the presence of a biomaterial. According to the effects induced by the biological system on the biomaterial, a biomaterial is:

- *Biostable*, if it is not altered by biological fluids. This is a requirement for long-lasting devices.
- *Biodegradable*, if it undergoes a progressive chemical modification that degrades the material when in contact with biological fluids.

Meanwhile, according to the effect of a biomaterial on the body, a biomaterial can be classified as:

- *Bioinert*, if it does not interact with the tissue, but also does not show incompatibility.
- *Bioactive*, if its implantation favors biological activity, so bonds between the material and the surrounding tissue are formed.

- *Bioresorbable*, when it undergoes a continuous degradation in the biological environment without the formation of toxic or undesired products.
- *Biotossic*, if it provokes rejection by the host.

It is clear that the choice of a peculiar biomaterial depends on the application for which it is intended.

1.2.1 Bioactivity

In the past, biomaterials for bone-tissue engineering were designed to be bioinert. Inert synthetic polymers, for example, were used since the ’60 as biomaterials, to replace natural body tissues, to construct artificial organs, rehabilitation devices, or prostheses. Bioinert biomaterials are used to minimize the immune response and the foreign body reaction. Nevertheless, after the implantation of a bioinert device, cellular activity causes the formation of a fibroblastic sheath all around the implant as an answer to the foreign body, and this produces the aseptic loss of many implants [6]. Furthermore, the survivability of bioinert implants decrease in long-term periods (>10 years), so development of new bioactive materials that minimize failure and extend long-term survivability was necessary [7]. These problems have caused the rise of bioactive biomaterials over bioinert ones (which were considered superior only in the early years).

Bioactive biomaterials interact with the biological environment thus enhancing the biological response as well as tissue-surface bonding. The term “bioactivity” refers to “any interaction or effect that materials exert on cells with the aim of leading or activating them to specific responses and behaviors” [8]. Bioactive biomaterials show a better survivability than bioinert biomaterials. They are also able to react at a cellular level in the body to enhance bone proliferation (Class A bioactivity) or to lead only to bone growth along the implant surface (Class B bioactivity).

However, there are also methods to induce bioactivity on a bioinert biomaterial. These methods rely on surface modification in order to introduce a specific reactive functional group in the desired quantity [9]. The techniques used to modify a material’s surface will be described further on this work.

1.2.2 Polymeric biomaterials

Polymeric materials are organic compounds consisting of long chains of repeating units, named monomers, chemically bonded together by a polymerization reaction. Polymers can be classified according to many properties.

The first important distinction relates to thermal behavior: we can have a thermoplastic if the material becomes moldable with increasing temperature and solidifies upon cooling, and a thermoset if the material can't be melted without chemical degradation occurring.

According to their structure, polymers can also be classified in homopolymers, when they contain only one type of monomer, and copolymers, when they contain two or more repeating units.

Finally, polymeric materials can be classified, according to their origin, in natural and synthetic. Both of these have gained popularity in tissue engineering due to their chemical tunability for scaffold production, flexibility, chemical inertia, biocompatibility and lightweight. Natural polymers include polysaccharides, proteins, and nucleic acids. They are more easily accepted by the body and can be metabolized through established pathways, but, on the other hand, they have inferior biomechanical properties and can increase the chances of immunogenicity [10].

The most used synthetic polymers for tissue engineering include polylactic acid (PLA), polyglycolic acid (PGA), polylactide-co-glycolic acid (PLGA), polyetheretherketone (PEEK), polyethylene oxide (PEO) and polyurethane foams (PU). Synthetic polymers can be easily tuned to fulfill specific purposes, have no batch-to-batch variations, and they are generally biologically inert [11].

Scaffolds designed for bone-tissue engineering should match as far as possible the mechanical properties and composition of human bone. Generally, polymers do not have a Young modulus as high as natural bone, so they are typically used for temporary, degradable scaffolds. To enhance their stiffness, natural and synthetic polymers have been blended with hydroxyapatite (HA), the main inorganic constituent of bone, in many applications [12, 13, 14].

1.3 PEEK

Polyetheretherketone is a semi-crystalline linear aromatic thermoplastic which belongs to the family of polyaryletherketones (PAEKs), which are polymers made of a 1,4-substituted aryl groups chain

interconnected by keto (R-CO-R) and ether (R-O-R) functional groups (Figure 1.2). Its structural formula is:

$(-C_6H_4-O-C_6H_4-O-C_6H_4-CO-)_n$

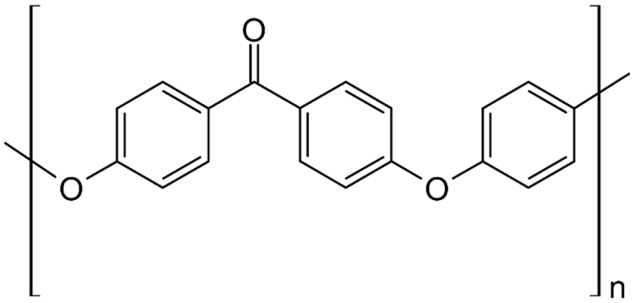

Figure 1.2 *– PEEK structure*

PEEK is obtained through step-growth polymerization by the dialkylation of bisphenolate salts. A typical reaction is the one between the disodium salt of hydroquinone and 4,4'-difluorobenzophenone, as shown in Figure 1.3.

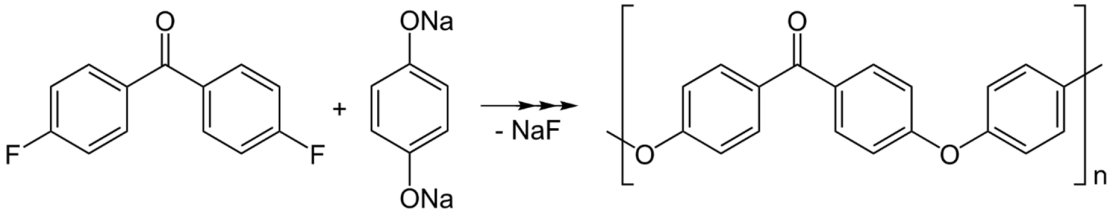

Figure 1.3 *– Synthesis of PEEK*

The reaction must occur at very high temperatures (>300 °C) in order to reach high molecular masses, and in the presence of aprotic solvents like diphenyl sulfone. Because of these difficult conditions, PEEK production needs dedicated plant facilities that work under strict safety rules, so typically PEEK is produced in batches instead of a continuous process. This contributes to the high cost of the polymer [15].

1.3.1 A brief history of PEEK

PEEK was invented in 1978 by English company Imperial Chemical Industries (ICI), but another English group, Victrex, was responsible for the main developments and the widespread use of this material. The first commercialization of the new polymer came in 1981, in the form of Victrex PEEK.

At first, PEEK was employed in aerospace and transport industry (manufacture of aircraft, turbine blades, piston parts, cable insulation, bearings and compressor plate valves [16], Figure 1.4, b) thanks to its potential for high-load, high-temperature applications, but the usage in other industrial sectors was limited due to its cost, which is much higher than that of low temperature thermoplastics like polyethylene. However, later on PEEK industry knew an expansion, and in 1999 it was launched as an implantable polymer for medical devices, in the form of PEEK-OPTIMA, commercialized by Invibio Biomedical Solutions. In 2001, Victrex established Invibio Biomaterial Solutions to specifically provide grades of PEEK suitable for long-term implantations. All PEEK polymers by ICI, Victrex, and Invibio were produced at the same plant location. Today, PEEK biomaterials are designated by the OPTIMA trade name based on their molecular weight, at which different flow properties of the melt correspond.

Recently, two new manufacturers approached PEEK medical market. In 2007, Solvay announced an implantable grade of PEEK under the trade name of Zeniva. In 2009, Evonik commercialized an implantable grade of PEEK under VESTAKEEP trade name. Neither of these two products have been tested in scientific studies for their applications in long-term implants.

Invibio and Oxford Performance Materials (OPM) also designed PAEK alternatives to PEEK, for example PEK, a candidate biomaterial for tribological testing, which however has not been commercialized yet, and PEKK, marketed as medical and implantable grades under OXPEKK trade name.

Since the 90s, PEEK has been recognized as one of the best candidates for metal implants substitute. Generally, PEEK in biomedical industry is employed for orthopedic, trauma and spinal implants, dental implants, joint replacement, cardiac valves and stents (Figure 1.4, a). Popular are the applications of PEEK for skull defect correction: in 2013 for the first time ever most of a human's skull was replaced with a 3D-printed PEEK one [17].

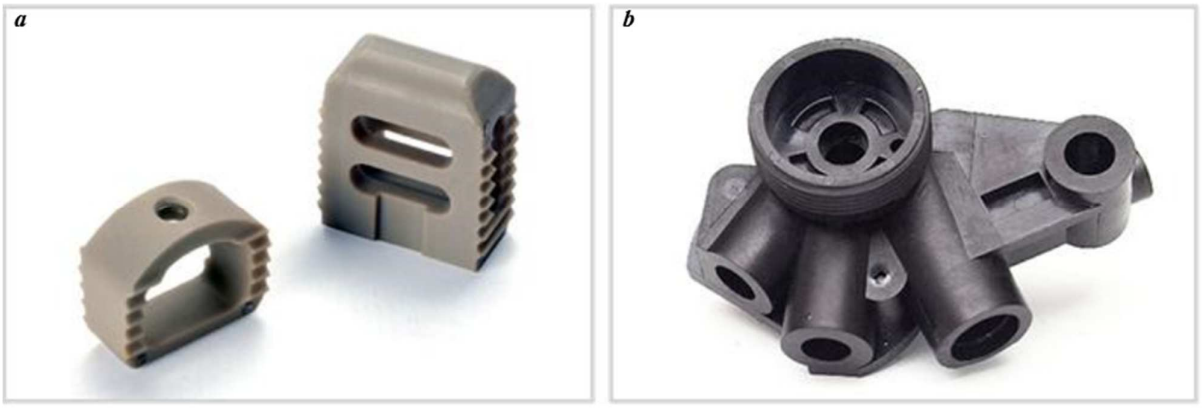

***Figure 1.4 – a**: Cervical cage made of PEEK. ©Eisertech, LLC. **b**: Complex PEEK injection part for Oil & Gas and automotive industry. ©MING-LI Precision Steel Molds CO.*

1.3.2 Crystalline structure and physical-chemical properties

PEEK consists of an amorphous phase and a crystalline phase. Like many semi-crystalline polymers, the crystalline content of PEEK varies depending upon its thermal processing history. Typically, the crystalline content of injection-molded grades of PEEK contains around 30-35% crystallinity, but amorphous PEEK can also form in the surface of large injection-molded products when the cooling rate is high. The polymer crystallizes into an orthorhombic cell structure.

PEEK is a white, radiolucent rigid material. Its chemical structure, which causes delocalization of higher orbital electrons along the entire macromolecule, confers stability at high temperatures (exceeding 300 °C), as well as outstanding resistance to chemical damage [18]. PEEK is insoluble in all conventional solvents at room temperature, with the exception of sulfuric acid, so the polymer is not affected by long-term exposure to water, not even at high temperatures (up to 260 °C) [19].

Thermal stability of PEEK has been widely studied for its high-temperature industrial applications and processing conditions. The glass transition and melting temperatures are, respectively, 143 °C and 343 °C; thermal degradation occurs between these two temperatures, at about 300 °C. It is clear then that thermal degradation is not a concern for biomedical applications, as the average temperature of bodily fluids is around 37 °C.

Thanks to the aromatic chemical structure, PEEK is also remarkably resistant to gamma and electron beam radiation, with lower radical formation than aliphatic polymers [20]. This indicates that PEEK is suitable for sterilization by gamma irradiation in air. Even though free radicals are generated during PEEK irradiation, they rapidly decay thanks to electron mobility along the macromolecule.

1.3.3 Mechanical properties

PEEK has excellent mechanical properties: its elastic modulus ranges from 3 to 4 GPa, which is close to that of human trabecular bone (1 GPa). The molecular structure is sturdy and rigid; however, the material has a ductile behavior and deforms both in tensile and compressive tests [21]. As the other semi-crystalline polymers, PEEK exhibits good fatigue resistance and impact strength, yet it must be noted that PEEK mechanical properties depend on strain rate, temperature, molecular weight, and size and orientation of crystalline regions. PEEK's mechanical properties can also be influenced by the level of crystallinity of the material: an increase in crystallinity can produce an increase in working temperature ranges, elastic modulus and yield strength, while conferring lower toughness and different tribological behaviors [22]. Obviously, the thermal processing conditions can influence significatively the crystallinity and mechanical properties of PEEK materials.

1.3.4 Biocompatibility and bioactivity

PEEK biocompatibility has been thoroughly studied since the late 1980s, and no adverse side effects have been founded when the material was tested for systemic and intracutaneous toxicity and intramuscular implantation. No sensitization or chromosome aberration due to PEEK has been detected in the specific tests either. However, concern has been raised over the inertness of PEEK: the polymer's surface is hydrophobic, and this does not allow protein absorption nor promotes cell adhesion [23]. To overcome this problem, during the last few years various techniques to improve PEEK bioactivity have been studied:

- Plasma treatment: plasma, an ionized gas mixture, breaks the chains of the macromolecules creating free bonds, to which other functional groups can be anchored, thus improving surface properties. This method has proven successful in increasing PEEK wettability, for example by Inagaki *et al*., who were able to decrease the water contact angle by an O_2-plasma treatment after only 30 seconds [24].
- Chemical treatment: the most used chemical treatments of PEEK surface for biomedical applications are two wet-amination procedures, one coined by Noiset *et al*., the other by Becker *et al*. The former consists in a reduction of the keto groups in PEEK backbone by sodium borohydride, then a reaction with hexamethylene diisocyanate and, finally,

hydrolyzation with sodium hydroxide [25]. The latter is easier as it consists only in a treatment with ethylene diamine [26].

- Coating: it is the deposition of a thin layer of bioactive material on PEEK surface, archived by various techniques, such as spray-coating, dip-coating, spin-coating, aerosol-coating and physical vapor deposition [27].
- Biofunctionalization: the immobilization of biomolecules such as polysaccharides, proteins, peptides etc. on a material's surface. It can be achieved, for example, through physical adsorption via week interactions, inclusion in a carrier or covalent attachment. A further description of biofunctionalization techniques will be presented in paragraph 1.5.

In this thesis work, biofunctionalization was applied in order to improve PEEK bioactivity.

1.3.5 Processing techniques

PEEK-based materials are processed by traditional plastic processing methods. Although PEEK pellets are supplied essentially dried, there is a moisture content around 0.5% w/w, thus a drying phase is necessary for certain processing methods such as injection molding. The main techniques are discussed below.

Injection molding: it is a batch technique, useful for mass production, with which products of multiple shapes and sizes can be obtained. PEEK is collected in pellets or granules and then is poured in a hopper on top of the machine. The pellets are introduced to a heated screw assembly that melts and pressurizes the molten polymer, which then flows rapidly to a heated mold thanks to a piston. The mold temperature is lower than the one in the injection chamber, so the material inside the mold solidifies and is then ejected, and another cycle can take place. Figure 1.5 shows a diagram of the process.

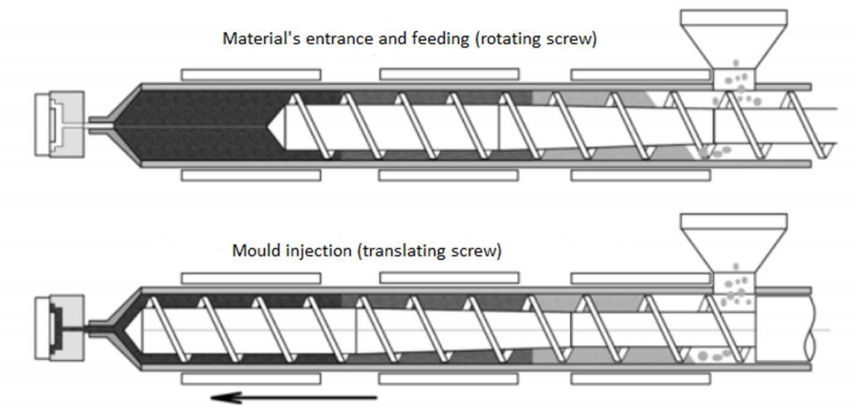

Figure 1.5 *– Injection molding process*

Compression molding: it is typically used for low volume productions, prototypes and in the production of components with very thick sections. This technique is useful even for reinforced polymers (for example, with glass or carbon fibers) and thermosetting resins. The compression molding press consists of two heated platens. The lower platen has a cavity the shape of the final product and is charged with resin powder or granules. The upper platen is connected to a punch that presses the material in the cavity, and heat is applied to both platens in order to consolidate the resin. After some time, the polymer melts and spreads through all the cavity, taking the correct shape. If we have a thermosetting resin, the high temperatures enable the crosslinking. The material then cools down and solidifies, and it is finally extracted from the die. Compared to injection molding, it is a more inexpensive process, but the time cycles are longer, so it is not suited for mass production.

Extrusion: extrusion is a process where a material is forced, by the application of a force, to flow through an orifice that has the same shape of the final product. Similar to injection molding, the pellets are poured into a hopper that feeds into a heated screw assembly that melts and pressurizes the material. The polymer is then forced through a heated die, and cools to room temperature along the extrusion line. Extrusion is useful to obtain constant-section, long-shaped products, such as rods, sheets and monofilament fibers. A schematic representation of extrusion is shown in Figure 1.6.

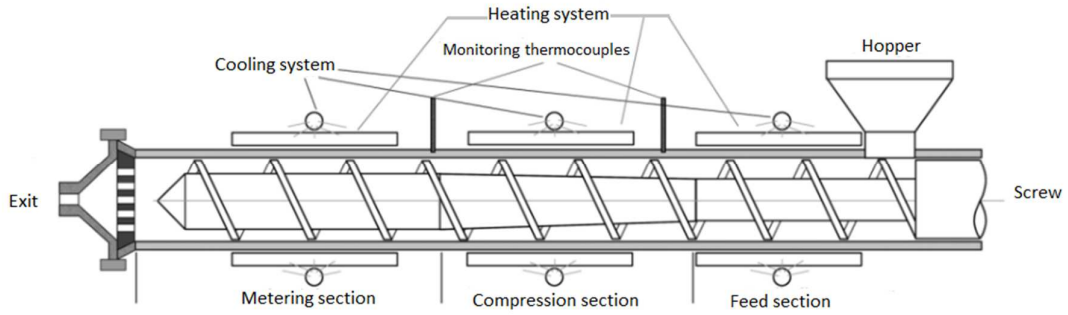

Figure 1.6 *- Schematic representation of an extruder*

3D printing: 3D printing is a technique in which an object is formed after depositing the material layer by layer. It has become popular in the recent years and it is very promising because it enables the production of very complex shapes, which are beyond the scope of conventional technologies. 3D printing has established itself as a very useful process in biomedical industry as it can supply unique biomedical implants, customized to the needs of every patient. Among the different types of 3D printing, Selective Laser Sintering (SLS) and Fused Deposition Modeling (FDM) are frequently used for the processing of PEEK in medical implants [28] [29] [30] [31].

1.4 Biochemical Factors

A biochemical factor is a molecule, mostly a protein, which promotes cell adhesion, proliferation, and differentiation. These molecules are normally synthesized by ECM cells and are employed in tissue engineering as signal factors for the detection, migration, and adhesion of cells to the scaffold. They can be divided in adhesion and growth factors.

1.4.1 Peptides

Peptides are organic macromolecules composed of short aminoacidic sequences linked by peptide bonds. They differ from proteins as they generally contain less than 50 amino acid sequences, and they are not able to self-organize in complex structures like proteins. Peptides can be subdivided in oligopeptides, which contain 2 to 20 amino acids, and polypeptides, which contain more than 20

amino acids. Synthetic peptides are applied in bioengineering because they offer a more convenient solution than full-length proteins. In fact, whole-length proteins are typically obtained from living organisms, may contain endotoxins or immunogenic material from donor tissue, are enzymatically degradable and susceptible of changes in pH, temperature and solvents, while synthetic peptides are produced chemically, possess no risk of immunogenic reaction, are more stable to pH, temperature and solvent changes and less susceptible to enzymatic degradation [32].

Surface biofunctionalization with peptides in bone-tissue engineering is carried out to promote osteoblast adhesion and growth.

Adhesion factors

A mechanism used to promote adhesion is the binding of osteoblast integrins to RGD peptide sequences; meanwhile, another mechanism involves an interaction between cell membrane heparan sulfate proteoglycans and heparin-binding sites on ECM proteins [33]. Dee *et al*. tested the ability of heparin-binding sequences X-B-B-X-B and X-B-B-B-X-X-B-X (B is a basic amino acid and X is a hydropathic amino acid) to promote cell adhesion: they assumed that an ideal bone-related adhesive protein should contain Lys-Arg-Ser-Arg as B-B-X-B sequence and found out that proteoglycan-mediated osteoblast adhesion is necessary to maximize osteoblast adhesion [33].

Starting from this discovery, Dettin *et al*. tested the X-B-B-B-X-B-B-X heparin-binding sequence contained in (339–364)HVP (Human Vitronectin Precursor) and reproduced in the peptide (351–359)HVP and found out that this nonapeptide is a well-suited molecule to promote proteoglycan-mediated cell adhesion, as it was more bioactive than the other tested sequences [34].

Vitronectin is a multifunctional glycoprotein that can be found in blood and in ECM. Vitronectin structure is composed of different domains, thus it can bind different molecules such as integrins, thrombin-antithrombin III complex (TAT), collagen, urokinase receptor (uPAR), plasminogen activator inhibitor-1 (PAI-1), plasminogen and heparin. Vitronectin promotes cell adhesion, spreading and migration thanks to the adhesive sequence RGD, that binds to integrins [35].

Growth factors

Growth factors are molecules that bind to specific receptors on cell membrane and stimulate cell proliferation and differentiation. Among the most important growth factors are Insulin-like Growth Factors (IGF), the main actors of bone growth, Fibroblast Growth Factors (FGF), heparin-binding

proteins responsible for proliferation and differentiation in multiple tissues and Transforming Growth Factors (TGF).

One of the members of the TGF family is Bone Morphogenetic Protein (BMP), a multifunctional acidic polypeptide. Among its different subtypes, particular attention is reserved to BMP2, a protein composed of 396 amino acids, that has a relevant role in osteogenesis, and induces osteogenic differentiation of mesenchymal stem cells. This last feature is enhanced when BMP2 is replaced by one of its derivates, GBMP1α, a 22 amino acids peptide. GBMP1α proved to significantly enhance calcium deposition and expression of genes involved in osteoblast differentiation, thus offering a cheaper and easier alternative to BMP2 [36].

1.4.2 Self-Assembling Peptides

Self-assembling peptides (SAPs) are oligopeptides characterized by the ability to self-organize in ordered structures through noncovalent interactions, such as hydrophobic interactions, hydrogen bonding, electrostatic interactions, and Van der Waals forces, that maintain the thermodynamic equilibrium. The first SAP was discovered by Zhang *et al*. at the Massachusetts Institute of Technology's laboratories: Zhang identified a protein, which he named *Zuotin*, that contains a particular repeating sequence, EAK16 [37]. This peptide was further researched by Zhang, which discovered that it organized itself in a β-sheet structure in aqueous solution. This happens because of its two distinct surfaces, one hydrophilic, and the other hydrophobic (Figure 1.7). EAK16 spontaneously associated in an insoluble macroscopic membrane, resistant to enzymatic degradation [38]. Zhang classified SAPs into five different classes [39]:

- Type I peptides, or "Molecular lego", that form beta sheets in aqueous solutions because of its two distinct surfaces, one hydrophilic, and the other hydrophobic.
- Type II peptides, or "Molecular switches", that show changes in conformation, passing from beta-sheet to alpha-helical with an increase in temperature, and then again to beta-sheet after some weeks at room temperature.
- Type III peptides, called "Molecular Paint" and "Molecular Velcro". They form monolayers on surfaces and are employed in surface treatments.
- Type IV peptides, that show a very dynamic assembly and disassembly and form nanotubes and nanovesicles.

- Type V peptides, employed in drug delivery and gene therapy, or in scaffolding, to promote biomineralization.

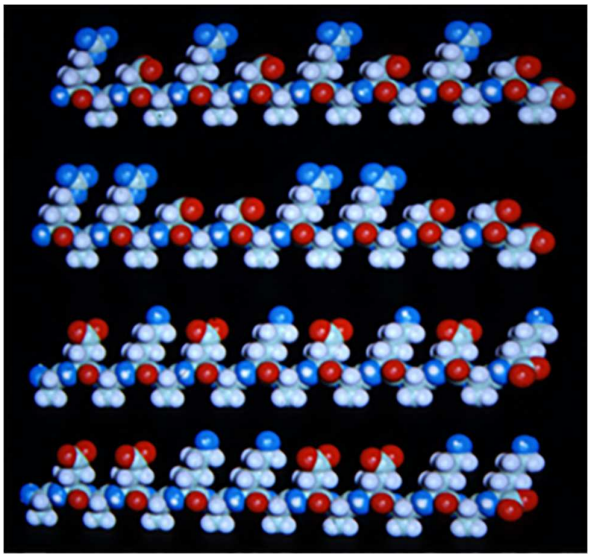

Figure 1.7 *– EAK16 three-dimensional model. In this conformation, the peptide has two distinct faces: one hydrophobic, made by alanine side chains only, and one hydrophilic, made by lysine or glutamic acid side chains. The reds are oxygen atoms, the blues are nitrogen atoms, and the whites are hydrogen atoms.*

1.5 Biochemical Functionalization

Biochemical functionalization, or biofunctionalization, can be defined as "one particular form of surface modification involving the immobilization of biomolecules as proteins, peptides and polysaccharides or bioactive drugs with the same purpose" [40]. Surface modification is an easy way to improve the surface bioactivity and reduce implant-related infections [41]. Usually, molecules employed for biochemical functionalization are proteins derived from the extracellular matrix: this promotes the formation of new tissue, simulating the natural interactions between cells and ECM. The methods available for biomolecule immobilization are essentially three:

- Superficial adsorption of biologically active molecules.
- Inclusion of biomolecules within a resorbable carrier.
- Covalent bonding.

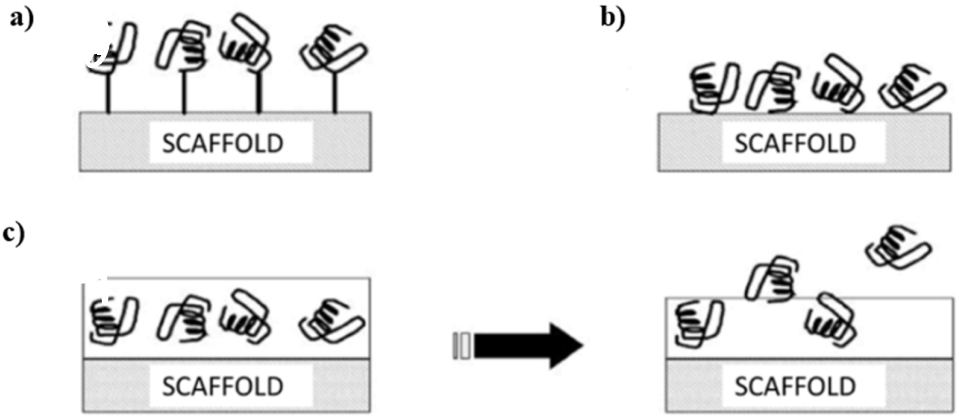

***Figure 1.8 – a)**: adhesion through covalent bond in the presence of a s er; **b)**: superficial adsorption through weak interactions; **c)**: biomolecule inclusion within a carrier*

Superficial adsorption

Adsorption is the adhesion of a protein or another molecule to a solid surface through weak interactions, such as Van der Waals forces. It is realized by leaving the solution containing the target biomolecule in contact with the surface under controlled conditions for an established period of time. It is a simple and inexpensive method, but it does not allow an evaluation of the precise number of biomolecules adsorbed per unit of surface, as the orientation is not controlled. Furthermore, bond breakage due to weakness of the bond itself is a risk (Figure 1.8, b).

Inclusion in a resorbable carrier

This method involves the inclusion of the target biomolecule within a carrier that allows its transport and release following a kinetic depending on the biomolecule characteristics and the technique used for inclusion. Molecules can be dissolved or chemically attached to the carrier. The materials used as carriers have some requirements: they must be biocompatible, biodegradable, and bioresorbable. Usually, carriers are made of PLA or PGA copolymers, or natural polymers like hyaluronic acid (Figure 1.8, c).

Covalent bonding

Covalent adhesion (Figure 1.8, a) is the most stable biofunctionalization technique. It consists in the formation of a chemical bond that allows the attachment of biomolecules to the material surface. This chemical bond can be direct or realized thanks to the introduction, between the molecule and the material surface, of a spacer that is able to enhance the flexibility of the peptide chain, minimize steric hindrance and multiply the available functional groups. For example, polyethyleneimine has been found to increase surface functionality thanks to its high concentration of amino groups, therefore it is widely used for enzyme and whole cell immobilization [42].

Covalent functionalization allows a better control over molecule orientation, bond stability and surface density as compared to the other methods. However, normally biomolecules tend to bind to the material surface in a random way, thus it is not possible to determine if a molecule will be recognized and covalently attached. This can nullify the effectiveness of the functionalization (Figure 1.9, left).

***Figure 1.9** – Aspecific covalent functionalization (left) and specific covalent functionalization (right)*

This issue can be solved with a specific functionalization, in which molecules bind to the surface thanks to a peculiar functional group, allowing proper molecule orientation and maximizing their exposition and their interaction with the active site (Figure 1.9, right). Specific functionalization is feasible through the following techniques:

- Photoactivation: an UV-activable group is added to the aminoacidic sequence. This guarantees selectivity of the reaction and homogeneity in the anchoring.
- Selective reversible protection of all the side chains groups except for the one that will be anchored. In this way, it is possible to guarantee the selectivity of the reaction, but, after that, it is necessary to remove all the artificially introduced protective groups.

- Introduction of a particular functional group that wasn't originally included in the peptide chain; this group allows the covalent adhesion to specific groups in the material surface.

In this thesis work, specific covalent functionalizations were performed using 7-aminoheptanoic acid as a spacer.

1.6 Chemoselective ligation

Chemoselective ligation consists in binding covalently biological molecules in a selective manner, in aqueous medium and mild conditions, and without the use of activating substances. This technique is often employed for the creation of peptide conjugates and the condensation of unprotected peptide fragments. A typical chemoselective ligation approach is oxime ligation. It is a typical example of the so-called "click chemistry", an approach defined for the first time by Sharpless *et al*. that involves the building of complex substances starting from simple molecules, following nature's examples. A reaction can be considered an example of click chemistry if it fulfills a few criteria: it must be "modular, wide in scope, give very high yields, generate only inoffensive byproducts that can be removed by nonchromatographic methods, and be stereospecific" [43].

Oxime ligation involves a conjugation between an aldehydic or ketonic group with a hydroxylamine. The aminooxy linker, present in compounds synthesized by SPPS [44], is among the most used for the modification of biological molecules. Compared to primary ammines, the reactivity of aminooxy groups with carbonyl groups is significantly higher, and the formed oximes have the advantage of being highly stable to hydrolysis [45].

In order for the reaction to occur, it is necessary to previously modify the N-terminal end of the peptide. Francis *et al*. developed a method that consists in transforming the amino group in an aldehydic or ketonic group through a reaction with the coenzyme pyridoxal-5'-phosphate (PLP, Figure 1.10), in an aqueous medium at 37° and 6.5 pH. This reaction is helpful particularly for its selectivity towards the amide end of the peptide. The reaction involves the condensation of the protein's N-terminal group with pyridoxal-5-phosphate and the subsequent hydrolysis, that gives pyruvamide (Figure 1.11), then the reaction of the $protein_{aldehyde/ketone}$ with an oxyamine, that yields an oxime [46].

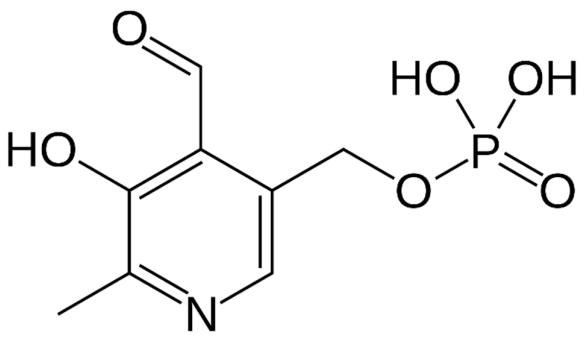

Figure 1.10 *- Pyridoxal-5'-phosphate*

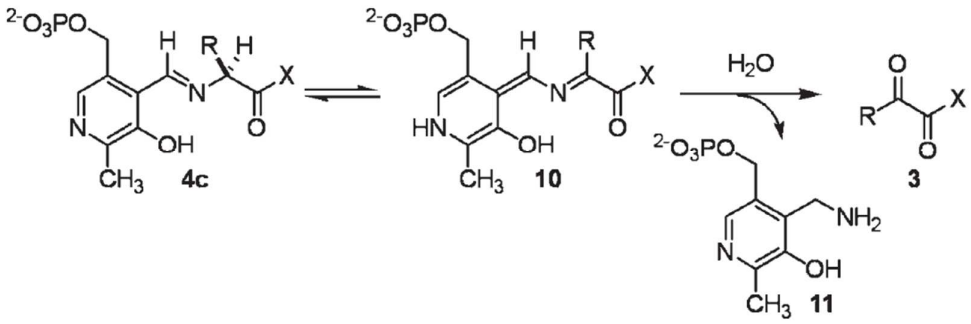

Figure 1.11 *- Formation of pyruvamide*

In this thesis work, chemoselective ligation was utilized to bind the N-terminal ends of Aoa-x-HVP, Aoa-x- GBMP1α and Aoa-x-EAK to PEEK ketonic groups.

1.7 Aim of the thesis

Nowadays, polyetheretherketone is considered as one of the best candidates for metallic implants substitution due to its excellent biocompatibility and mechanical properties. However, the major limitation is the lack of osseointegration with bone tissue due to its inertness, that makes healing time longer. The novelty of this project consists in functionalizing the surface of a PEEK scaffold, thus combining the good properties of this material with tissue engineering methods, in an interdisciplinary approach between material science and bioengineering. PEEK surface will be modified by covalent bonds between ketone groups of the polymer and an aminooxy group introduced

ad hoc at the end of three bioactive peptide sequences (HVP, GBMP1α, EAK). The different surfaces will be characterized through water contact angle (WCA) measurements, atomic force microscopy (AFM), X-ray photoelectron spectroscopy (XPS), and biologically at King's College of London laboratories.

Chapter 2

Materials and methods

2.1 Materials

Columns:

- Nova-Pak HR C18 (4 μm, 60 Å, 3.9 x 300 mm, Waters);
- Vydac C18 218TP54 (5 μm, 300 Å, 4.6 x 250 mm, Grace);
- Delta-Pak C18 (15 μm, 100 Å, 7.8 x 300 mm, Waters);
- Jupiter C18 (5 μm, 300 Å, 4.6 x 250 mm, Phenomenex);
- Zorbax 300SB C18 (5 μm, 300 Å, 9.4 × 250 mm, Agilent).

Reagents purchased from *Merck Millipore* (Burlington, Massachusetts, United States):

- 7-amino heptanoic acid, Fmoc protected;
- Acetic Acid;
- Acetone;
- Acetonitrile;
- Amino acids used;
- Bis-Boc-aminooxy acetic acid (Aoa);
- Dichloromethane (DCM);
- N,N-Diisopropylethylamine (DIPEA);
- N,N-dimethylformamide (DMF);
- Ethyl cyano(hydroxyimino)acetate (Oxyma Pure);
- Methanol;
- Rink-Amide MBHA resin;
- Triethylamine (TEA);
- Triethylsilane (TES);

- 2-(1H-benzotriazol-1-yl)-1,1,3,3-tetramethyluronium hexafluoro phosphate (HBTU)

Reagents purchased from *Biosolve* (Valkenswaard, Holland):

- Diethyl ether;
- Trifluoroacetic acid (TFA).

Reagents purchased from *PanReac AppliChem* (Darmstadt, Germany):

- 2-Propanol for HPLC

Reagents purchased from *Carlo Erba* (Milan, Italy):

- Ethanol.
- Sodium phosphate monobasic.

Reagents purchased from *Iris Biotech GmbH* (Marktredwitz, Germany):

- N-Methyl-2-pyrrolidone (NMP).

Kaiser Test reagents purchased from *Applied Biosystem* (Perkin-Elmer, Waltham, MA, USA):

- Monitor 1: Phenol solution, 76% (w/w) Phenol/Ethanol;
- Monitor 2: Potassium cyanide solution, 0.2 mM KCN/Pyridine;
- Monitor 3: Ninhydrin solution, 0.28 M Ninhydrin/Ethanol.

2.2 Laboratory instrumentation

Synthesizer Syro I (MultiSynTech, GmbH, Witten, Germany):

Figure 2.1 *– Synthesizer Syro I (MultiSynTech)*

Spectrophotometer UV/Vis model Lambda 2 (Perkin-Elmer) for ninhydrin analysis:

Figure 2.2 *– Spectrophotometer UV/Vis Lambda 2 (Perkin-Elmer)*

Mass analyses were performed at the Department of Chemical Science and at the Department of Pharmaceutical Science (University of Padua). MALDI-TOF (MALDI-TOF 4800 Plus, AB SCIEX) and ESI-TOF (ESI-TOF Mariner System 5220, Perkin-Elmer) instruments were used.

For chromatographic analysis, two chromatographic systems were used:

- HPLC Waters 600 Controller (Figure 2.3), coupled with UV/Vis multichannel detector, model 2487, with programmable wavelength. Data acquisition is carried out with a recorder, model BD40/BD41, obtained from Carlo Erba Strumentazione and produced by Kipp&Zonen (Delft, Holland).

- HPLC Waters 1525 Binary Pump coupled with Waters 2707 autosampler and UV/Vis multichannel detector, model 2498, with programmable wavelength. Empower Pro software (Waters, Milford, MA. U.S.A) has been used to obtain chromatograms and data integrations.

Figure 2.3 *– HPLC Waters 600 Controller (Waters)*

Figure 2.4 *– HPLC Waters 1525 Binary Pump with Waters 2707 autosampler and UV/Vis multichannel detector, model 2498*

FreeZone2.5 Liter Benchtop freeze dryer (Labconco, Kansas City, Missouri, USA) for lyophilization:

Figure 2.5 *– Freeze dryer (Labconco)*

Rotary evaporator (Laborota 4100-Efficient, Heidolph Instruments s.r.l., Milan, Italy):

Figure 2.6 *– Rotary evaporator (Laborota 4100-Efficient, Heidolph Instruments s.r.l., Milan, Italy)*

2.3 Methods

2.3.1 Solid Phase Peptide Synthesis

In order to synthesize the peptides for this thesis work, Solid Phase Peptide Synthesis (SPPS) was employed. SPPS is a technique that involves the use of a solid support made of an insoluble resin, to which peptides are bound (*coupled*) in succession.

Introduced in 1963 by Bruce Merrifield [47], it consists in four different steps:

1. Coupling of the first amino acid of the chain with a solid polymeric resin through a covalent bond between the resin and the carboxyl end of the amino acid.
2. Removal of the protecting group, generally obtained with piperidine.

3. Anchoring of the N-end of the resin-bound peptide with the C-end of another amino acid through a condensation reaction. Steps 2 and 3 are repeated until the desired peptide sequence is obtained.
4. Removal of the peptide from the solid support.

A schematic representation of the aforementioned process is shown in Figure 2.7.

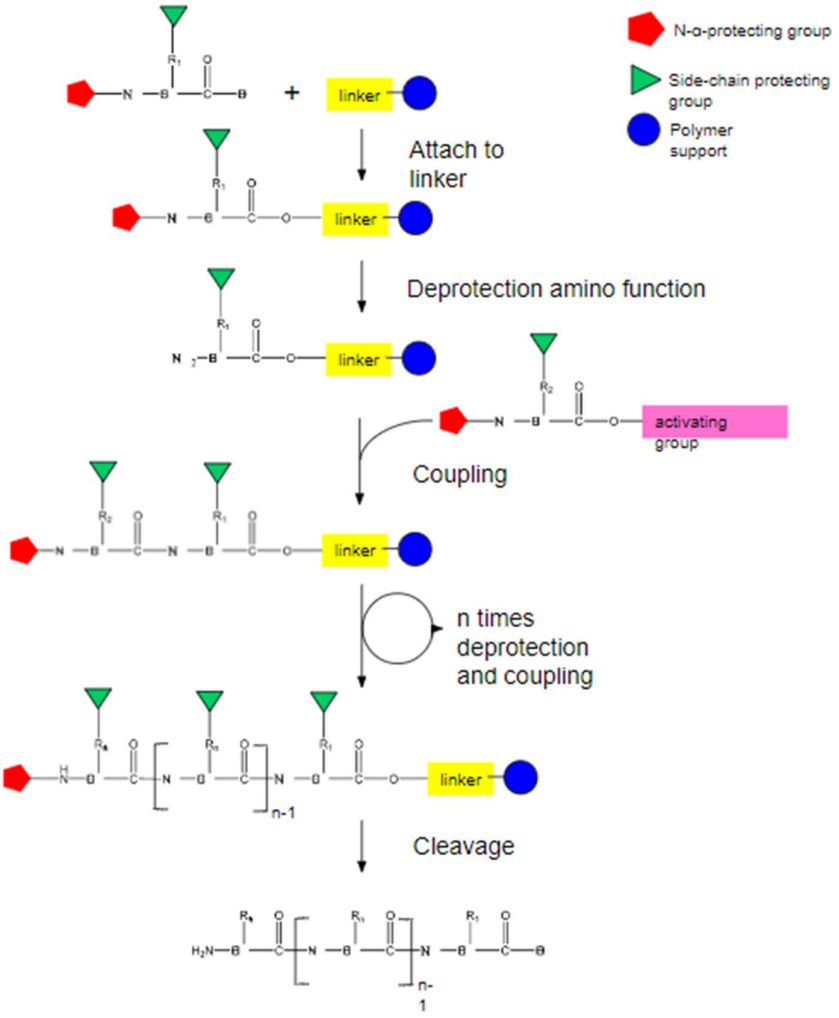

Figure 2.7 *– Schematic representation of a SPPS process*

SPPS, along with liquid phase peptide synthesis (LPPS), is one of the main techniques for the artificial production of peptides in scientific research and in pharmaceutical/commercial sector. However, unlike LPPS, SPPS has the advantage of an insoluble solid matrix; this solid support allows us to isolate the growing peptide at each reaction step, so the whole process can take place in a single reactor. This allows high automation of the process and less handling of the reagents.

There are two possible strategies for the protection of the amino functional group and the side chains:

- Boc chemistry
- Fmoc chemistry

In Boc chemistry, the amino functional group is protected with terz-butossicarbonyl group (Boc), that is removed with mildly strong organic and inorganic acids, for example with TFA. The side chains' protection is obtained with ether, ester and urethan groups. These groups are stable in Boc removal conditions and are instead removed by hydrofluoric acid.

In the case of Fmoc chemistry, developed by Carpino *et al*. and used for this thesis project, the amino acids for SPPS are protected on the α-aminic group with the base-labile group 9-Fluorenylmethoxycarbonyl (Fmoc) [48] [49]. On the reactive functional groups of the side chains other more stable, acid-labile protecting groups are present: these are necessary to avoid undesired reactions that could create bonds different from the α-amidic ones in the backbone. Temporary α-aminic protecting groups are removed in every step of peptide growth. In fact, each SPPS cycle involves at first the deprotection of the amino functional group with 40% piperidine solution in DMF for 3 minutes, then a condensation between the free amino group on the resin and the carboxyl group of the new amino acid introduced. This last step is called coupling, and it can be repeated in order to maximize the reaction yield; for example, in this thesis work a double coupling was performed. The reaction yield can also be monitored through a ninhydrin test, that assesses a quantitative percentage of the yield. At the end of the synthesis all the side chain protecting groups are removed using TFA, and the peptide is cleaved from the resin support.

The selection of the resin depends on the type of chemistry used in the synthesis and on the type of peptide desired. Usually, polymer-based resins are used: these resins swell when in contact with aprotic polar solvents like DMF, NMP and DCM. Different types of resins are available commercially, with a wide variety of linkers or with the C-terminal amino acid already attached. During this thesis project we used the Rink-Amide MBHA resin, shown in Figure 2.8.

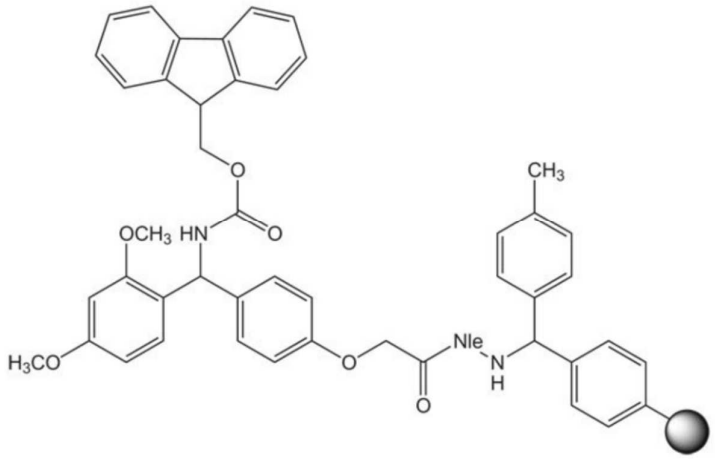

Figure 2.8 *– Structure of Fmoc-protected Rink-Amide MBHA resin*

2.3.2 Ninhydrin test

The ninhydrin test, or Kaiser test, is a qualitative and quantitative test that evaluates the coupling yield of a synthesis reaction by detecting free amino groups in the peptide chain.

The procedure used in this thesis project was the following:

- A certain amount of resin, in a range from 2 to 8 mg, was picked up and put in a test tube;
- The test tube with the resin was filled with the following solutions: 100 µl of monitor 1, 75 µl of monitor 2 and 100 µl of monitor 3. In another, empty test tube the same solutions were poured in the same order: this sample is the reference (control) of the test;
- Both test tubes were placed in a laboratory block heater at 100°C for 5 minutes;
- Once the test tubes were removed from the heater, 4.8 ml of monitor 4 were rapidly added to them, to block the reaction. If the solution, after some time, changes color into a blue or purple one, it is an index that there are a lot of free aminic groups, so probably the reaction yield is low;
- Two cuvettes with only monitor 4 were placed in the spectrophotometer at 570 nm, and the machine was reset; one of the two cuvettes was then removed and replaced with a cuvette full of the control solution. The absorbance was therefore registered;
- The test tube with the resin was centrifugated and the supernatant was moved in a cuvette that replaces the one with the control in the spectrophotometer. The absorbance was registered again.

A qualitative indication of the coupling yield is obtained by observing the color intensity of the solution, as described before. The quantitative measurement is instead obtained by the below reported formula:

$$\mu mol/g = \frac{\Delta Abs \cdot V \cdot 10^6}{\varepsilon \cdot P}$$

Where ΔAbs is the difference of absorbance between the sample with the resin and the control, V is the volume of the mixture (in ml), ε is the coefficient of molar extinction equal to 15000 $M^{-1}cm^{-1}$, and P is the sample weight (in mg).

The coupling efficiency is given by:

$$Yield\% = \left\{ 1 - \left[\frac{\frac{\mu mol}{g_{amino\ groups}}}{new\ substitution \left[\frac{mmol}{g}\right] \times 10^3} \right] \right\} \times 100$$

Where $new\ substitution$ is the new resin substitution, obtained by:

$$new\ substitution = \frac{1000}{MW_{growing\ peptide}}$$

And $MW_{growing\ peptide}$ is obtained by the sum of the resin's molecular weight,

$$MW_{resin} = \frac{1000}{substitution}$$

With the molecular weight of all the amino acidic residues. A percentage above 95% is considered a good result.

2.3.3 Cleavage

When in SSPS an acid-labile resin is used, it is possible to cleave both the peptide from the resin and the side chain protecting groups at the same time. The cleavage procedure takes place in acidic environment with the help of some nucleophilic reagents called *scavengers*, that have similar properties as the species that we want to protect.

In this project, the cleavage was performed with the subsequent procedure:

1. The resin is washed with DCM to remove DMF and dried under vacuum for 1 hour;

2. The resin is treated with 0.125 ml of MilliQ water, 0.125 ml of TES and 4.75 ml of TFA, then left to react for 1.5 hours. At the end of the reaction, the mixture is washed with TFA;
3. The liquid obtained is put in a rotary evaporator and reduced to a small volume;
4. The peptide is precipitated with cold diethyl ether under magnetic stirring, then it is filtered with a Gooch 4 and dried under vacuum for 1 hour.

2.3.4 Mass spectroscopy

Mass spectroscopy (MS) is a destructive analysis method that allows to measure the molecular weight of unknown substances, thus recognizing their structural formula. Before the mass analysis, a molecule must be ionized, then the gas ions can be separated, in time or space, on the basis of their mass/charge ratio (m/z).

The sample is ionized in a special chamber, called ionization chamber, thanks to the impact with an electron, atom, ion, or photon beam. Some ionization techniques operate at high energy levels and cause a high fragmentation (hard techniques), while some others operate at low energy and produce a lesser number of ions (soft techniques).

The ionization techniques can be divided by the source used. In this project, two ionization techniques were employed:

- Matrix Assisted Laser De-sorption Ionization (MALDI) technique;
- ElectroSpray Ionization (ESI) technique.

MALDI technique consists in hitting a sample soaked in a matrix with a laser beam. The laser beam hits the matrix molecules, that absorb the ultraviolet light, switch to an excited status, and heat the close area. The solvated analyte is separated from the matrix molecules, and then it is de-solvated, causing a proton transfer (acid-base reaction between the analyte and matrix molecules, Figure 2.9).

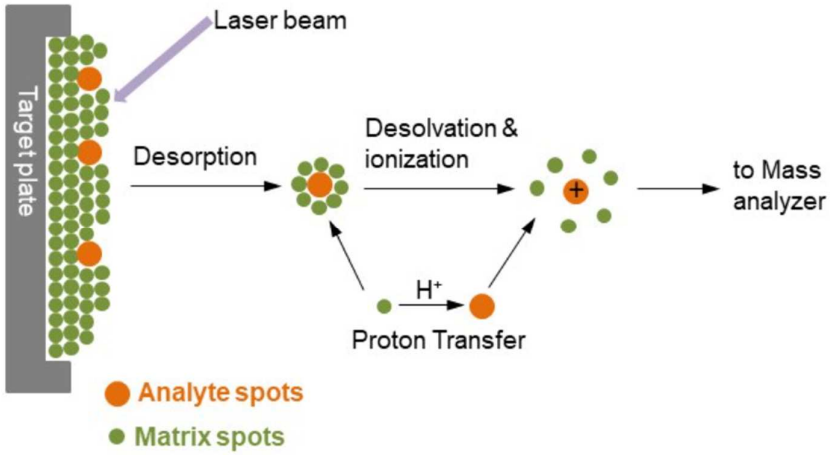

Figure 2.9 *– MALDI ionization process*

ESI technique utilizes an inert gas (usually nitrogen) to facilitate nebulization. Nebulization is caused by a high potential difference applied to the injector's metallic needle, that produce droplets of the solution (analyte and solvent). The most important features of ESI technique are the ionization that takes place at atmospheric pressure and the fact that a multiple charge can form on the molecule. This process takes place in an aqueous and organic solution, that is then nebulized at 80°C after applying an electric field. A schematic workflow of a typical ESI ionization process is shown in Figure 2.10.

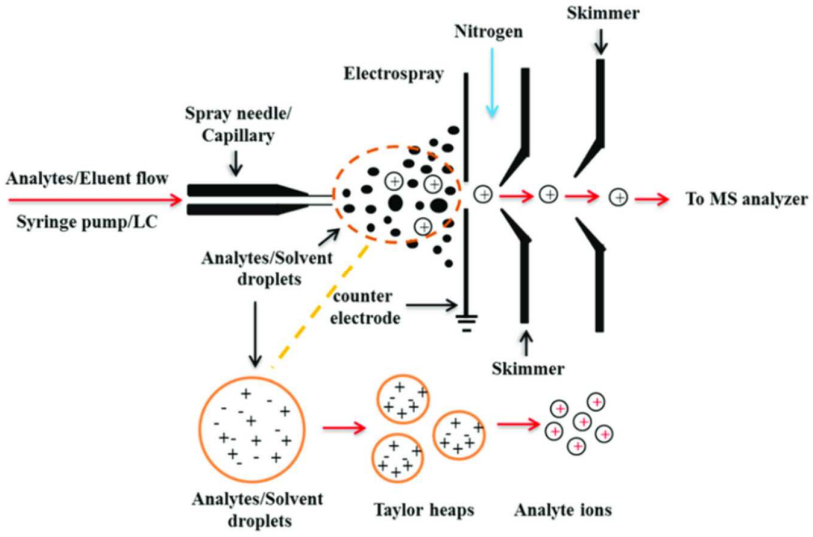

Figure 2.10 *– ESI ionization process [50]*

After the sample ionization, the signal measurement is performed using a Time of Flight (TOF) analyzer. The principle is that different m/z values have the same kinetic energy but different speed

after ionization: this means that the time spent crossing the analyzer is different for every ion. So, the ions from the source are accelerated by a strong electric field and they cross with different speeds the analyzer, that works under vacuum without any electrical or magnetic fields. This analyzer measures mass values with a high sensitivity.

2.3.5 Chromatographic purification and characterization

The purification and characterization of the different peptides synthetized in this thesis work was conducted with a Reverse Phase-High Performance Liquid Chromatography (RP-HPLC).

Chromatography is a chemical-physical approach that relies on the equilibrium between two different phases, one stationary, made of a gas or a liquid on a solid support, and one mobile, made of a gas, a liquid, or a supercritical fluid. The sample is dissolved in the mobile phase and flows continuously through the immiscible stationary phase. The components with the most affinity to the stationary phase are retained for a considerable amount of time, while the others with less affinity move faster. In this way, different components of the sample are separated and analyzed or collected. In liquid chromatography, the mobile phase is a liquid, while the stationary phase can be a solid or another immiscible liquid. An evolution of classic liquid chromatography is HPLC, where columns filled with functionalized silica gel are employed.

The Reverse Phase HPLC is a partition chromatography where the stationary phase is non-polar, and the mobile phase can be a mixing of different percentage of water and organic solvents (in this particular case, isopropanol). For the stationary phase, columns containing silica gel functionalized with linear, 18 C atoms hydrocarbon chains were used.

The interaction which allows the retention of peptides in the stationary phase is a hydrophobic one. The chromatography can be performed in “isocratic mode” or in “gradient mode”. In the latter case, increasing the organic solvent concentration leads to an increase in the mobile phase hydrophobicity. This leads to a competition between the two phases, so the analyte is de-adsorbed at a specific percentage (concentration) of the organic solvent.

Generally, peptides are better separated in acidic environment, so most of the mobile phases includes low concentration of TFA (0.05% in our case). In this thesis work, analyses were performed using 0.05% TFA in MilliQ water and 0.05% TFA in 40% isopropanol and 60% MilliQ water as eluents. Usually, 0.05% TFA in acetonitrile is used in lieu of isopropanol-based eluent, but aminooxy-acetylated peptides showed a high reactivity to ketones [51], so an eluent change was necessary.

A UV-spectrophotometer detector is placed at the column output, with a wavelength (λ) of 214 nm, which is the peptide bond's absorption peak.

HPLC preparative analysis allows the isolation and purification of compounds starting from a mixture, while HPLC analytic is used to obtain information on a sample, for example the identification and characterization of a peptide. Once the chromatographic conditions (column, mobile phase, and gradient) are fixed, the retention time represents a fingerprint of the molecule. The area under the peak is directly proportional to the injected sample amount. So, by integrating all the chromatogram peaks, it is possible to evaluate the homogeneity grade of the purified product.

2.3.6 Scaffold functionalization

In this thesis work, PEEK scaffolds were covalently functionalized with the peptides obtained by SPPS. The linkages between the aminooxy group at the end of the peptide chain and ketonic groups in PEEK surface are realized by means of chemoselective ligation. The buffer solution employed, i.e., a solution used for keeping the pH at a nearly constant value, was 40 mM of monobasic sodium phosphate at 6 pH. All the details about scaffold functionalization for this project are provided in paragraph 3.2.

2.3.7 Biological assays

All biological assays were performed at the Tissue Engineering laboratory of Professor Lucy Di Silvio, Centre of Clinical Translation Science, KCL. A thorough description of the principles and the procedures used is presented below.

2.3.7.1 Cell culture preparation

PEEK disks functionalized in this work of thesis were treated with a cell culture media containing immortalized Human Osteoblast (HOB) cells, using microseeding technique. 575 ml of osteoblast differentiation media were prepared using 500 ml of Dulbecco's Modified Eagle Medium (DMEM) combined with phenol red, 10 ml of 1 M HEPES, 5 ml of 200 mM L-glutamine, 5 ml of 100x penicillin/streptomycin, 50 ml of Fetal Calf Serum (FCS), 5 ml of minimal essential medium and

0.075 g of solid ascorbate powder. Prior to seeding, PEEK specimens were sterilized with 70% ethanol for 24 hours on a rolling machine. When all the samples were sterilized and culture media was ready, $1x10^5$ HOB cells were micro-seeded on the specimens by suspending them in 20 µl of culture media. Finally, the seeded scaffolds were incubated for 30 minutes at 37°C and 5% CO, and submerged in 1 ml of culture medium. For gene expression tests, $2x10^5$ HOB cells were seeded.

2.3.7.2 Alamar Blue test for cell proliferation

Alamar Blue™ (AB) is a dyeing solution based of resazurin that is used to evaluate cell proliferation. It is preferred to traditional tests such as MTT assay because it is non-toxic to the cells and extremely stable [52], allowing us to use the same samples at the different time points. When resazurin, the active ingredient of AB dye that is blue in color, is applied to cells cultured in media, it reduces to resorufin, that is red in color and fluorescent (Figure 2.11). This happens because the dye accepts electrons from the growing cells' metabolites. The continuing growth of cells maintains the reducing environment red and fluorescent, so that it can be detected by using a colorimetric or fluorometric plate reader.

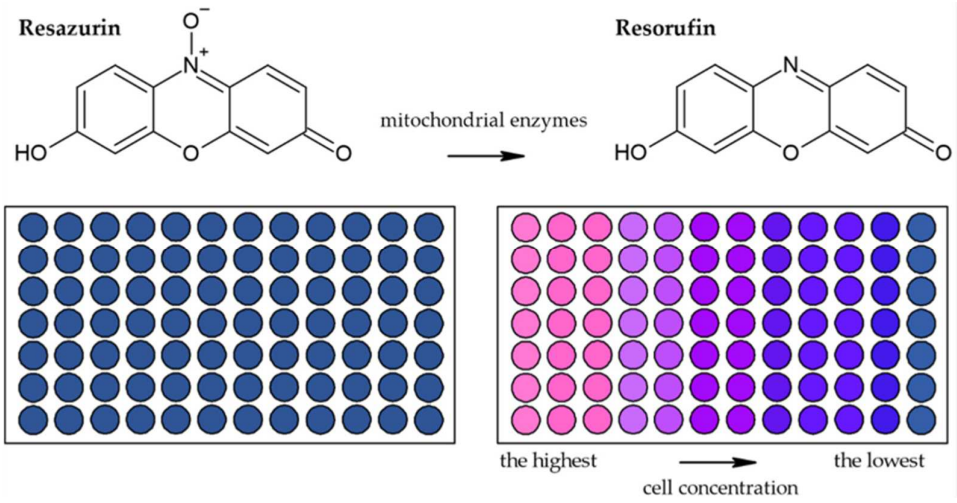

Figure 2.11 *- Scheme of the reduction of resazurin to resorufin including the color change [53]*

In the followed procedure, HOB cells were cultured for 1, 4, 7, 14 and 21 days. At each time point, 10x of AB were diluted to 1x by adding cell culture media, then 1 ml of the solution were added to each sample and left to react for 4 hours. Three replicates were collected for each sample, with 100 µl of solution each, all placed in a 96 multiwell plate. The plate was put into a Dynex Opsys MR

microplate reader, that measured the fluorescence values at 570 nm test wavelength and 630 nm reference wavelength.

2.3.7.3 Alizarin red S staining test

Calcium deposition was evaluated by Alizarin Red S staining on HOB cells. Alizarin red S is an anthraquinone dye that reacts with calcium and forms an Alizarin Red S/calcium complex that is birefringent.

HOB cells were cultured for 21 days, then the disks were washed in PBS, fixed with 10% formal saline for 15 minutes and then washed with deionized water three times. 2% Alizarin red S solution in water was added to the specimens, staining them for 15 minutes, then the samples were washed 5 times with 50% ethanol. For qualitative assessment, images of the stained scaffolds were taken.

Quantitative assessment was conducted using Lee *et al*. protocol [54]. The bound stain taken up by the cells on the disks was released using 1 ml of 10% cetylpyridium chloride (CPC) solution added to each well overnight (24 well plates). Aliquots (100 µL) of the supernatant were removed and read using a microplate reader (Opsys MR™ 96-well microplate reader, Dynex Technologies, VA, USA) at 570 nm. A standard curve for Alizarin red S was created, for quantification, using known concentrations of alizarin red S in CPC solution. Cell mineralization results were expressed as µmoles of calcium per well as 1 mole of Alizarin red S binds to 2 moles of calcium in an Alizarin red S-calcium complex [55].

2.3.7.4 Cell viability assessment

Cell viability was assessed using a LIVE/DEAD™ Viability/Cytotoxicity Kit (Thermo Fisher Scientific, Waltham, MA, USA) after 48 hours of cell culture. The kit consists of Calcein AM which stains live cells green and Ethidium homodimer-1 which stains dead cells red. Calcein AM itself is non-fluorescent, but it is cell-permeant, so it diffuses into intact cell membranes of live cells and once inside, it is hydrolyzed into fluorescent Calcein by the non-specific intracellular esterase activity of live cells. Calcein is retained within the cells with green fluorescence (around 530 nm). Ethidium homodimer-1 is cell-impermeant and can only enter compromised membranes of dead cells. Once inside dead cells, it binds to nucleic acids which enhance its red fluorescence (>600 nm), and also

binds to the DNA. Two PBS washings were performed prior to exposure to live/dead stain.The samples were then imaged with an Olympus IX51 fluorescent microscope. ImageJ software was used to display and merge images of live cells and dead cells of the same location into one image and enumerate them for viability calculation.

2.3.7.5 *Real time* Polymerase Chain Reaction

Polymerase Chain Reaction is one of the most powerful technologies of molecular biology. Developed by Nobel Prize Kary Mullis in the 80s, it can amplify exponentially specific sequencies of a DNA or RNA fragment. Some elements are necessary to carry out this technique:

- DNA or RNA that act as a "template" to carry out the amplification;
- Two primers (Forward and Reverse), i.e., two oligonucleotides that are complementary to 5' and 3' ends of the two regions of the filament that needs to be reproduced;
- A DNA polymerase, an enzyme that can create a copy of the amplifiable region. Usually, it is used the Taq polymerase, which is extracted from *Thermus aquaticus* bacteria and is stable at high temperatures;
- Nucleotides for the synthesis of new DNA;
- Buffer solution with $MgCl_2$, where Mg^{2+} ion is necessary for the enzyme to work.

PCR relies on a succession of amplification cycles that is realized by a thermal cycler, in this case Stratagene Mx3000P by Agilent Technologies was employed.

The number of cycles is generally a few tens, and every cycle is structured as follows:

1. Denaturation at high temperatures;
2. Annealing of the primers to the original DNA, at lower temperatures;
3. Extension, again at higher temperatures.

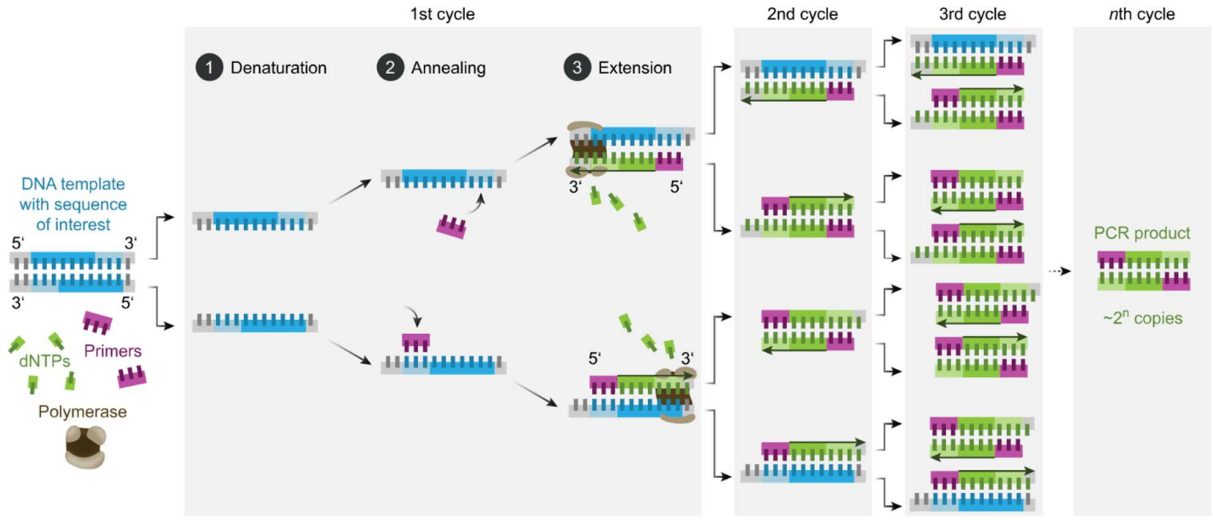

Figure 2.12 *– Schematic example of a complete PCR cycle*

Real Time Polymerase Chain Reaction, also called *quantitative PCR* or *qPCR*, is a particular form of PCR that allows to both amplify and quantify simultaneously a DNA or RNA target filament. The polymerase product quantity is measured at the end of every cycle. The quantification takes place thanks to the use of fluorescent markers embedded in the PCR product; these markers are called "amplicons" and are generated during the reaction. The instrument draws a quantitative chart of the fluorescence according to the number of cycles; thus, it allows to determine the product accumulation during the reaction. When the DNA or RNA produced increase, the fluorescence rises until the reaction stops (plateau phase in the chart curves, Figure 2.13). The point where the fluorescence rises rapidly is called "threshold" (also known as Ct). Higher is the cycle number necessary to get past the threshold, less will be the gene quantity expressed by the sample.

When RNA is used instead of DNA, as in this case, it is necessary to transform the RNA molecule into a complementary DNA (cDNA) molecule before proceeding with Real Time PCR.

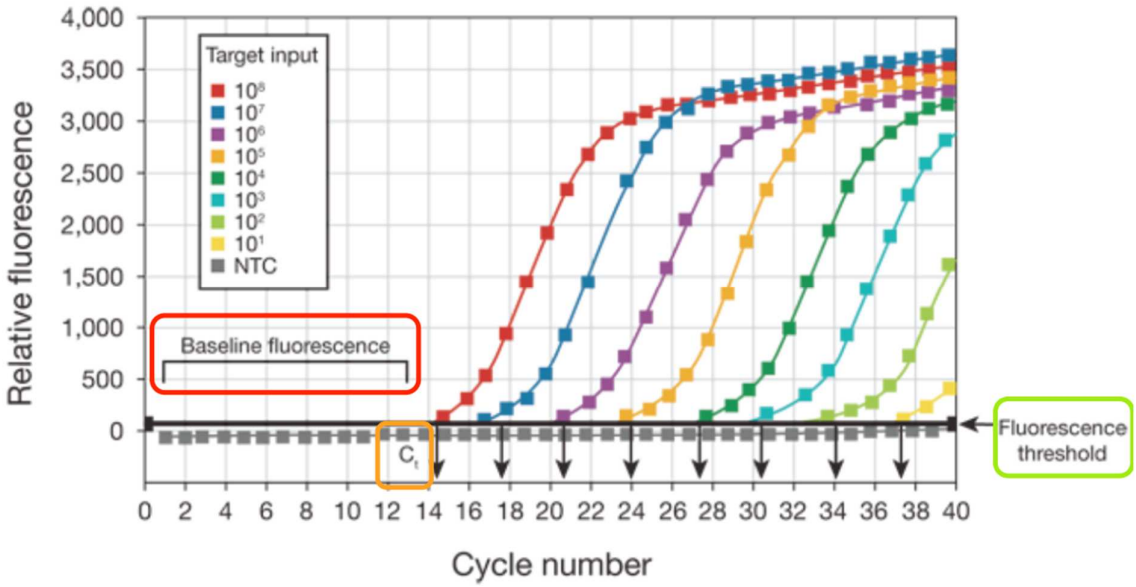

Figure 2.13 *– Plot of the fluorescence as a function of the cycle number*

In this thesis work, five genes were analyzed:

- Glyceraldehyde-3-phospahte (GAPDH) is the *housekeeping gene*, i.e., a gene that is normally expressed by cells, so the amount of DNA analyzed can be normalized to the amount in this housekeeping gene.
- SOX9 and RUNX2 are transcription factors that control mesenchymal cell differentiation into chondrocytes and osteoblasts [56].
- Alkaline phosphatase (ALP) and osteocalcin (OCN) are early and late markers for osteoblastic proliferation and differentiation, respectively [57].

Our functionalized samples were analyzed after 1 and after 7 days of HOB cells culturing. The RNA extraction procedure followed by King's College's Tissue Engineering laboratory involved some steps:

1. Samples cultured in media were washed with TRIzol to obtain all the genetic component;
2. The aqueous phase of the samples with TRIzol was transferred to a RNase-free tube, where an equal volume of ethanol (≥ 95%) was added. The solution was mixed thoroughly;
3. The mixture was transferred to an RNA spin column, assembled with a collection tube that removes gDNA from the sample;
4. 500 µl of RNA priming buffer were added to the spin column and the mixture was centrifuged for 30 seconds, then the flow-through was discharged. The same procedure was repeated with 500 µl of RNA wash buffer;

5. Another 500 µl of RNA wash buffer were added to the spin column and the mixture was centrifuged for 2 minutes, then the column was transferred to a RNase free microfuge tube;
6. For RNA elution, 50 µl of nuclease-free water were added to the spin column and the mixture was centrifuged for 30 seconds.

After RNA extraction, RNA was prepared for reverse transcription. First of all, a Master Mix was prepared with 2 µl of 10xRT buffer, 0.8 µl of 25xdNTP mix, 2 µl of 10x RT random primers, 1 µl of MultiScrive reverse transcriptase and 4.2 µl of nuclease-free water. 4 µl of Master Mix were added to 16 µl of extracted RNA for every sample, and then the sample was reverse transcribed to obtain cDNA thanks to a Veriti 96 Wall Thermal Cycler instrument by Applied Biosystems.

Reverse transcription consisted of an incubation period of 10 minutes at 25 °C, and then 60 minutes at 37 °C for the activation of reverse transcriptase enzyme. After that, the temperature was raised to 85 °C for 5 minutes to conduct RNA and cDNA primer denaturation and, finally, the temperature was lowered to 4 °C to avoid reverse transcription on the newly synthetized cDNA.

For Real Time PCR it was essential to prepare the PCR Amplification Mix for every tested gene. This mix is composed of 5 µl of Primer Stock and 5 µl of SYBR Green. Primer Stock is composed of 10 µl of forward primers, 10 µl of reverse primers and 180 µl of nuclease-free water. After obtaining the PCR Amplification Mix, 5 µl of it were added to the well associated with the specific gene, and 5 µl of cDNA mix were added to it. Once all the 96 multiwells were full, the multiwell plate was put into a Stratagene Mx3000P instrument. The concentration of cDNA employed for Real Time PCR was 200 ng/ml.

PCR phases consisted of 10 minutes at 95 °C, in which the enzyme Taq polymerase was activated, then 30 seconds at 95 °C to conduct DNA denaturation. Right after that, the temperature was lowered to 55 °C for 1 minute to permit the binding of primers with the complementary sequences on the DNA filament (annealing phase), then the temperature was raised to 72 °C for 1 minute for the filament extension phase. This cycle is repeated about 40 times, to obtain a measurable quantity of DNA.

2.3.8 Scanning electron microscopy

Scanning electron microscopy is an electrical-optical morphological analysis that is carried out with a Scanning Electron Microscope (SEM). The analysis relies on the emission of an optical beam by means of an incandescent filament, and on the analysis of the interaction between the electron beam

with the sample. Numerous types of samples can be analyzed with this technique, but the main constraint is that fluids must be absent, because the instrument works under high vacuum. Samples must be conductive; when they are not, they can be made so by coating them with a thin conductive layer.

A SEM is composed by:

- An electron column, where the electron beam is created.
- A vacuum chamber, where the electron beam interacts with the sample.
- Various types of detectors, that acquire the beam-sample interactions and transfer them to the elaborators.
- A screen, where the image is assembled.

Electrons are obtained by thermionic emission from a tungsten filament at high temperature, and are accelerated by an anode located under the filament. The electron beam is then focused by electromagnetic lenses and by slits inside the electron column. A set of coils deflects the beam and make it hit a predefined area of the sample. The sample is located in the vacuum chamber, and is hit by the electron beam. This interaction causes the emission of X-rays, secondary electrons, Auger electrons and backscattered electrons; every one of them is scanned by a specific detector and converted in a LCD screen image (Figure 2.14).

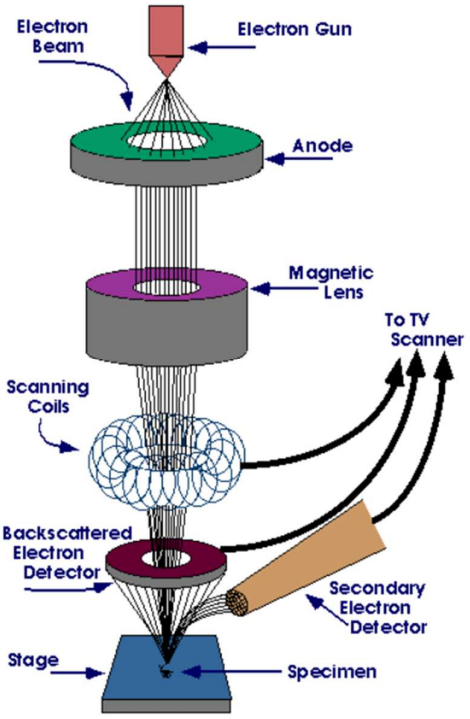

Figure 2.14 *– Diagram of a scanning electron microscope*

In this thesis work, morphology of HOB cells on PEEK structures was observed using SEM (Zeiss Gemini SEM 360) at a voltage of 10kV, by KCL's Tissue Engineering laboratory. Before SEM imaging, it was necessary to modify the samples' surface to preserve the structure of cells, so samples cultured in media were fixed with 2.5% glutaraldehyde in 0.1 M sodium cacodylate buffer for at least 24 hours at 4 °C. Then the glutaraldehyde was removed, and the samples were rinsed with 0.1 M sodium cacodylate buffer solution before treatment with 1% osmium tetroxide in 0.1 M sodium cacodylate buffer for 1 hour. The osmium tetroxide was then removed, and the samples were again rinsed with 0.1 M sodium cacodylate buffer. The samples were treated for 1 hour with a solution of 1% tannic acid in 0.1 M sodium cacodylate buffer. This solution reacts with osmium tetroxide to increase lipid retention and formation of links to proteins and carbohydrates. After another rinse with 0.1 M sodium cacodylate buffer, the samples were dehydrated with a series of aqueous ethanol solutions (20%, 30%, 40%, 50%, 60%, 70%, 90%, 96% and 100%). For each concentration, the samples were treated twice, and each treatment was 5 mins. After dehydration, the samples were air dried, and sputter coated with gold to make them conductive before being observed with SEM.

PEEK disks cultured for 24 h and 48 h were used as controls to determine normal cell behavior, to compare the other functionalized samples' results. Two separate wells without any PEEK disks were also set up as cell viability controls.

2.3.9 X-ray photoelectron spectroscopy

X-ray photoelectron spectroscopy (XPS) is a quantitative analysis that relies on the photoelectric effect to identify the elements that cover the surface of a sample, and their properties. XPS instrument uses metallic anodes as X-ray sources; these anodes are exposed to electrons characterized by an elevated energy. The ionization of the core level of the metal atom causes an X-ray release by the metal anodes. The sample is irradiated by the X-rays produced and emits photoelectrons. In fact, in the photoelectron effect when a material is hit by an electromagnetic radiation with an adequate energy content, the atom's electrons can be emitted.

Irradiation by photons with an energy hv produces an electron that has a kinetic energy equal to the photon's energy minus the bond energy of the atom and minus the work function Φ:

$$KE = hv - BE - \Phi$$

By measuring the KE of the expelled electron, it is possible to trace its energy of linkage, which is indicative of the chemical element involved, so, by analyzing the photoemitted electrons' spectrum, it will be possible to determine which elements are present on the sample surface.

XPS spectrum is composed by a series of peaks:

- Core level emission peaks, distinctive of the energetic levels of an atom's inner shells. They have a bond energy which is higher than 20 eV.
- Valence level emission peaks, which have less intensity than core peaks. These peaks derive from external energy levels of electrons and have a bond energy lower than 0.3 KeV.
- Auger emission peaks, caused by electrons emitted from the material due to an internal relaxation process. These peaks are typical of the material considered and appear in the low KE region.

A representation of the XPS equipment is shown in Figure 2.15.

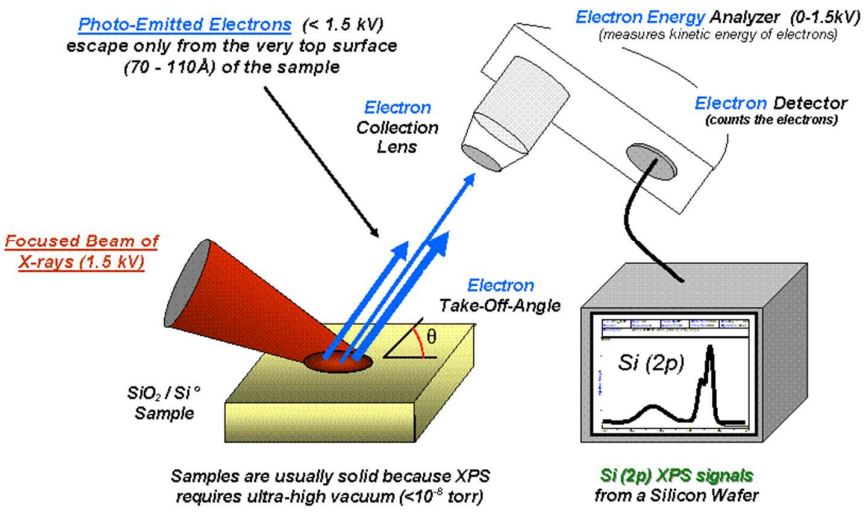

Figure 2.15 *– XPS equipment*

In this work, XPS analysis was conducted in collaboration with the University of Rome (Professor Giovanna Iucci). As described by Professor Iucci's report, XPS analysis was performed with a homemade instrument, consisting of a preparation and an analysis UHV chambers, separated by a gate valve. The analysis chamber is equipped with a six-degree-of freedom manipulator and a 150 mm mean radius hemispherical electron analyzer with a five-lens output system combined with a 16-channel detector giving a total instrument resolution of 1.0 eV as measured at the Ag $3d_{5/2}$ core level. Samples were introduced in the preparation chamber and left outgassing overnight at a base pressure of about 10^{-8} Torr, before introduction in the analysis chamber. Typical vacuum pressure in the analysis chamber during measurements was in the 10^{-9}–10^{-10} Torr range. The used X-ray radiation was a non-monochromatized Mg Kα(1253.6 eV).

2.3.10 Water contact angle

Water contact angle (WCA) is a thermodynamic quantity determined by the measure of a surface's wettability (Figure 2.16). The concept of wettability describes the ability of a liquid to wet completely or partially the surface in which it is settled. A surface characterized by a high wettability is called hydrophilic, and has a WCA that is less than 90°, while a surface with a low wettability is hydrophobic, and has a WCA higher than 90°. Hydrophilic scaffolds tend to react easily with water

due to the presence of polar functional groups, while hydrophobic scaffolds tend not to react with water.

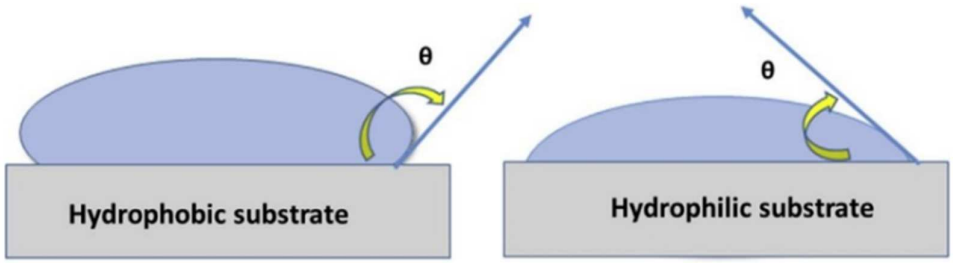

Figure 2.16 *– Contact angle for a hydrophobic surface (left) and a hydrophilic surface (right)*

The contact angle is the internal angle between liquid-vapor interface and solid-liquid interface (Figure 2.17).

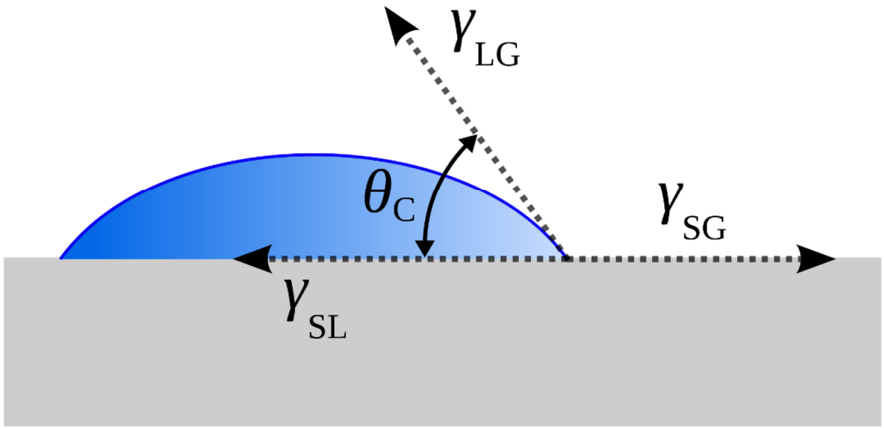

Figure 2.17 *– Contact angle (θ_c) between a liquid droplet and a solid surface*

WCA is linked to surface tension γ, which is the quantity of free energy observed on the surface of a material, so it is possible to determine the wettability of a surface by using γ values. A less wettable material has a higher contact angle and surface tension. The contact angle is described by Young's equation:

$$\cos\theta_c = \frac{\gamma_{SG} - \gamma_{SL}}{\gamma_{LG}}$$

This equation represents the thermodynamic equilibrium of a drop under the activity of three interfacial tensions, namely the tension between solid and vapor (γ_{SG}), the tension between solid and liquid (γ_{SL}) and, finally, the tension between liquid and vapor (γ_{LG}). It should be borne in mind that

Young's equation is valid on the hypothesis that the scaffold's surface is stiff, flat, non-reactive, inert, homogeneous, insoluble, smooth and non-porous (ideal surface).

WCA measurements in this thesis work were performed in the lab of the Department of Chemical Sciences of Catania, in collaboration with Professor Giovanni Marletta.

2.3.11 Atomic Force Microscopy

Atomic Force Microscopy (AFM) is a subtype of Scanning Probe Microscopy (SPM) that relies on scanning the sample surface to determine its morphology. This is accomplished with the help of a sharp tip, generally made of silicon or silicon nitride, and assembled at the end of a cantilever with a nanometric bend radius. The main forces exerted on the AFM tip are the van der Waals forces, Pauli repulsion and electrostatic forces, but the main forces of interest are Van der Waals forces. A schematic diagram of AFM operation is shown in Figure 2.18. A piezoelectric ceramic scanner is used to move either the tip or the sample surface. The attraction, or repulsion, between the tip and the surface atoms due to Van der Waals forces creates deflections on the cantilever, whose elastic constant is known. Typically, a laser diode is focused onto the back of the cantilever. The laser then reflects back onto a four quadrant photodiode; in this way, every deflection of the cantilever is measured and registered during scanning.

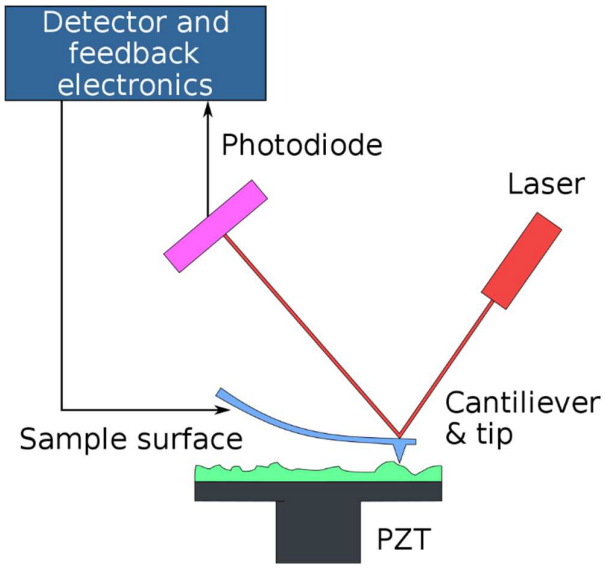

***Figure 2.18** – Schematic representation of an Atomic Force Microscopy operation*

The main working methodologies of AFM are:

- Contact mode;
- Non-contact mode;
- Dynamic mode.

In contact mode, the force acting between the tip and the surface is constant during scanning, and it causes a constant deflection. In non-contact mode, the cantilever oscillates at resonant frequency, and this frequency changes thanks to the interaction forces between the tip and the surface. The ratio between these oscillations and the reference oscillation gives information on the sample. This mode is often desirable since it avoids contact, and thus degradation of the surface in question. In practice, however, a purely non-contacting mode is often not achieved, and the tip will intermittently come into contact, or "tap" the sample. Hence this method is often referred to as tapping mode. In dynamic mode, the cantilever oscillates so that it comes into contact with the sample at every cycle, and then a force necessary to detach the tip from the sample is applied.

Thanks to the ability of AFM to be performed in aqueous solutions, this technique has been used even to determine mechanical properties of several types of cells, including osteoblasts [58]. For example, the elastic modulus and adhesion forces, i.e., the tip-cell interaction forces, were assessed with this technology [59] [60]. Obviously, living cells need a sensitive control over the loading force applied, that must be minimized in order not to damage the soft samples with the sharp tip.

AFM measurements in this thesis work were performed in the lab of the Department of Chemical Sciences of Catania, in collaboration with Professor Giovanni Marletta. A NTEGRA (ND-MDT) microscope was employed. This instrument is characterized by a silicon nitride cantilever with a nominal radius that is less than 10 nm, a resonance frequency of 300 kHz and a strength constant of 40 N/m. To obtain the Young modulus, every sample was analyzed with approximately 300 strength curves thanks to the Derjaguin-Muller-Toporov (DMT) model:

$$F + F_{ad} = \frac{4E_s}{3(1-\nu_s^2)} R^{1/2} \delta^{3/2}$$

Where F is the applied force, F_{ad} is the adhesion force, E_s is the Young modulus, ν_s is the Poisson's ratio, R is the cantilever's radius and δ is the elastic indentation depth. With the DMT model, Young modulus was evaluated in the elastic region of the curve.

2.3.12 Statistical analysis

Data obtained by biological and surface assays were analyzed and processed with Prism (GraphPad Software 9). Alizarin Red S results were compared by using one-way analysis of variance (ANOVA) test. Tukey's multiple comparisons test was carried out to confront every condition. AB and gene expression results were compared with two-way ANOVA tests, followed by Tukey's post-hoc test. The significance level applied was 5%.

Chapter 3

Experimental part

3.1 Peptide synthesis and purification

3.1.1 Aoa-x-HVP

This peptide was already synthesized, and it was present as crude peptide in the laboratory. In this project Aoa-x-HVP peptide was only purified.

The peptide sequence is:

H-Aoa-(7-aminoheptanoic acid)-Phe-Arg-His-Arg-Asn-Arg-Lys-Gly-Tyr-NH_2

The theoretical weight is 1432.587 Da.

3.1.1.1 Peptide purification

The crude Aoa-x-HVP peptide was purified through a RP-HPLC semipreparative (SP) analysis. 30.1 mg of crude peptide were dissolved first with 30.1 ml of MilliQ water. The solution was filtered using a PVDF filter with 0.45 µm pore diameter. The analysis was performed under the following conditions:

- Column: Zorbax 300SB C_{18} (5 µm, 300 Å, 9.4 × 250 mm)
- Injected volume: 30.1 ml
- Flow rate: 2 mL/min
- Detector wavelength: 214 nm
- Full-scale: 4.0
- Eluent A: 0.05% TFA in MilliQ water
- Eluent B: 0.05% TFA in 40% isopropanol and 60% MilliQ water
- Gradient: from 10% to 40% of B in 60 minutes

- Paper velocity: 0.5 cm/min

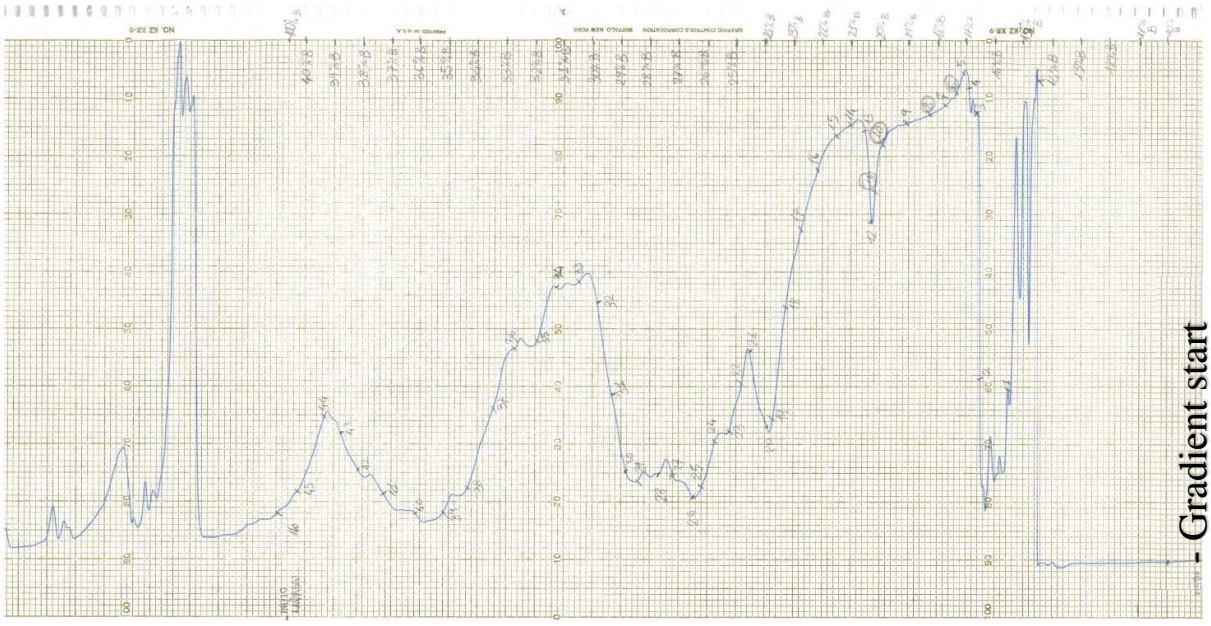

Figure 3.1 *- Crude Aoa-x-HVP semipreparative RP-HPLC chromatogram. Column: Zorbax C_{18}, flow: 2 ml/min, eluent A: 0.05% TFA in MilliQ water, eluent B: 0.05% TFA in 40% isopropanol and 60% MilliQ water solution, gradient: from 10% to 40% of B in 60 minutes, injected volume: 30.1 ml, detector wavelength: 214 nm, full-scale: 4.0, paper velocity: 0.5 cm/min*

In figure 3.1 it is possible to identify a large peak. The eluate was fractioned in different vials. Different pools were created: 6, 7÷8 and 9÷10. Several analytical RP-HPLC analyses were carried to evaluate the purity of the collected fractions. These analyses were carried out at the following conditions:

- Column: Jupiter C_{18} (5 µm, 300 Å, 4.6 x 250 mm)
- Injected volume: 50 ul
- Flow rate: 0.5 mL/min
- Detector wavelength: 214 nm
- Eluent A: 0.05% TFA in MilliQ water
- Eluent B: 0.05% TFA in 40% isopropanol and 60% MilliQ water
- Gradient: from 20% to 50% of B in 30 minutes

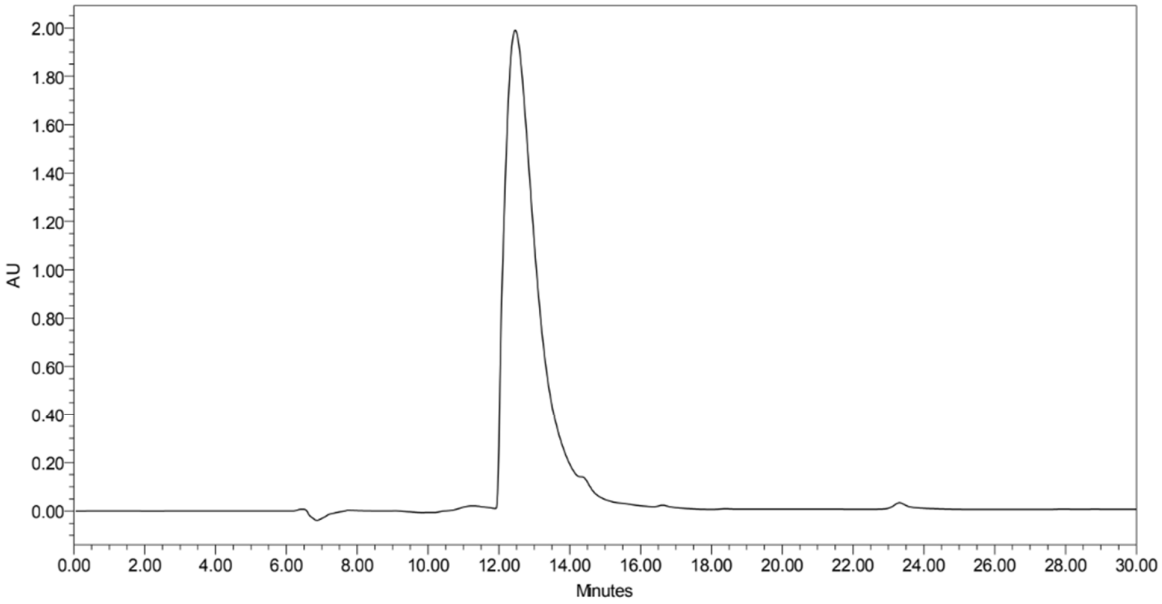

Figure 3.2 *- Purified Aoa-x-HVP RP-HPLC analytical chromatogram. Column: Jupiter C_{18}, flow: 0.5 ml/min, eluent A: 0.05% TFA in MilliQ water, eluent B: 0.05% TFA in 40% isopropanol and 60% MilliQ water solution, gradient: from 20% to 50% of B in 30 minutes, injected volume: 50 µl, detector wavelength: 214 nm*

Figure 3.2 is the analytical of fraction 6. Both pool 6, 7÷12 and 9÷10 showed a high purity. The purified fractions were immediately frozen with liquid nitrogen and lyophilized, because the aminooxy acetylated peptides have a tendency to react with ketones when in contact with traces of certain substances (like acetone) or even when stored [51]. The total weight of pure peptide obtained was 4.84 mg.

3.1.2 Aoa-x-GBMB1α

Aoa-x-GBMP1α was obtained through solid phase peptide synthesis using a Syro I automatic synthesizer and Fmoc chemistry. The resin Rink Amide MBHA (substitution 0.52 mmol/g) was used as a solid support. 240 mg of resin were used, which is equal to 0.125 mmol (scale of synthesis).

The peptide sequence is:

H-Aoa-(7-aminoheptanoic acid)-Pro-Phe-Pro-Leu-Ala-Asp-His-Leu-Asn-Ser-Thr-Asn-His-Ala-Ile-Val-Gln-Thr-Leu-Val-Asn-Ser-NH_2

The theoretical weight is 2587.86 Da.

Aoa group was attached separately as different conditions are needed. In fact, the aminooxy group tends to react with itself.

3.1.2.1 Peptide synthesis

A 0.62 M DMF solution was prepared for each of the following amino acids:

- Fmoc-Ala-OH
- Fmoc-Asp(OBut)-OH
- Fmoc-His(Trt)-OH
- Fmoc-Ile-OH
- Fmoc-Leu-OH
- Fmoc-Asn(Trt)-OH
- Fmoc-Pro-OH
- Fmoc-Gln(Trt)-OH
- Fmoc-Ser(But)-OH
- Fmoc-Thr(But)-OH
- Fmoc-Val-OH
- Fmoc-7-aminoheptanoic acid
- BisBoc-Aoa

A 0.62 M NMP solution was prepared for the following amino acids:

- Fmoc-Phe-OH

To increase the efficiency of the coupling, 5 equivalents of each amino acid were used with respect to resin reactive groups.

The three solutions needed for the reaction were prepared:

- 0.5 M solution of HBTU/Oxyma Pure in DMF
- 40% piperidine solution in DMF
- 1.8 N solution of DIPEA in NMP

The synthesis reaction is composed of 23 cycles, all set to double coupling, each one with a 45 minute span time. Fmoc group removal was obtained by treating the growing peptide with 1 ml of 40% piperidine solution in DMF for 3 minutes, then again with 0.9 ml of 40% piperidine solution in DMF

for 12 minutes. The activation of the carboxyl group, during the condensation reaction, was obtained by dissolving 1 ml of amino-acid solution in 1.4 ml of HBTU/Oxyma Pure in DMF and 0.695 ml of DIPEA solution in NMP.

At the end of the 23rd cycle, so after the binding of the spacer, a ninhydrin test was performed to evaluate the reaction yield. The yield obtained was 97%, which was considered acceptable.

After the ninhydrin test, another cycle was set for the double coupling of Aoa group. In this case, the following solutions were prepared, to maximize the yield:

- 0.5 M solution of HATU/Oxyma Pure in DMF
- 40% piperidine solution in DMF
- 2 N solution of collidine in NMP

A deprotection cycle for the Fmoc group was set, and then the double coupling of Aoa. At the end of the synthesis, some washings with DCM were performed, then the resin was dried under vacuum for 1 hour.

3.1.2.2 Peptide cleavage from the resin

Peptide cleavage from the resin was carried out on 1/4 of the resin obtained, to see if the aminooxy group had bound correctly. 730.43 mg of resin were weighed, and 178 mg were taken.

The cleavage solution was composed of:

- 0.125 ml of MilliQ water
- 0.125 ml of TES
- 4.75 ml of TFA

The solution was reacted for 1 hour and 30 minutes at room temperature, manually rotating the reactor occasionally. Once finished, the solution was filtered and some washings with TFA were carried out, then the solution was dried out with the help of the rotary evaporator. The obtained peptide was precipitated adding cold ethyl ether (4°C) under low magnetic stirring, then it was filtered in a Gooch 4 and dried under vacuum for 1 hour.

The dried crude peptide was weighed, obtaining 50 mg of crude peptide.

3.1.2.3 Crude peptide characterization

To characterize Aoa-x-BMP peptide, 1 mg of crude peptide was dissolved in 1 ml of MilliQ water, and then the solution was filtered using a PVDF filter. The analysis was performed at the following conditions (Figure 3.3):

- Column: Vydac 218TP C18 (5 µm, 300 Å, 4.6 x 250 mm)
- Injected volume: 25 µl
- Flow rate: 0.5 ml/min
- Detector wavelength: 214 nm
- Eluent A: 0.05% TFA in MilliQ water
- Eluent B: 0.05% TFA in 40% isopropanol and 60% MilliQ water
- Gradient: from 60% to 80% of eluent B in 40 minutes

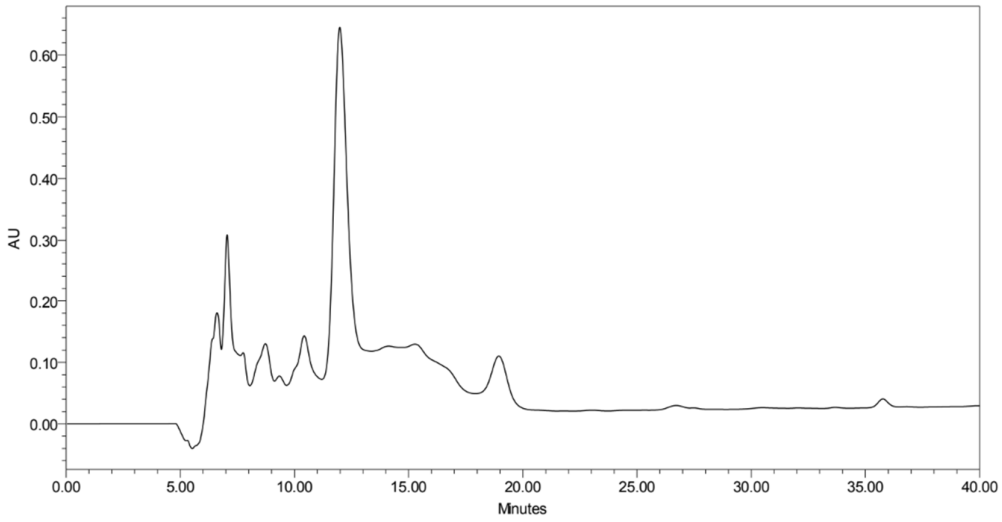

Figure 3.3 *- Crude Aoa-x-GBMP1α RP-HPLC analytical chromatogram. Column: Vydac C_{18}, flow: 0.5 ml/min, eluent A: 0.05% TFA in MilliQ water, eluent B: 0.05% TFA in 40% isopropanol and 60% MilliQ water solution, gradient: from 60% to 80% of B in 40 minutes, injected volume: 25 µl, detector wavelength: 214 nm*

Then, a mass spectroscopy analysis was performed to ensure the correct molecular weight. Maldi-TOF result is reported in Figure 3.4. We can see that the theoretical weight is found.

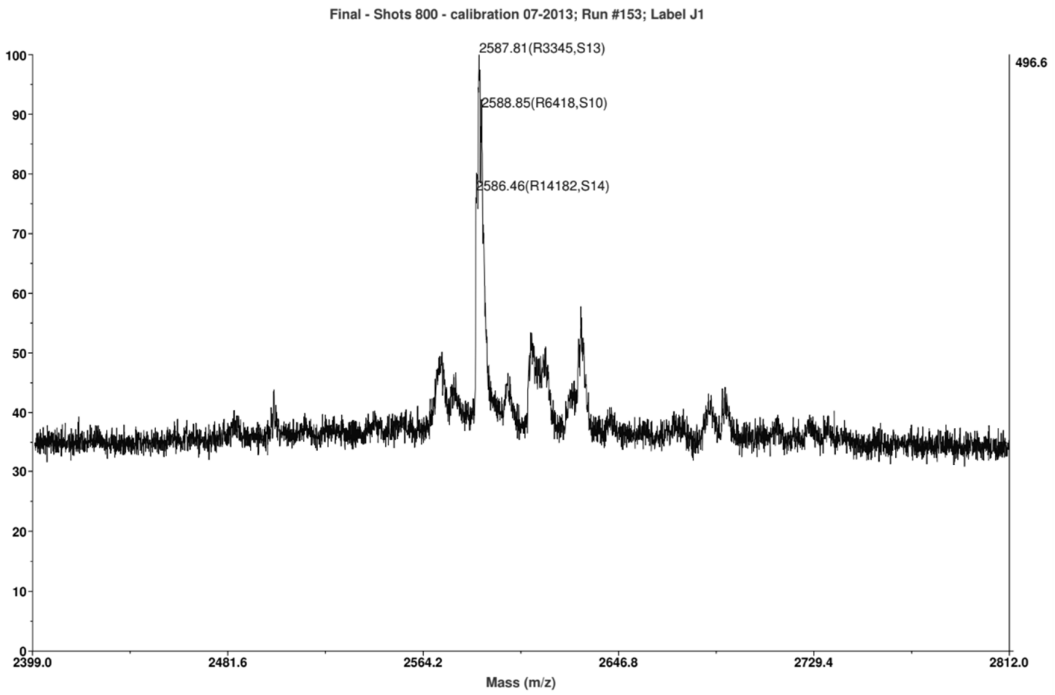

Figure 3.4 *– Mass analysis of crude Aoa-x-GBMP1α peptide (theoretic weight: 2587.86 Da, experimental weight: 2587.81 Da).*

3.1.2.4 Peptide purification

The crude Aoa-x-GBMP1α peptide was purified through a RP-HPLC SP analysis. Aoa-x-GBMP1α is highly insoluble, so 30.2 mg of crude peptide were dissolved first with some drops of hydrochloric acid, then with 30.2 ml of MilliQ water. The solution was filtered using a PVDF filter with 0.45 µm pore diameter. The analysis was performed under the following conditions:

- Column: Zorbax 300SB C_{18} (5 µm, 300 Å, 9.4 × 250 mm)
- Injected volume: 30.2 ml
- Flow rate: 2 mL/min
- Detector wavelength: 214 nm
- Full-scale: 4.0
- Eluent A: 0.05% TFA in MilliQ water
- Eluent B: 0.05% TFA in 40% isopropanol and 60% MilliQ water
- Gradient: from 60% to 80% of B in 80 minutes
- Paper velocity: 0.5 cm/min

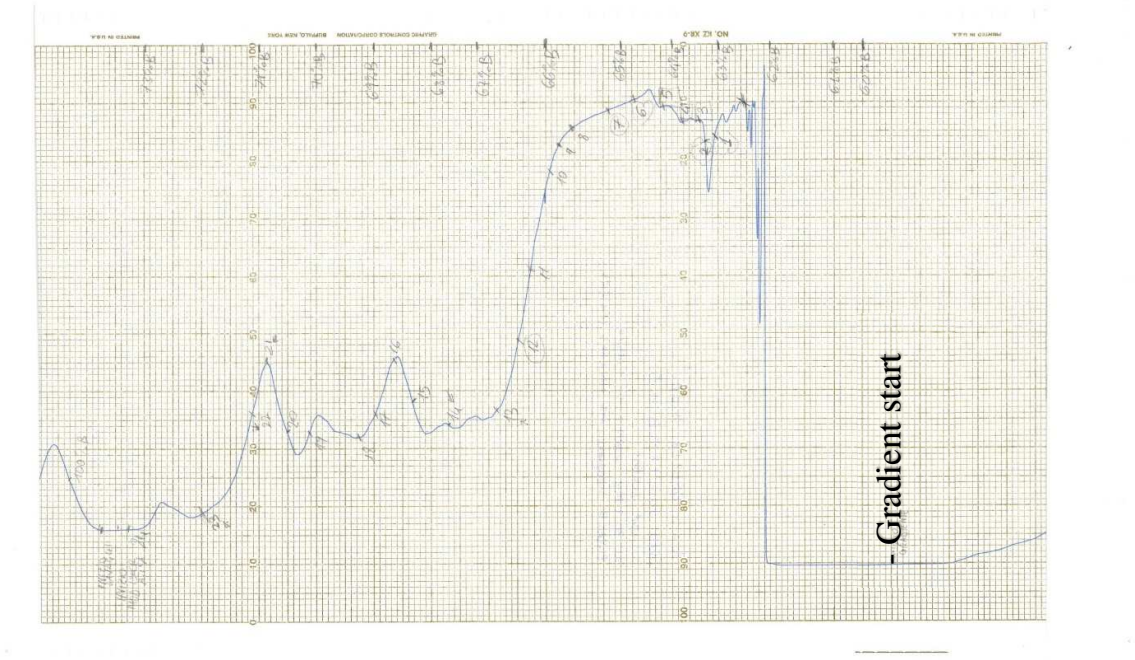

Figure 3.5 *– Crude Aoa-x-GBMP1α semipreparative RP-HPLC chromatogram. Column: Zorbax C_{18}, flow: 2 ml/min, eluent A: 0.05% TFA in MilliQ water, eluent B: 0.05% TFA in 40% isopropanol and 60% MilliQ water solution, gradient: from 60% to 80% of B in 80 minutes, injected volume: 30.2 ml, detector wavelength: 214 nm, full-scale: 4.0, paper velocity: 0.5 cm/min*

In figure 3.5 it is possible to identify a large peak. The eluate was fractioned in different vials. Different pools were created: 1÷2, 3÷5, 6 and 7÷12. Several analytical RP-HPLC analyses were carried to evaluate the purity of the collected fractions. These analyses were carried out at the following conditions:

- Column: Vydac 218TP C18
- Injected volume: 20 µl
- Flow rate: 0.5 mL/min
- Detector wavelength: 214 nm
- Eluent A: 0.05% TFA in MilliQ water
- Eluent B: 0.05% TFA in 40% isopropanol and 60% MilliQ water
- Gradient: from 60% to 80% of B in 40 minutes

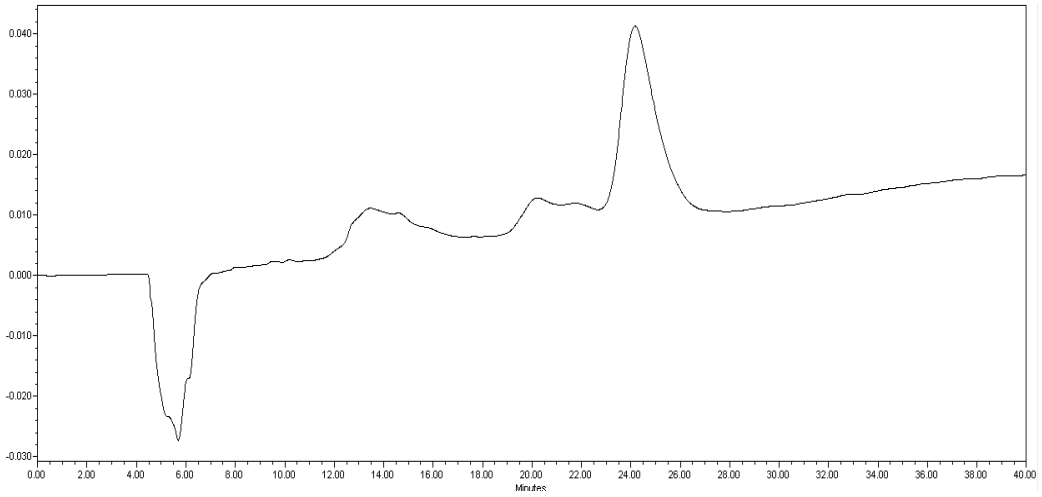

Figure 3.6 *- Purified Aoa-x-GBMP1α RP-HPLC analytical chromatogram. Column: Vydac C_{18}, flow: 0.5 ml/min, eluent A: 0.05% TFA in MilliQ water, eluent B: 0.05% TFA in 40% isopropanol and 60% MilliQ water solution, gradient: from 60% to 80% of B in 40 minutes, injected volume: 20 µl, detector wavelength: 214 nm*

Figure 3.6 is the analytical of fraction 6. Both pool 6 and pool 7÷12 showed a high purity. The total weight of pure peptide obtained was 11.69 mg.

The collected pools were analyzed by Maldi-TOF to identify the pure peptide (Figure 3.7).

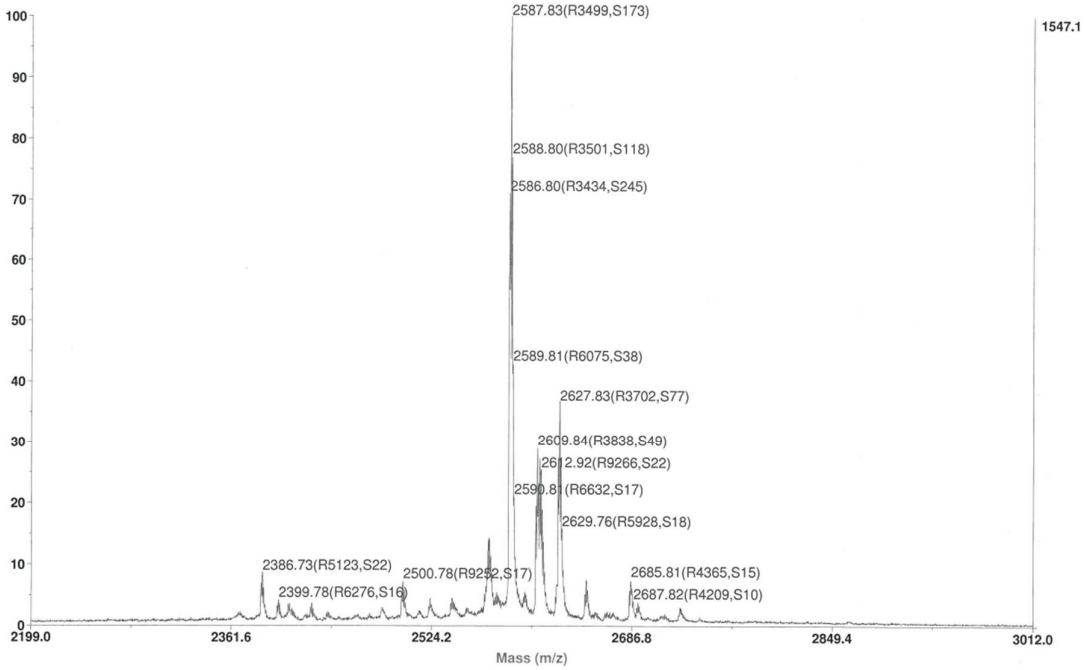

Figure 3.7 *– Mass analysis of purified Aoa-x-GBMP1α peptide (theoretic weight: 2587.86 Da, experimental weight: 2587.83 Da).*

The analysis shows a mass peak of 2587.83 Da, which is equal to the theoretical weight of the pure peptide.

3.1.3 Aoa-x-HVP with Fluorine

Aoa-x-HVP-F was obtained through solid phase peptide synthesis using a Syro I automatic synthesizer and Fmoc chemistry. The resin Rink Amide MBHA (substitution 0.52 mmol/g) was used as a solid support. 240 mg of resin were used, which is equal to 0.125 mmol (scale of synthesis). A special phenylalanine with fluorine in the side chain, Fmoc-parafluoro-phenylalanine (Fmoc-PFP, residual MW = 165.166 Da) was used instead of normal phenylalanine.

The peptide sequence is:

H-Aoa-(7-aminoheptanoic acid)-PFP-Arg-His- Arg-Asn-Arg-Lys-Gly-Tyr-NH_2

The theoretical weight is 1450.58 Da.

Aoa group was attached separately as different conditions are needed.

3.1.3.1 Peptide synthesis

A 0.62 M DMF solution was prepared for each of the following amino acids:

- Fmoc-Arg(Pbf)
- Fmoc-His(Trt)
- Fmoc-Lys(Boc)-OH
- Fmoc-Gly
- Fmoc-Tyr(tBu)
- Fmoc-amino-heptanoic acid

A 0.062 M NMP solution was prepared for each of the following amino acids:

- Fmoc-PFP-OH.

To increase the efficiency of the coupling, 5 equivalents of each amino acid were used with respect to resin reactive groups.

The three solutions needed for the reaction were prepared:

- 0.5 M solution of HBTU/Oxyma Pure in DMF
- 40% piperidine solution in DMF
- 1.8 N solution of DIPEA in NMP

The synthesis reaction is composed of 10 cycles, all set to double coupling, each one with a 45 minute span time. Fmoc group removal was obtained by treating the growing peptide with 1 ml of 40% piperidine solution in DMF for 3 minutes, then again with 0.9 ml of 40% piperidine solution in DMF for 12 minutes. The activation of the carboxyl group, during the condensation reaction, was obtained by dissolving 1 ml of amino-acid solution in 1.4 ml of HBTU/Oxyma Pure in DMF and 0.695 ml of DIPEA solution in NMP.

At the end of the 9th cycle, so after the binding of PFP, a ninhydrin test was performed to evaluate the reaction yield. The yield obtained was 94%, which was considered too low, so the resin was split in two halves, each one of these weighing 293.08 mg, and one half was acetylated, to block peptide chains with free amino groups. The acetylation procedure was conducted following two steps:

1. 2 ml of 10% acetic anhydride and 5% lutidine in DMF solution were added to the reactor with the weighed resin. The solution was left to react for 20 minutes.
2. The resin was washed 5 times with DMF.
3. Some washes of the resin with DCM were carried out, then the reactor was dried under vacuum for 1 hour.

After acetylation, the resin continued the synthesis with a double coupling of 7-aminoheptanoic acid. After that, another cycle was set for the double coupling of Aoa group. In this case, the following solutions were prepared, to maximize the yield:

- 0.5 M solution of HATU/Oxyma Pure in DMF
- 40% piperidine solution in DMF
- 2 N solution of collidine in NMP

A deprotection cycle for the Fmoc group was set, and then the double coupling of Aoa. At the end of the synthesis, some washings with DCM were performed, then the resin was dried under vacuum for 1 hour.

3.1.3.2 Peptide cleavage from the resin

Peptide cleavage from the resin, and simultaneous chain groups deprotection, was carried out on all of the resin obtained.

The cleavage solution was composed of:

- 0.125 ml of MilliQ water
- 0.125 ml of TES
- 4.75 ml of TFA

The solution was reacted for 1 hour and 30 minutes at room temperature, manually rotating the reactor occasionally. Once finished, the solution was filtered and some washings with TFA were carried out, then the solution was dried out with the help of the rotary evaporator. The obtained peptide was precipitated adding cold ethyl ether (4°C) under low magnetic stirring, then it was filtered in a Gooch 4 and dried under vacuum for 1 hour.

The dried crude peptide was weighed, obtaining 72.98 mg of crude peptide.

3.1.3.3 Crude peptide characterization

To characterize Aoa-x-HVP-F peptide, 1 mg of crude peptide was dissolved in 1 ml of MilliQ water, and then the solution was filtered using a PVDF filter. The analysis was performed at the following conditions (Figure 3.8):

- Column: Jupiter 5u C18 300A
- Injected volume: 50 µl
- Flow rate: 0.5 ml/min
- Detector wavelength: 214 nm
- Eluent A: 0.05% TFA in MilliQ water
- Eluent B: 0.05% TFA in 40% isopropanol and 60% MilliQ water
- Gradient: from 20% to 50% of eluent B in 30 minutes

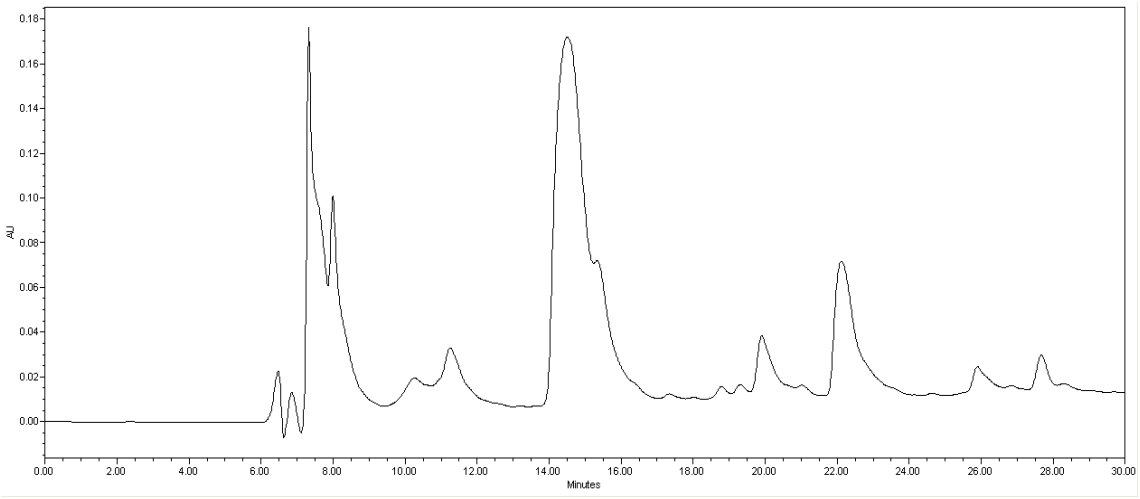

Figure 3.8 *- Crude Aoa-x-HVP with fluorine RP-HPLC analytical chromatogram. Column: Jupiter C_{18}, flow: 0.5 ml/min, eluent A: 0.05% TFA in MilliQ water, eluent B: 0.05% TFA in 40% isopropanol and 60% MilliQ water solution, gradient: from 20% to 50% of B in 30 minutes, injected volume: 50 µl, detector wavelength: 214 nm*

Then, a mass spectroscopy analysis was performed to ensure the correct molecular weight. Maldi-TOF result is reported in Figure 3.9.

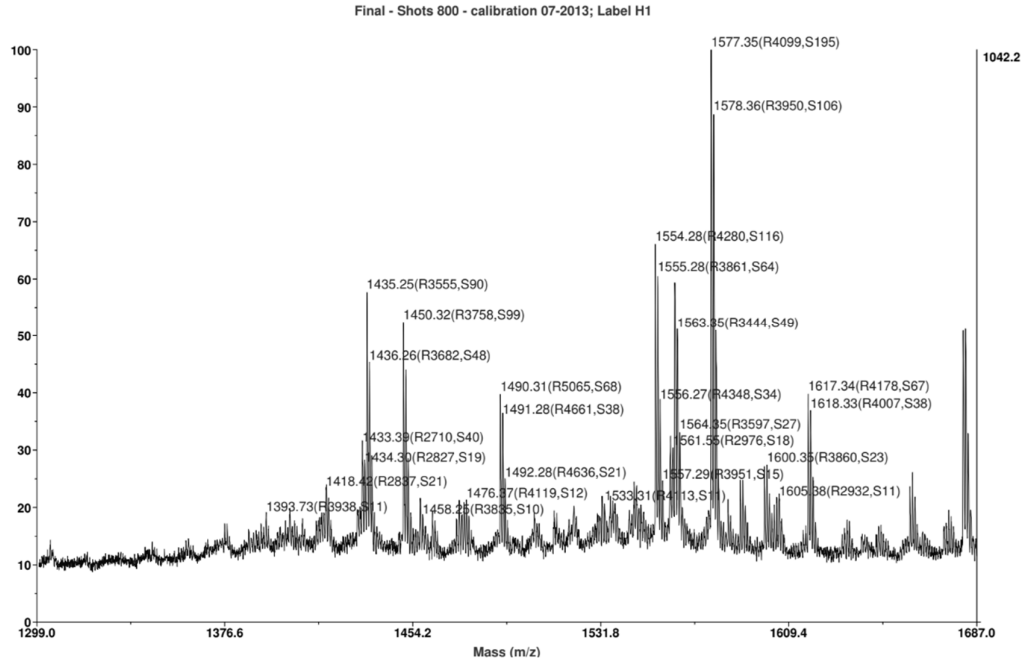

Figure 3.9 *– Mass analysis of purified Aoa-x-HVP with fluorine peptide (theoretic weight: 1450.58 Da, experimental weight: 1450.32 Da).*

3.1.3.4 Peptide purification

The crude Aoa-x-HVP-F peptide was purified through a RP-HPLC SP analysis. 35 mg of crude peptide were dissolved in 25 ml of MilliQ water. The solution was filtered using a PVDF filter with 0.45 µm pore diameter. The analysis was performed under the following conditions:

- Column: Zorbax 300SB C18 (5 µm, 300 Å, 9.4 × 250 mm)
- Injected volume: 35 ml
- Flow rate: 2 mL/min
- Detector wavelength: 214 nm
- Full-scale: 4.0
- Eluent A: 0.05% TFA in MilliQ water
- Eluent B: 0.05% TFA in 40% isopropanol and 60% MilliQ water
- Gradient: from 10% to 30% of B in 60 minutes
- Paper velocity: 0.5 cm/min

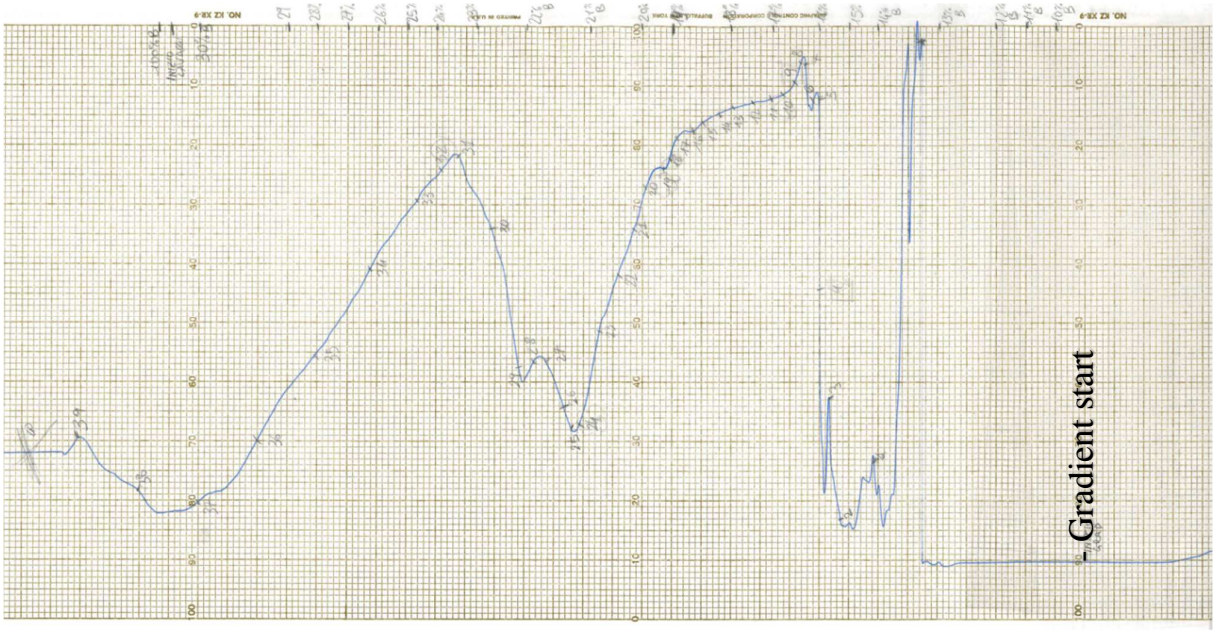

Figure 3.10 *– Crude Aoa-x-HVP with fluorine semipreparative RP-HPLC chromatogram. Column: Zorbax C_{18}, flow: 2 ml/min, eluent A: 0.05% TFA in MilliQ water, eluent B: 0.05% TFA in 40% isopropanol and 60% MilliQ water solution, gradient: from 10% to 30% of B in 60 minutes, injected volume: 35 ml, detector wavelength: 214 nm, full-scale: 4.0, paper velocity: 0.5 cm/min*

In figure 3.10 it is possible to identify one large peak, that corresponds to the pure peptide, and a second peak, which is peptide reacted with ketones. The eluate was fractioned in different vials, which were freezed at -20°C to prevent the reaction of Aoa group with ketones.

Different pools were then created: 4÷5, 10÷18, 19÷24 and 32. Several analytical RP-HPLC analyses were carried to evaluate the purity of the collected fractions. These analyses were carried out at the following conditions:

- Column: Jupiter C_{18} (5 µm, 300 Å, 4.6 x 250 mm)
- Injected volume: 50 µl
- Flow rate: 0.5 mL/min
- Detector wavelength: 214 nm
- Eluent A: 0.05% TFA in MilliQ water
- Eluent B: 0.05% TFA in 40% isopropanol and 60% MilliQ water
- Gradient: from 20% to 50% of B in 30 minutes

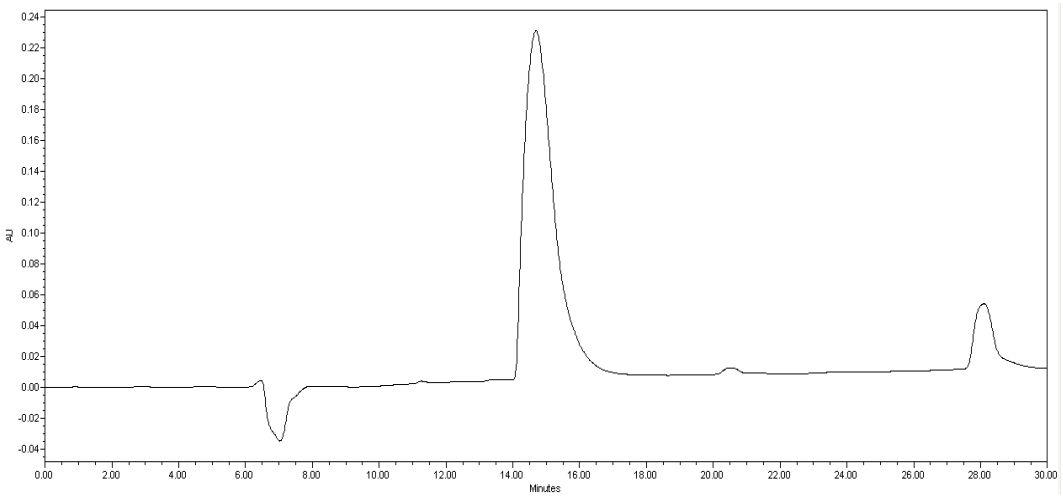

Figure 3.11 *- Purified Aoa-x-HVP with fluorine RP-HPLC analytical chromatogram. Column: Jupiter C_{18}, flow: 0.5 ml/min, eluent A: 0.05% TFA in MilliQ water, eluent B: 0.05% TFA in 40% isopropanol and 60% MilliQ water solution, gradient: from 20% to 50% of B in 30 minutes, injected volume: 50 µl, detector wavelength: 214 nm*

Figure 3.11 is the analytical of pool 10÷18. This pool shows a large peak of pure peptide and a smaller peak of peptide reacted with ketones, nevertheless the pool was considered suitable for functionalization. The total weight of pure peptide obtained was 3.70 mg.

The collected pools were analyzed by Maldi-TOF to identify the pure peptide (Figure 3.12).

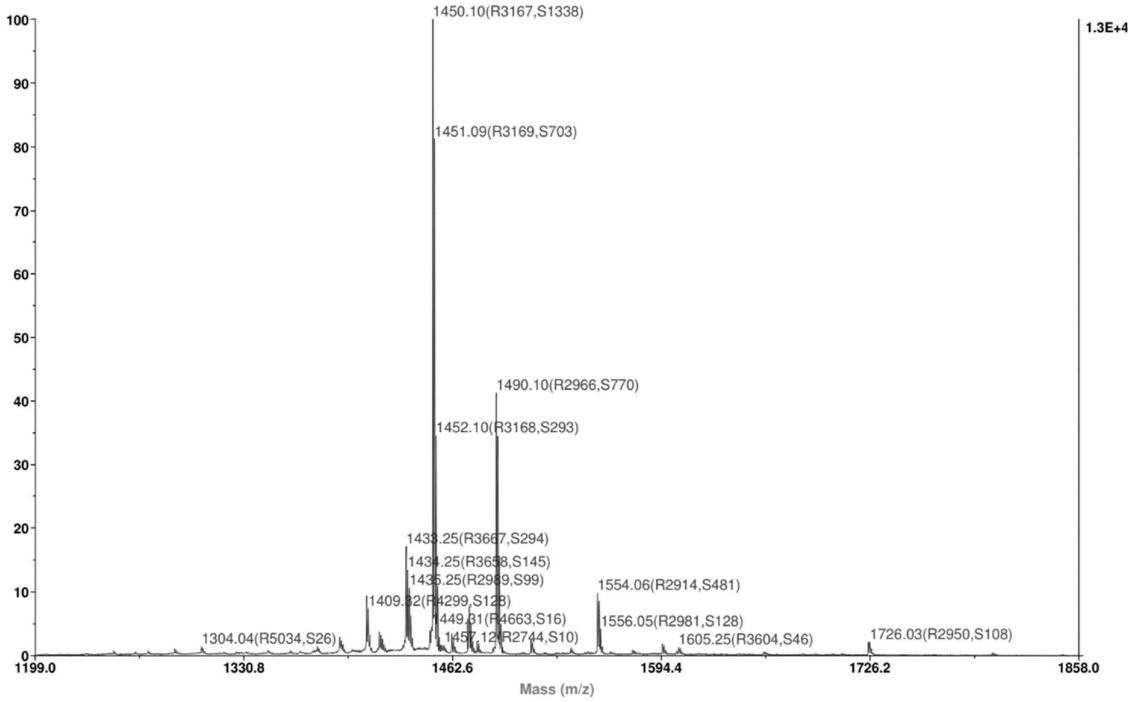

Figure 3.12 *– Mass analysis of purified Aoa-x-HVP with fluorine peptide (theoretic weight: 1450.58 Da, experimental weight: 1450.32 Da).*

The analysis shows a mass peak of 1450.10 Da, which is almost equal to the theoretical molecular weight of the pure peptide (1450.58 Da).

3.1.4 Aoa-x-EAK

Aoa-x-EAK was obtained through solid phase peptide synthesis using a Syro I automatic synthesizer and Fmoc chemistry. The resin Rink Amide MBHA (substitution 0.62 mmol/g) was used as a solid support. 202 mg of resin were used, which is equal to 0.125 mmol (scale of synthesis).

The peptide sequence is:

H-Aoa-(7-amino heptanoic acid)-Ala-Glu-Ala-Glu-Ala-Lys-Ala-Lys-Ala-Glu-Ala-Glu-Ala-Lys-Ala-Lys-NH_2

The theoretical weight is 1813.99 Da.

Aoa group was attached separately as different conditions are needed.

3.1.4.1 Peptide synthesis

A 0.63 M DMF solution was prepared for each of the following amino-acids:

- Fmoc-Ala-OH
- Fmoc-Glu(OBut)-OH
- Fmoc-Lys(Boc)-OH
- Fmoc-amino-heptanoic acid

To increase the efficiency of the coupling, 5 equivalents of each amino-acid were used with respect to resin reactive groups.

The three solutions needed for the reaction were prepared:

- 0.5 M solution of HBTU/Oxyma Pure in DMF
- 40% piperidine solution in DMF
- 1.8 N solution of DIPEA in NMP

The synthesis reaction is composed of 17 cycles, all set to double coupling, each one with a 45 minute span time. Fmoc group removal was obtained by treating the growing peptide with 1 ml of 40% piperidine solution in DMF for 3 minutes, then again with 0.9 ml of 40% piperidine solution in DMF for 12 minutes. The activation of the carboxyl group, during the condensation reaction, was obtained by dissolving 1 ml of amino-acid solution in 1.4 ml of HBTU/Oxyma Pure in DMF and 0.695 ml of DIPEA solution in NMP.

When the synthesis finished, another cycle was set for the double coupling of Aoa group. In this case, the following solutions were prepared, to maximize the yield:

- 0.5 M solution of HATU/Oxyma Pure in DMF
- 40% piperidine solution in DMF
- 2 N solution of collidine in NMP

A deprotection cycle for the Fmoc group was set, and then the double coupling of Aoa. At the end of the synthesis, some washings with DCM were performed, then the resin was dried under vacuum for 1 hour.

3.1.4.2 Peptide cleavage from the resin

Peptide cleavage from the resin, and simultaneous chain groups deprotection, was carried out on half of the resin obtained (267 mg).

The cleavage solution was composed of:

- 0.125 ml of MilliQ water
- 0.125 ml of TES
- 4.75 ml of TFA

The solution was reacted for 1 hour and 30 minutes at room temperature, manually rotating the reactor occasionally. Once finished, the solution was filtered and some washings with TFA were carried out, then the solution was dried out with the help of the rotary evaporator. The obtained peptide was precipitated adding cold ethyl ether (4°C) under low magnetic stirring, then it was filtered in a Gooch 4 and dried under vacuum for 1 hour.

The dried crude peptide was weighed, obtaining 140 mg of crude peptide.

3.1.4.3 Crude peptide characterization

To characterize Aoa-x-EAK peptide, 1 mg of crude peptide was dissolved in 1 ml of eluent A, and then the solution was filtered using a PVDF filter. The analysis was performed at the following conditions (Figure 3.13):

- Column: Nova-Pak C_{18} (4 µm, 60 Å, 3.9 x 300 mm)
- Injected volume: 50 µl
- Flow rate: 0.5 ml/min
- Detector wavelength: 214 nm
- Eluent A: 0.05% TFA in MilliQ water
- Eluent B: 0.05% TFA in 40% isopropanol and 60% MilliQ water
- Gradient: from 20% to 35% of eluent B in 15 minutes

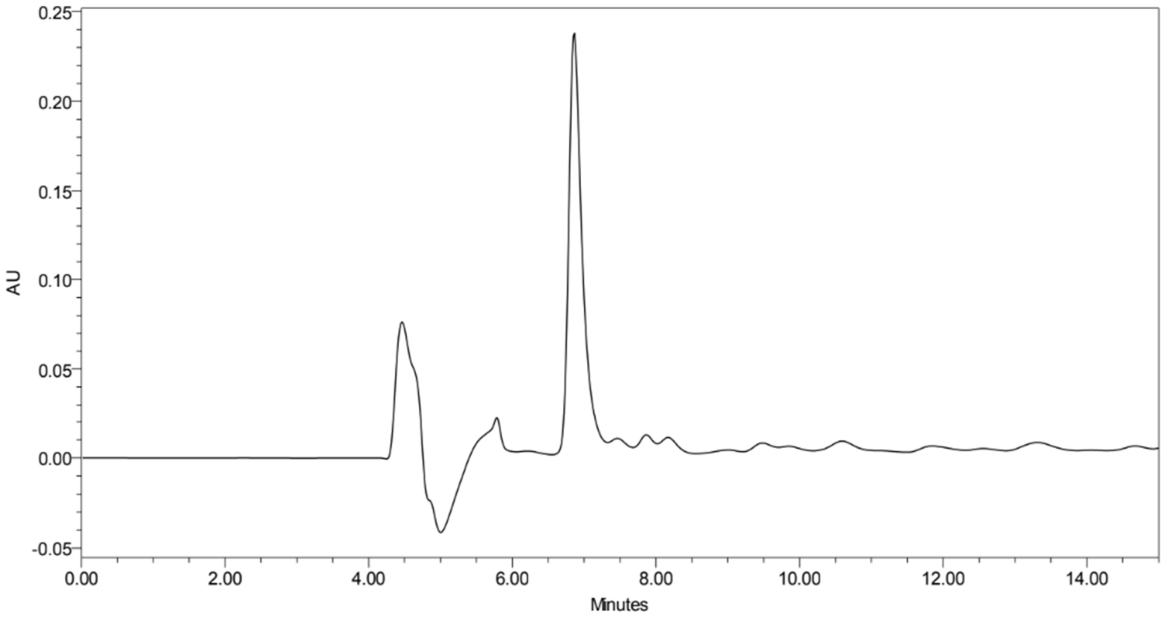

Figure 3.13 *- Crude Aoa-x-EAK RP-HPLC analytical chromatogram. Column: Nova-Pak C_{18}, flow: 0.5 ml/min, eluent A: 0.05% TFA in MilliQ water, eluent B: 0.05% TFA in 40% isopropanol and 60% MilliQ water solution, gradient: from 20% to 35% of B in 15 minutes, injected volume: 50 µl, detector wavelength: 214 nm*

Then, a mass spectroscopy analysis was performed to ensure the correct molecular weight. ESI-TOF result is reported in Figure 3.14.

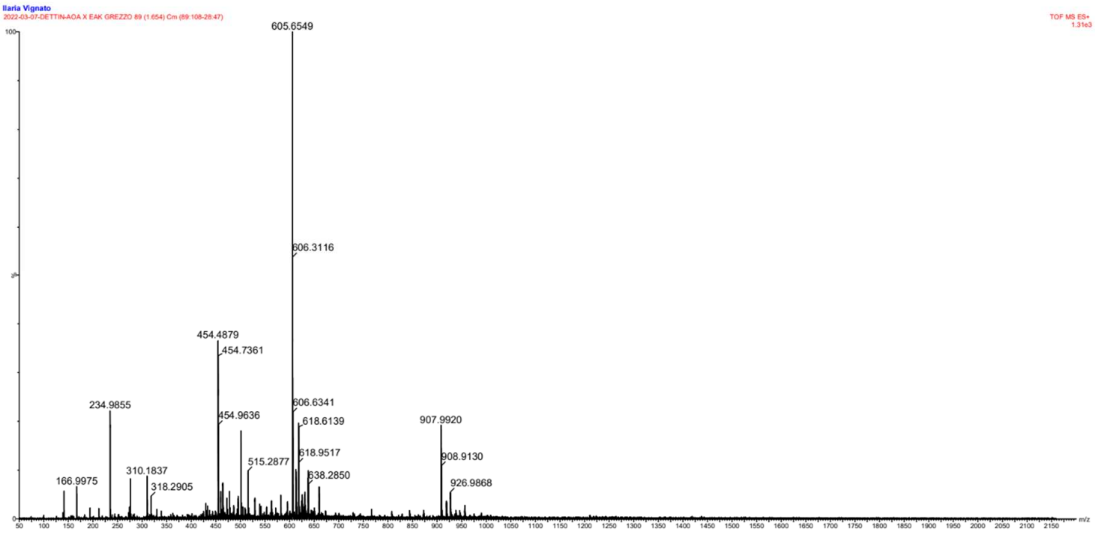

Figure 3.14 *– Mass analysis of crude Aoa-x-EAK peptide (theoretic weight: 1813.99 Da).*

Since ESI-TOF divides the molecule in equal parts depending on the number of charges, to find the real molecular weight the following formula must be used:

$$MW_{real} = \frac{MW + n_{charges}}{n_{charges}}$$

- 2 charges: $\frac{1814+2}{2} = 908\ Da$
- 3 charges: $\frac{1814+3}{3} = 605.65\ Da$
- 4 charges: $\frac{1814+4}{4} = 454.5\ Da$

Where 1814 is the molecular weight of pure peptide.

3.1.4.4 Peptide purification

The crude Aoa-x-EAK peptide was purified through a RP-HPLC SP analysis. 35.80 mg of crude peptide were dissolved in 35.80 ml of eluent A. The solution was filtered using a PVDF filter with 0.45 µm pore diameter. The analysis was performed under the following conditions:

- Column: Delta-Pak C_{18} (15 µm, 100 Å, 7.8 x 300 mm)
- Injected volume: 35.8 ml
- Flow rate: 2 mL/min
- Detector wavelength: 214 nm
- Full-scale: 4.0
- Eluent A: 0.05% TFA in MilliQ water
- Eluent B: 0.05% TFA in 40% isopropanol and 60% MilliQ water
- Gradient: from 10% to 60% of B in 50 minutes
- Paper velocity: 0.5 cm/min

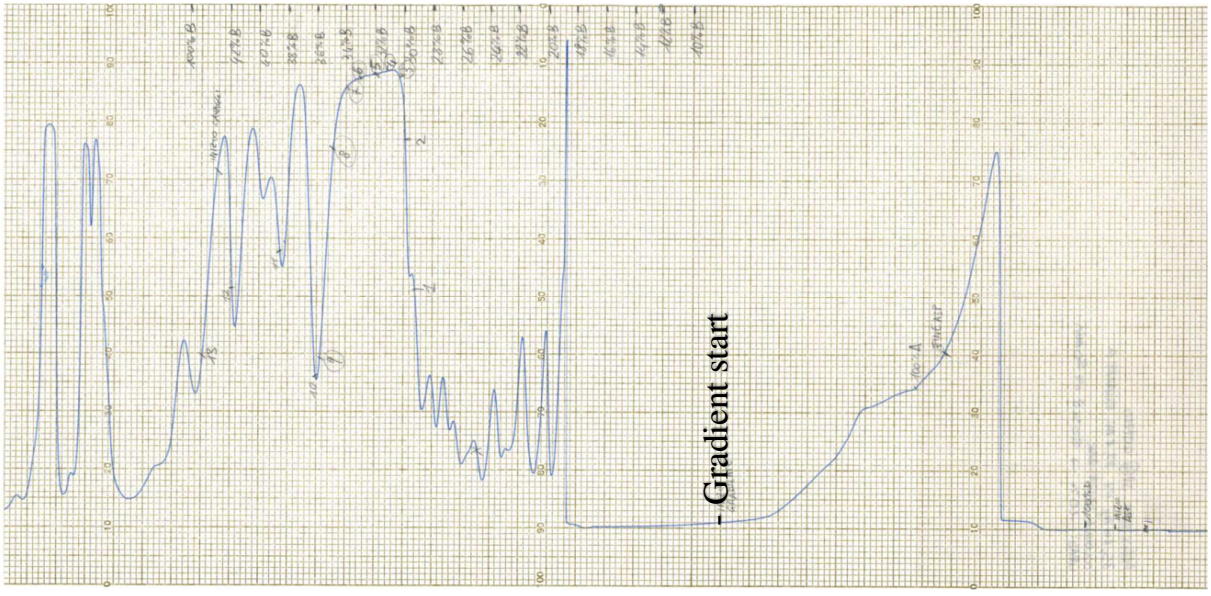

Figure 3.15 *– Crude Aoa-x-GBMP1α semipreparative RP-HPLC chromatogram. Column: Zorbax C_{18}, flow: 2 ml/min, eluent A: 0.05% TFA in MilliQ water, eluent B: 0.05% TFA in 40% isopropanol and 60% MilliQ water solution, gradient: from 10% to 60% of B in 50 minutes, injected volume: 35.8 ml, detector wavelength: 214 nm, full-scale: 4.0, paper velocity: 0.5 cm/min*

In figure 3.15 it is possible to identify one large peak, that corresponds to the pure peptide. The eluate was fractioned in different vials. Fractions from 3 to 9 were supposed pure, so they were collected together and instantly freezed in liquid nitrogen and then lyophilized, to avoid reaction of pure peptide with ketones.

An RP-HPLC analysis was carried to evaluate the purity of the collected pool. This analysis was carried out at the following conditions:

- Column: Nova-Pak C_{18} (4 µm, 60 Å, 3.9 x 300 mm)
- Injected volume: 50 µl
- Flow rate: 0.5 mL/min
- Detector wavelength: 214 nm
- Eluent A: 0.05% TFA in MilliQ water
- Eluent B: 0.05% TFA in 40% isopropanol and 60% MilliQ water
- Gradient: from 15% to 35% of B in 20 minutes

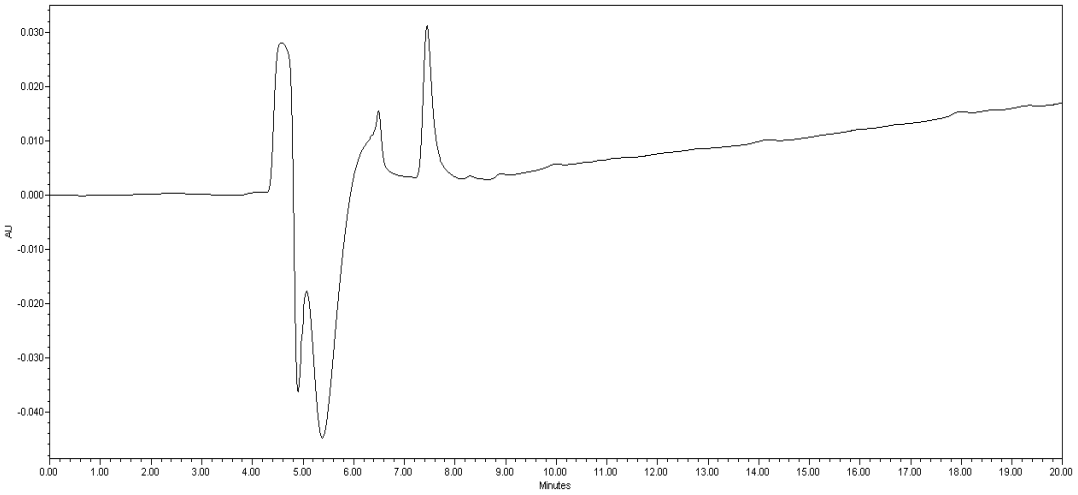

Figure 3.16 *- Crude Aoa-x-EAK RP-HPLC analytical chromatogram. Column: Nova-Pak C_{18}, flow: 0.5 ml/min, eluent A: 0.05% TFA in MilliQ water, eluent B: 0.05% TFA in 40% isopropanol and 60% MilliQ water solution, gradient: from 15% to 35% of B in 20 minutes, injected volume: 50 µl, detector wavelength: 214 nm*

Figure 3.16 is the analytical of pool 3÷9. The total weight of pure peptide obtained was 12.70 mg.

The collected pools were analyzed by ESI-TOF to identify the pure peptide (Figure 3.17).

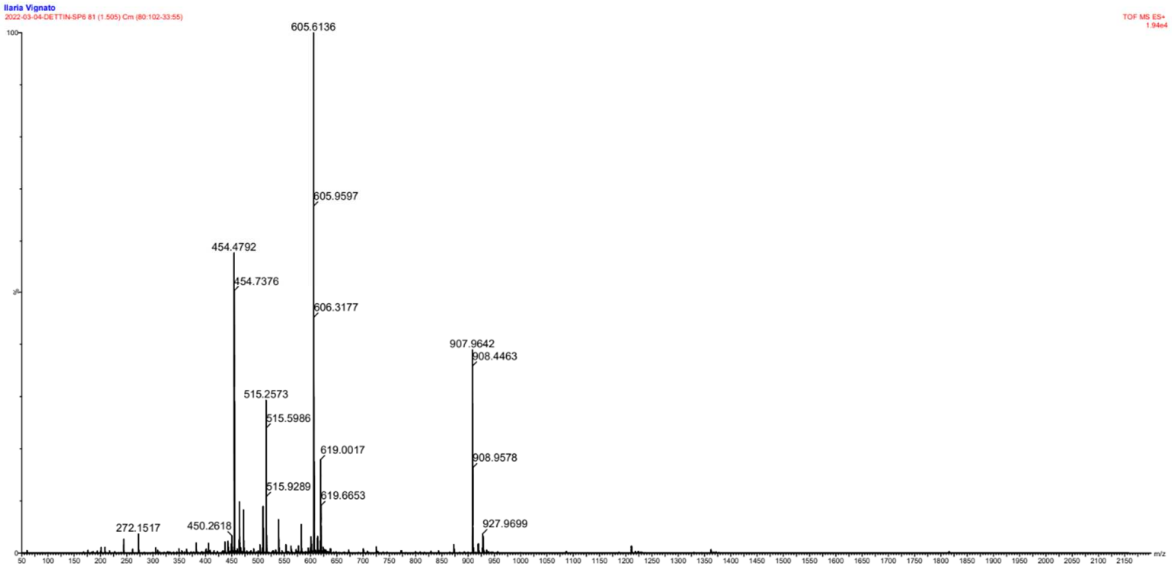

Figure 3.17 *– Mass analysis of purified Aoa-x-EAK peptide (theoretic weight: 1813.99 Da).*

- 2 charges: $\frac{1814+2}{2} = 908\ Da$
- 3 charges: $\frac{1814+3}{3} = 605.65\ Da$
- 4 charges: $\frac{1814+4}{4} = 454.5\ Da$

3.2 PEEK functionalization through covalent bond

3.2.1 PEEK functionalization for biological assays

3.2.1.1 PEEK functionalization with different concentrations of Aoa-x-HVP for AlamarBlue assay

The patterned surface of PEEK disks was functionalized with 3 different concentrations of Aoa-x-HVP in 40 mM, 6 pH sodium phosphate buffer solution:

- 7 disks were functionalized with 10^{-3} M peptide in buffer solution
- 7 disks were functionalized with 10^{-4} M peptide in buffer solution
- 7 disks were functionalized with 10^{-5} M peptide in buffer solution

Sodium phosphate buffer was prepared as follows: 1.10 g of monobasic sodium phosphate were dissolved in 208.12 ml of MilliQ water, then the solution was stirred with electromagnetic stirring to facilitate the dissolution. The solution pH was checked, and some drops of sodium hydroxide were added to stabilize the pH at 6.

For the 10^{-3} M solution, 1.97 mg of pure Aoa-x-HVP solid peptide were dissolved in 1.38 ml of sodium phosphate buffer solution.

For the 10^{-4} M solution, 200 µm of 10^{-3} M peptide solution were picked up and then 1.8 ml of buffer solution were added.

For the 10^{-5} M solution, 200 µm of 10^{-4} M peptide solution were picked up and then 1.8 ml of buffer solution were added.

PEEK disks were put in a 48 multiwell plate and 200 µm of the respective solution were added on the surface of each one of them. 200 µm of sodium phosphate buffer solution only were added to 7 additional disks, which were considered as control. The reaction took place at room temperature for 24 hours, then the disks were washed as follows:

- 3 wash cycles with 1 ml of 40 mM, 6 pH sodium phosphate buffer solution for each disk
- 3 wash cycles with 1 ml of MilliQ water for each disk

3.2.1.2 *PEEK functionalization with 10^{-4} M solution of different peptides*

21 PEEK disks for each peptide were needed:

- 9 disks for adhesion assays
- 12 disks for proliferation assays

The patterned surface of PEEK disks was functionalized with a 10^{-4} M solution of different peptides in 40 mM, 6 pH sodium phosphate buffer solution:

- 21 disks were functionalized with Aoa-x-HVP peptide in buffer solution
- 21 disks were functionalized with Aoa-x-GBMP1α peptide in buffer solution
- 21 disks were functionalized with Aoa-x-EAK peptide in buffer solution

For Aoa-x-HVP peptide, 2.11 mg of pure peptide were dissolved in 14.73 ml of sodium phosphate buffer solution, thus each disk was functionalized with 600 µl of the solution.

For Aoa-x-GBMP1α peptide, 3.66 mg of pure peptide were dissolved first in 10% of DMF (1.4 ml), then in 12.74 ml of sodium phosphate buffer solution, thus each disk was functionalized with 600 µl of the solution.

For Aoa-x-EAK peptide, 1.68 mg of pure peptide were dissolved first in 50% of eluent A (4.63 ml), then in 50% of sodium phosphate buffer solution (4.63 ml). The pH was adjusted with a drop of 10% sodium hydroxide solution, reaching a value of 6.02. Each disk was then functionalized with 400 µl of the solution obtained.

All of the 63 disks, which were put in different multiwell plates, were functionalized at room temperature for 24 hours, then the disks were washed as follows:

- 3 wash cycles with 1 ml of 40 mM, 6 pH sodium phosphate buffer solution for each disk
- 3 wash cycles with 1 ml of MilliQ water for each disk

3.2.2 PEEK functionalization for XPS analysis

The smooth surface of PEEK disks was functionalized with 3 different concentrations of Aoa-x-HVP with fluorine in 40 mM, 6 pH sodium phosphate buffer solution:

- 2 disks were functionalized with 10^{-3} M peptide in buffer solution

- 2 disks were functionalized with 10^{-4} M peptide in buffer solution
- 2 disks were functionalized with 10^{-5} M peptide in buffer solution

Sodium phosphate buffer was prepared as described in paragraph 3.2.1.1.

For the 10^{-3} M solution, 2.22 mg of pure Aoa-x-HVP solid peptide were dissolved in 1.53 ml of sodium phosphate buffer solution.

For the 10^{-4} M solution, 200 µm of 10^{-3} M peptide solution were picked up and then 1.8 ml of buffer solution were added.

For the 10^{-5} M solution, 200 µm of 10^{-4} M peptide solution were picked up and then 1.8 ml of buffer solution were added.

PEEK disks were put in a 24 multiwell plate and 600 µm of the respective solution were added on the surface of each one of them. 600 µm of sodium phosphate buffer solution only were added to 2 non-functionalized disks, which were considered as control. The reaction took place at room temperature for 24 hours, then the disks were washed as follows:

- 3 wash cycles with 1 ml of 40 mM, 6 pH sodium phosphate buffer solution for each disk
- 3 wash cycles with 1 ml of MilliQ water for each disk

3.2.3 PEEK functionalization for WCA and AFM measurements

The smooth surface of PEEK disks was functionalized with 10^{-4} M solution of different peptides in 40 mM, 6 pH sodium phosphate buffer solution:

- 3 disks were functionalized with Aoa-x-HVP peptide in buffer solution
- 3 disks were functionalized with Aoa-x-GBMP1α peptide in buffer solution
- 3 disks were functionalized with Aoa-x-EAK peptide in buffer solution

Sodium phosphate buffer was prepared as described in paragraph 3.2.1.1.

For Aoa-x-HVP peptide, 0.45 mg of pure peptide were dissolved in 3.14 ml of sodium phosphate buffer solution.

For Aoa-x-GBMP1α peptide, 0.54 mg of pure peptide were dissolved first in 10% of DMF (0.21 ml), then in 1.88 ml of sodium phosphate buffer solution.

For Aoa-x-EAK peptide, 0.42 mg of pure peptide were dissolved in 2.32 ml of sodium phosphate buffer solution.

PEEK disks were put in a 24 multiwell plate and 600 µm of the respective solution were added on the surface of each one of them. 600 µm of sodium phosphate buffer solution only were added to 3 additional disks, which were considered as control. The reaction took place at room temperature for 24 hours, then the disks were washed as follows:

- 3 wash cycles with 1 ml of 40 mM, 6 pH sodium phosphate buffer solution for each disk
- 3 wash cycles with 1 ml of MilliQ water for each disk

Chapter 4

Results

4.1 XPS results

PEEK functionalized with Aoa-x-HVP marked with fluorine samples were analyzed by XPS analysis, to quantify peptide presence. 10^{-3} M, 10^{-4} M and 10^{-5} M concentrations were considered. In each sample, XPS measurements were carried out at the following core levels:

- C1s,
- N1s,
- O1s,
- F1s.

XPS data (BE, fwhm, atomic ratios) of N1s and F1s core levels are reported in Table 4.1.

Sample	Signal	Assignment	Atomic ratios (%)
PEEK-Controllo	N1s F1s	C-N $-N^+$ F-C	1.7 0.2
PEEK-F-HVP_ 10^-3 M	N1s F1s	C-N F-C	3.2 0.4
PEEK-F-HVP_ 10^-4 M	N1s F1s	C-N F-C	2.5 0.3
PEEK-F-HVP_ 10^-5 M	N1s F1s	C-N F-C	3.0 0.2

Table 4.1 *– XPS results for untreated PEEK (control) and PEEK functionalized with Aoa-x-HVP-F at 10^{-3}, 10^{-4} and 10^{-5} M concentration.*

Table 4.1 shows that the electronic band of fluorine is present on functionalized surface, and this is indicative of peptide presence. F1s and N1s signals are detected even in the control sample, where nitrogen and fluorine should be absent; after functionalization, an increase in the atomic percentage of both elements is detected, particularly for PEEK + HVP-F at 10^{-3} M, corresponding to the highest peptide concentration. However, there is only a slight improvement with 10^{-3} M and 10^{-4} M concentrations respect to the control, and PEEK functionalized with a 10^{-5} M concentration shows no improvement as compared to control. On the other hand, it should be noted that the atomic ratios of nitrogen, indicative of peptide anchoring, are increasing, with 10^{-5} M having a value of 3.0 up to 3.2 for 10^{-3} M concentration.

4.2 WCA measurements

Water contact angle (WCA) was measured to determine functionalized PEEK's wettability at a concentration of 10^{-4} M (working solution). Surfaces with Aoa-x-HVP, Aoa-x-GBMP1α, or Aoa-x-EAK grafting were considered. The results are shown in Figure 4.1.

It is evident that both Aoa-x-HVP and Aoa-x-EAK are more wettable than unfunctionalized PEEK, as their WCA is lower than the control, while Aoa-x-GBMP1α (abbreviated in Figure 4. As Aoa-x-BMP) has a higher WCA than the control. This confirms that functionalized surfaces become more hydrophilic with more charged peptides like Aoa-x-HVP (net charge = +5), and more hydrophobic with less charged peptides like Aoa-x-GBMP1α (net charge = +1), while Aoa-x-EAK surface is hydrophilic (net charge = 0). The last result can be explained by considering the β-sheet conformation of EAK sequence that projects all hydrophobic side chains on one side and all charged side chains on the opposite side: our hypothesis is that the anchored peptide could interface the hydrophobic PEEK surface with its hydrophobic side leaving the side chains of charged amino acids open to solvent interactions.

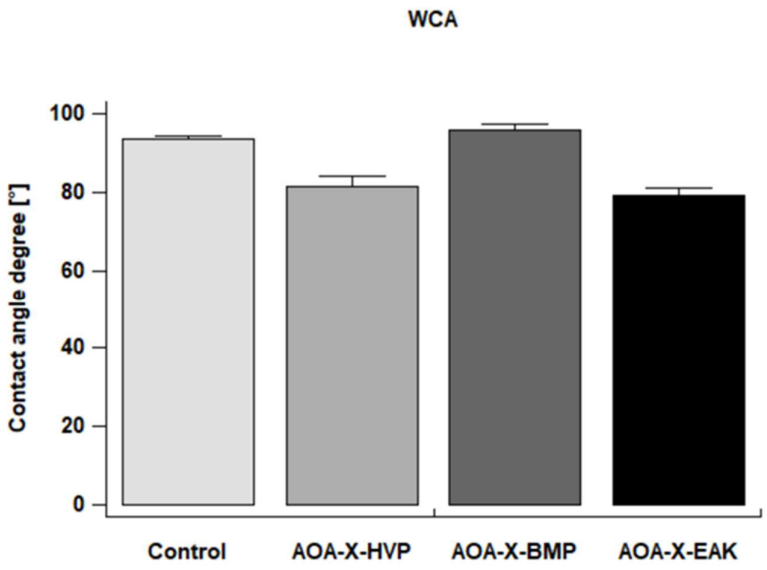

Figure 4.1 *– WCA measurements of functionalized PEEK scaffolds*

4.3 AFM measurements

Atomic Force Microscopy was performed on the scaffolds to determine differences in Young modulus and adhesion forces. Scaffold functionalized with 10^{-4} M of Aoa-x-GBMP1α, Aoa-x-HVP and Aoa-x-EAK were considered, and untreated PEEK was used as control.

In Figure 4.2, graphs of Young's modulus distribution are reported. It can be noted that untreated PEEK has the lowest Young modulus, thus it is more deformable. Surface functionalization has the effect of increasing stiffness at the interface, especially in PEEK functionalized with HVP and GBMP1α. In PEEK functionalized with EAK, substrate stiffness is lower as the Young modulus is approximately half the value of the other peptides.

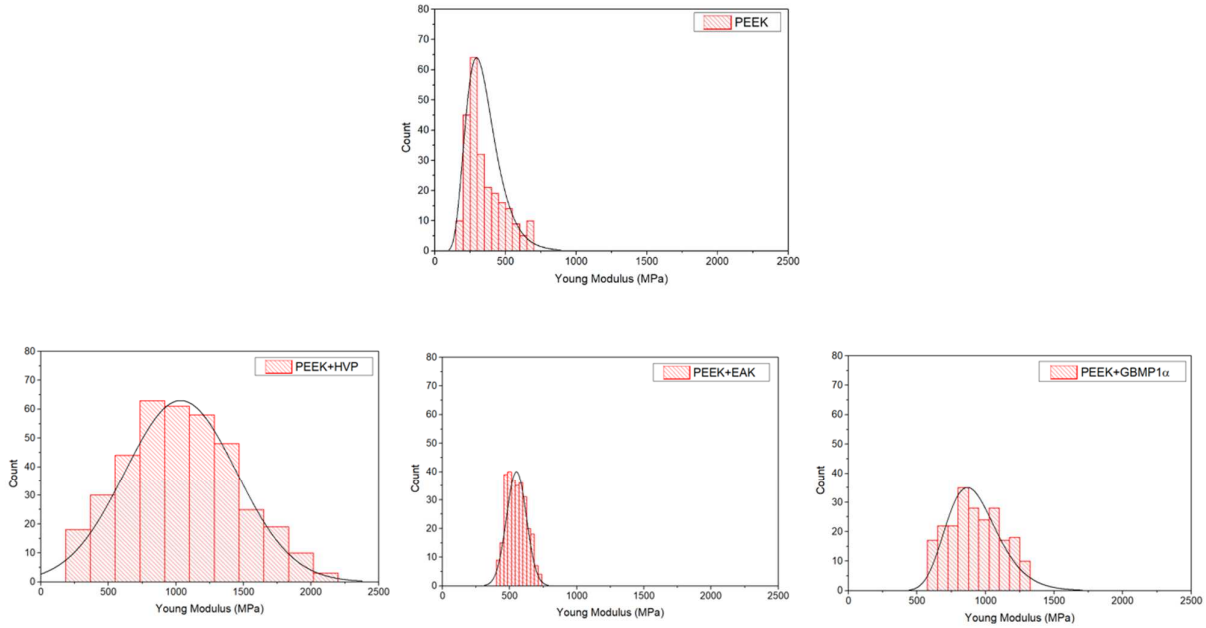

Figure 4.2 *– Young modulus curves obtained by AFM measurements*

Figure 4.3 shows values of adhesion forces between the tip and the sample. In this case, it should be noted that untreated PEEK has very low adhesion forces, while the values increase in functionalized PEEK. Among all the peptides analyzed, the highest adhesion forces pertain to Aoa-x-EAK.

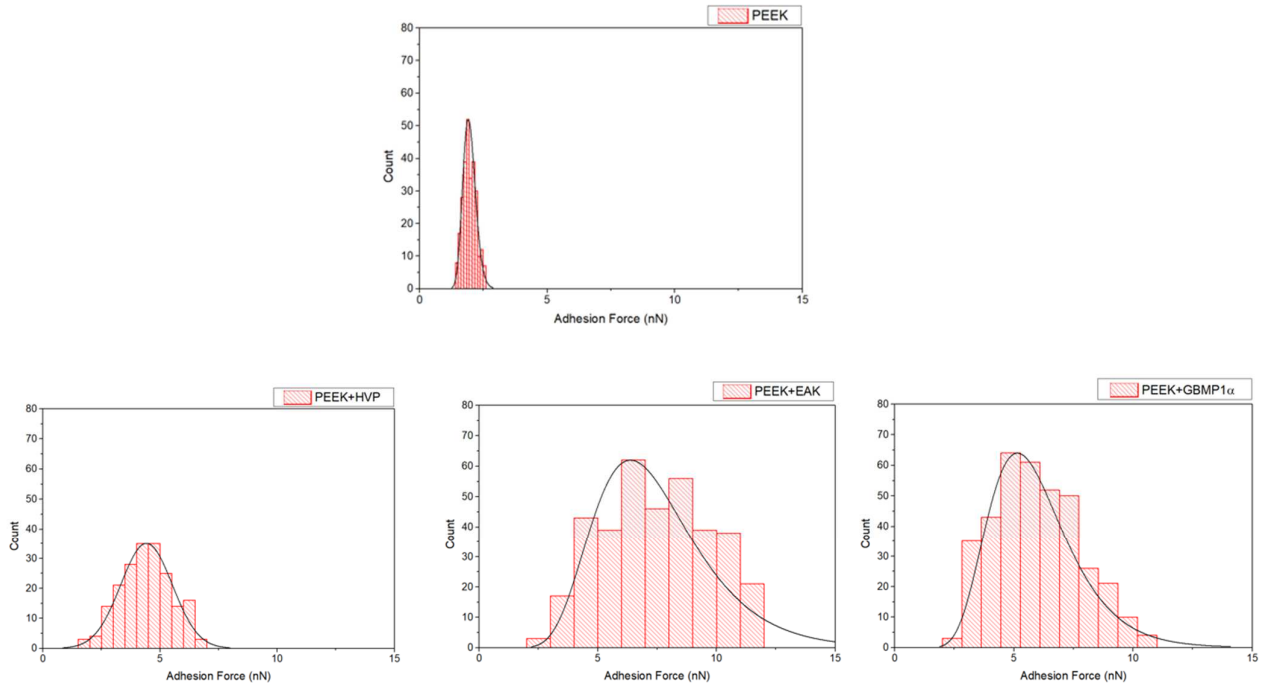

Figure 4.3 *– Adhesion force curves obtained by AFM measurements*

4.4 Live and Dead assay

Live and Dead assay images give us a qualitative measure of cell viability. The images were produced after 48 hours of HOB cells seeding, and with two magnifications: 10x (shown in Figure 4.4) and 20x (shown in Figure 4.5). All figures contain images of dead cells only, live cells only and live and dead cells merged together.

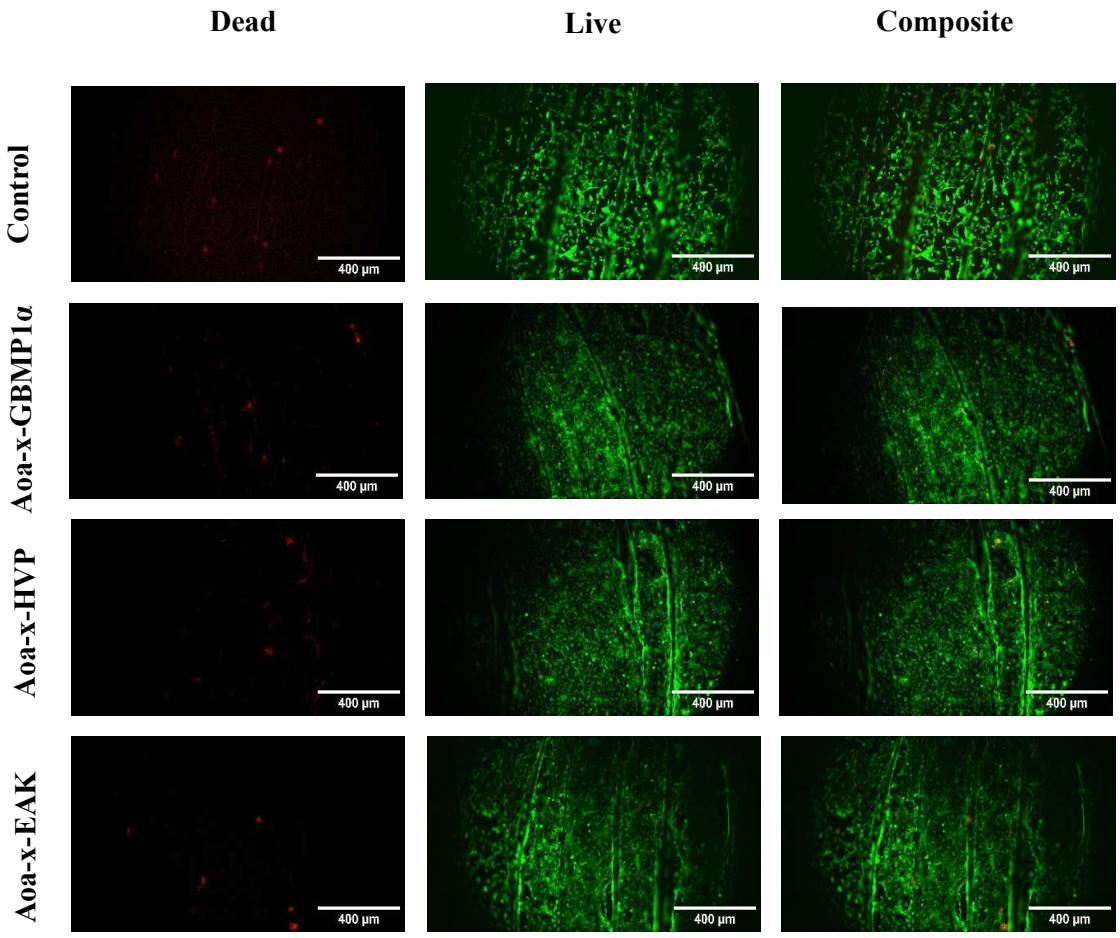

Figure 4.4 – *Live and Dead assay on unfunctionalized and functionalized PEEK at 10x magnification after 48 hours of HOB cells seeding. The top line refers to dead cells, the center line to live cells, while the bottom line is live and dead cells merged together*

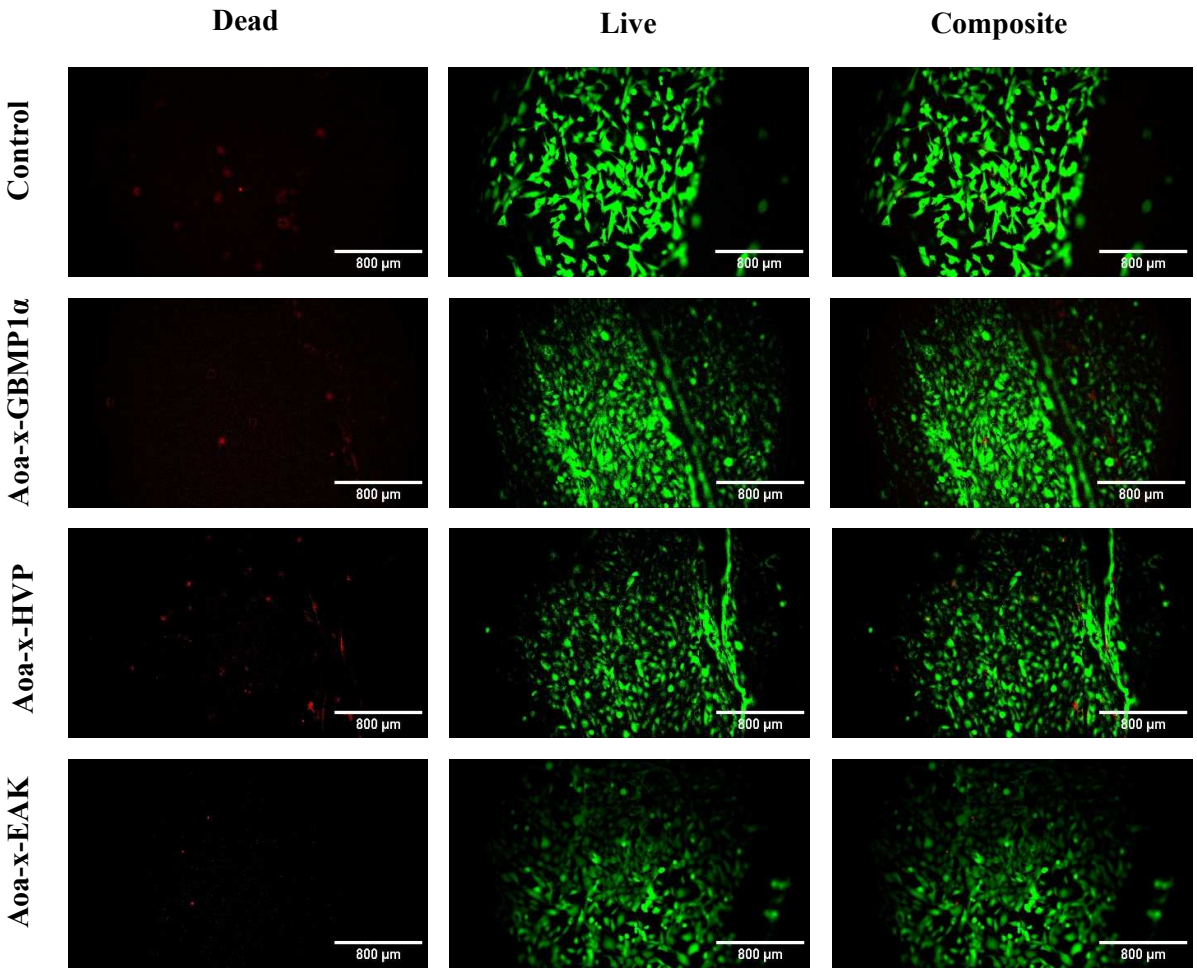

Figure 4.5 *– Live and Dead assay on unfunctionalized and functionalized PEEK at 20x magnification after 48 hours of HOB cells seeding. The top line refers to dead cells, the center line to live cells, while the bottom line is live and dead cells merged together*

The number of dead cells is very little in both 10x and 20x magnifications, approximately a few dozens. Therefore, we can say that the cytotoxicity is very low.

We can see that there is an increase in cell viability in functionalized scaffolds as compared to unfunctionalized PEEK. Scaffolds functionalized with Aoa-x-GBMP1α and Aoa-x-HVP show an increased number of cells compared to Aoa-x-EAK, qualitatively. The higher cell density is found in the cavities of the patterned surface, so cells tend to accumulate in these regions.

4.5 SEM analysis

The patterned scaffolds seeded with HOB cells were observed with the scanning electron microscope after 24 and 48 h from the seeding procedure to qualitatively assess the morphology of the samples and the cells. Scaffold functionalized with 10^{-4} M of Aoa-x-GBMP1α and Aoa-x-HVP were considered, and untreated PEEK was used as control. Samples functionalized with Aoa-x-EAK are still under analysis. Images of the preliminary results reported in Figure 4.9 refer to day 1 from the seeding (on the left) and day 2 from the seeding (on the right).

Control

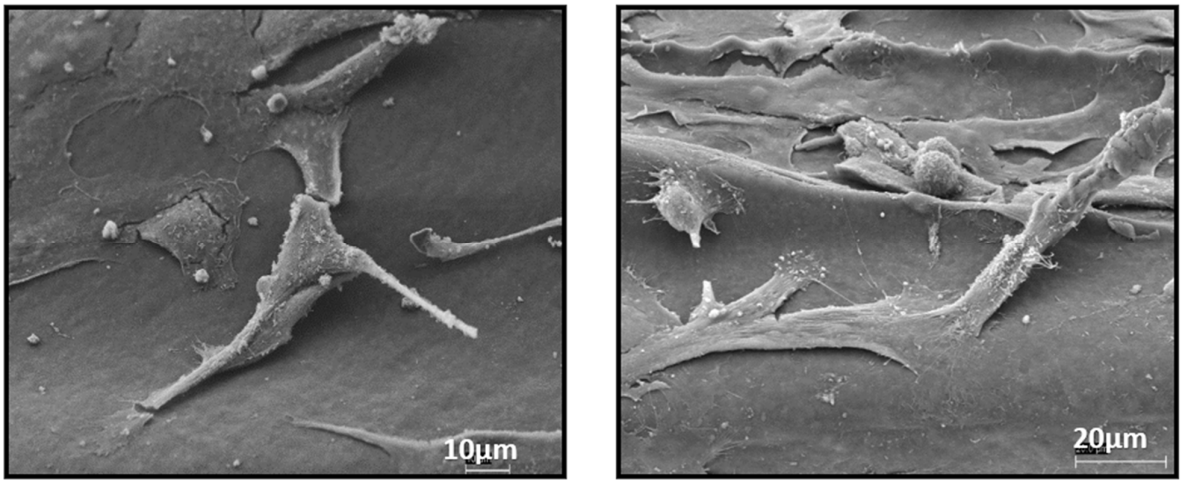

PEEK + Aoa-x-GBMP1α

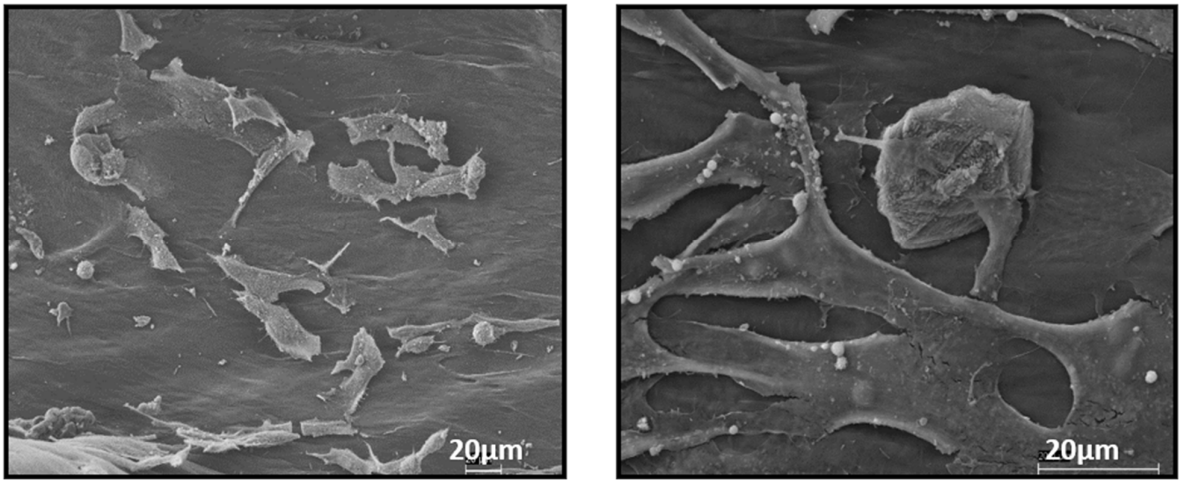

PEEK + Aoa-x-HVP

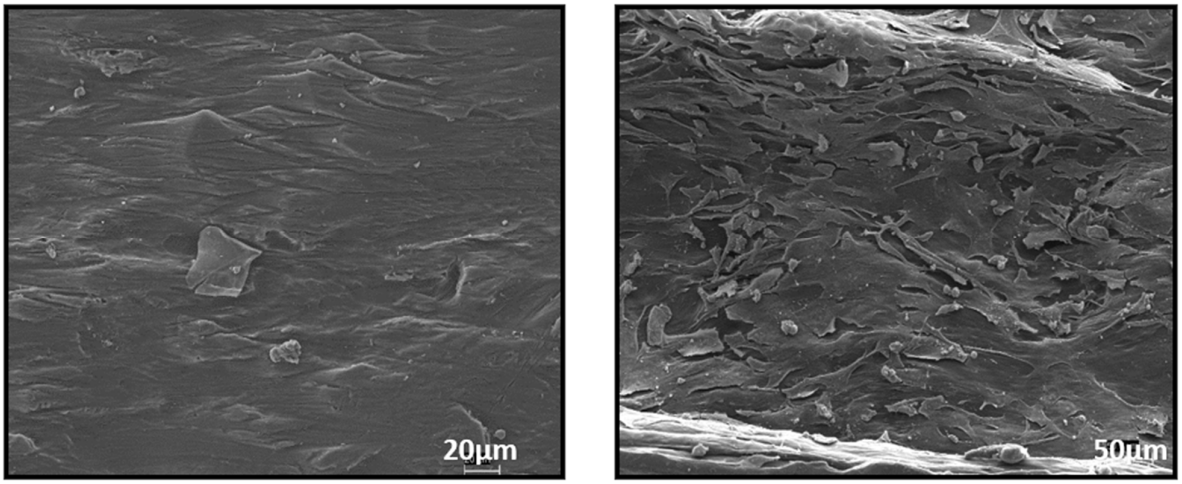

Figure 4.6 *– SEM analysis of untreated PEEK, PEEK + Aoa-x-GBMP1α and Aoa-x-HVP patterned scaffolds after 24 hours of seeding (left) and 48 hours of seeding (right)*

Functionalized scaffolds, especially PEEK + Aoa-x-HVP, present a higher level of cell stratification than the control, which has more round cells on its surface. Moreover, PEEK + Aoa-x-HVP has more cells than PEEK + GBMP1α.

AlamarBlue ™ assay

4.5.1 AlamarBlue ™ assay of Aoa-x-HVP scaffolds at different concentrations

PEEK disks were covalently functionalized with three different concentrations of Aoa-x-HVP, to see which concentration stimulates better the osteoblast proliferation.

An AlamarBlue™ test was performed at KCL on the samples (Figure 4.7). As shown in the figure, from day 1 to day 12, all samples showed an increased cell activity.

In particular, 10^{-4} and 10^{-5} M concentration test samples showed an increased cell proliferation activity compared to 10^{-3} M and untreated.

A higher cell proliferation between 10^{-4} M and all the other groups was observed qualitatively, indicating that 10^{-4} M concentration produces a greater stimulatory effect on osteoblast cells. For this reason, 10^{-4} M concentration was employed for every functionalization destined to biological assays.

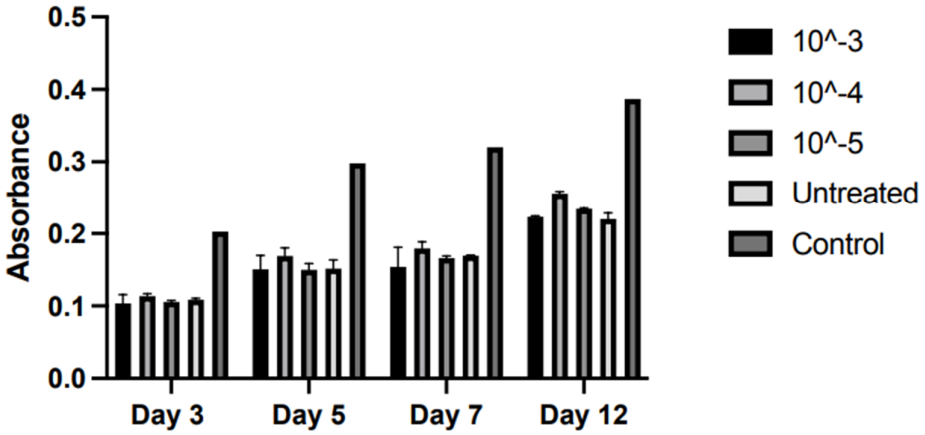

Figure 4.7 *– AB assay on PEEK functionalized disks at 3, 5, 7 and 12 days after HOB cell culture. Three peptide concentration were considered: 10^{-3} M, 10^{-4} M and 10^{-5} M. "Untreated" is non-functionalized PEEK*

4.5.2 AlamarBlue ™ assay of functionalized PEEK at 10^{-4} M concentration

PEEK disks were covalently functionalized with 10^{-4} M concentration of Aoa-x-GBMP1α, Aoa-x-HVP and Aoa-x-EAK. Untreated PEEK was considered as control, while only cells is the positive control.

AB assays were performed after 1, 4, 7, 14 and 21 days of HOB cells seeding. Then, a two-way ANOVA with a Tukey multiple comparison post-hoc test was performed with GraphPad software. Data are presented as mean ± standard deviation. The level of significancy was set at 5%.

Aoa-x-EAK-treated scaffolds were analyzed in a different batch from the other functionalized scaffolds because EAK is a SAP, so data analysis was performed separately with respect to Aoa-x-GBMP1α and Aoa-x-HVP-treated scaffolds.

Results are shown in Figure 4.8 and Figure 4.9.

As regards the self-assembling peptide's batch, at day 1 we can observe that functionalization stimulates cell proliferation significantly better than the control.

At day 4, absorbance values are generally higher than day 1, but, in this case, no significant differences among the scaffolds were found.

At 7 days after seeding, it is possible to appreciate significant differences between untreated PEEK and Aoa-x-EAK functionalized scaffolds.

After 14 days of cell seeding, there are still significant differences between functionalized scaffolds and untreated ones.

At day 21 there are still significant differences between functionalized scaffolds and untreated ones, but we can see a decrease in cell activity compared to the other time points.

Regards the other batch, we can see that from day 1 to day 21, all samples of the Figure 4.8 showed an increased cell activity. At day 1, cell proliferation in the functionalized disks was significantly higher than that in the control. The bar related to Aoa-x-HVP is higher than the bar of Aoa-x-GBMP1α, but not in a significative way. The positive control is significantly higher than the other values, except for Aoa-x-HVP.

At day 4, absorbance values are generally higher than day 1, but, in this case, no significant differences among the scaffolds were found.

At 7 days after seeding, it is possible to appreciate significant differences between untreated PEEK and Aoa-x-GBMP1α functionalized scaffolds, as well as between PEEK + Aoa-x-GBMP1α and PEEK + Aoa-x-HVP.

After 14 days of cell seeding, PEEK + Aoa-x-GBMP1α, although more performing than PEEK + Aoa-x-HVP, is not significatively better than untreated PEEK.

Finally, after 21 days of cell seeding, every functionalized scaffold stimulated cell proliferation significatively more than the respective control.

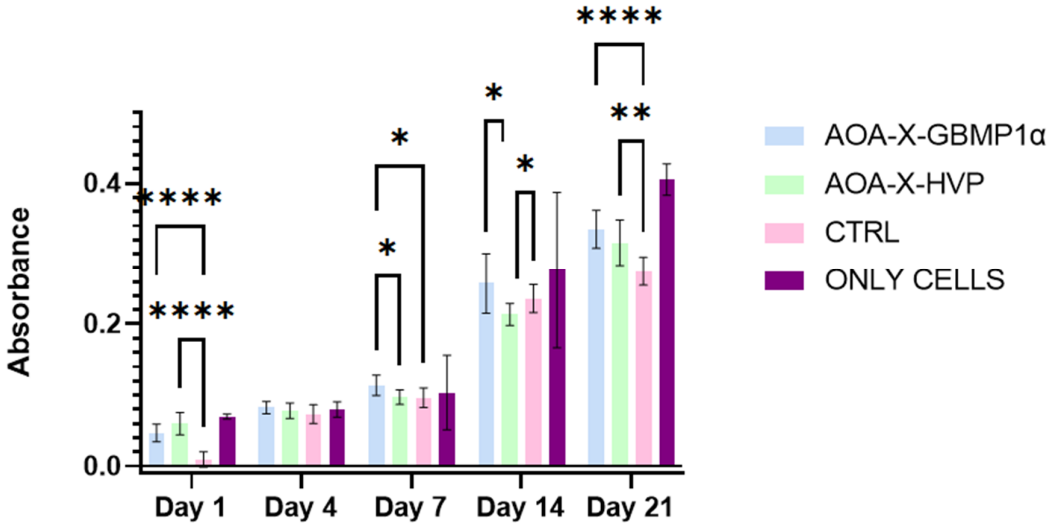

Figure 4.8 – *AB assay on 10^{-4} M functionalized disks at day 1, 4, 7, 14 and 21 after cell seeding. Aoa-x-GBMP1α, Aoa-x-HVP and untreated PEEK (ctrl) were considered. Significance levels: * <0.05 ** < 0.01, **** <0,0001.*

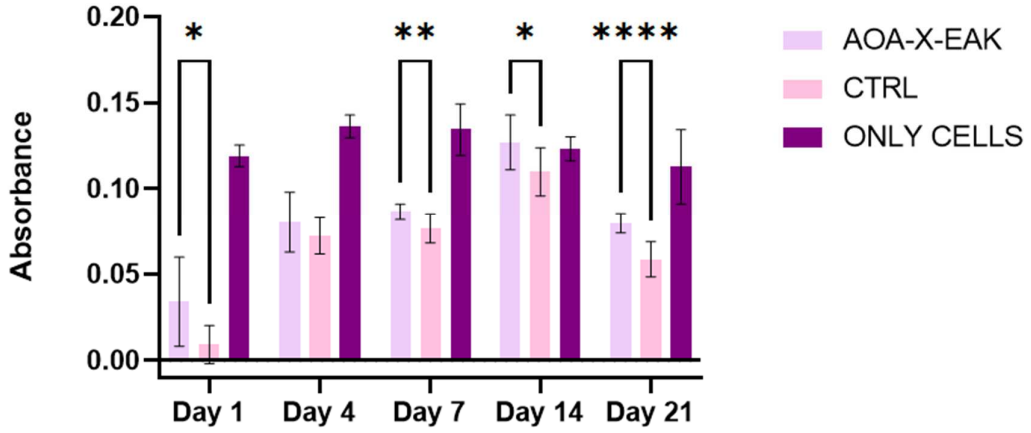

Figure 4.9 – *AB assay on 10^{-4} M functionalized disks at day 1, 4, 7, 14 and 21 after cell seeding. Aoa-x-EAK and untreated PEEK (ctrl) were considered. Significance levels: * <0.05, ** < 0.01, **** <0,0001*

4.6 Alizarin Red S assay

PEEK disks were covalently functionalized with 10^{-4} M concentration of Aoa-x-GBMP1α, Aoa-x-HVP and Aoa-x-EAK.

Alizarin red S staining test for calcium deposition was performed after 21 days of HOB cells seeding at KCL, then, a one-way ANOVA with a Tuckey multiple comparison post-hoc test was performed with GraphPad software. Data are presented as mean ± standard deviation. The level of significancy was set at 5%.

Results are shown in Figure 4.10.

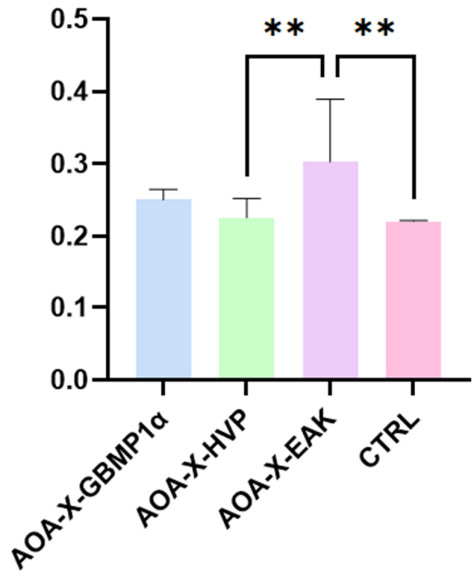

Figure 4.10 – *Alizarin Red S staining test at day 21 after HOB cells seeding. Ctrl is untreated PEEK. Significance levels: ** < 0.01*

The figure shows that calcium deposition was not achieved in a significative way with respect to the control, except for Aoa-x-EAK.

4.7 Gene expression

Functionalized and unfunctionalized scaffolds were tested for the expression of SOX9, RUNX2, ALP and osteocalcin, as described in paragraph 2.3.7.5, after 1 and 7 days of HOB cells seeding. PEEK disks were covalently functionalized with 10^{-4} M concentration of Aoa-x-GBMP1α, Aoa-x-HVP and Aoa-x-EAK.

After qPCR, data obtained was elaborated: for every sample, the number of cycles needed by a specific gene to get past the threshold (set when the curve becomes exponential), Ct, was normalized to the Ct value of the housekeeping gene GAPDH:

$$\Delta Ct_{sample} = Ct_{gene} - Ct_{GAPDH}$$

Then, this value was normalized to the control (untreated PEEK):

$$(\Delta\Delta Ct)_{sample} = \Delta Ct_{sample} - \Delta Ct_{ctrl}$$

Thanks to this normalization, gene expression for every gene and time point is equal to 1 for the control. In this way, we can determine whether a gene is over- or under-expressed respect to the control.

After that, a two-way ANOVA with a Tuckey multiple comparison post-hoc test was performed with GraphPad software. Data are presented as mean ± standard deviation. The level of significancy was set at 5%. Figure 4.11 and Figure 4.12 represent the gene expression after 1 and 7 days of cell seeding, respectively.

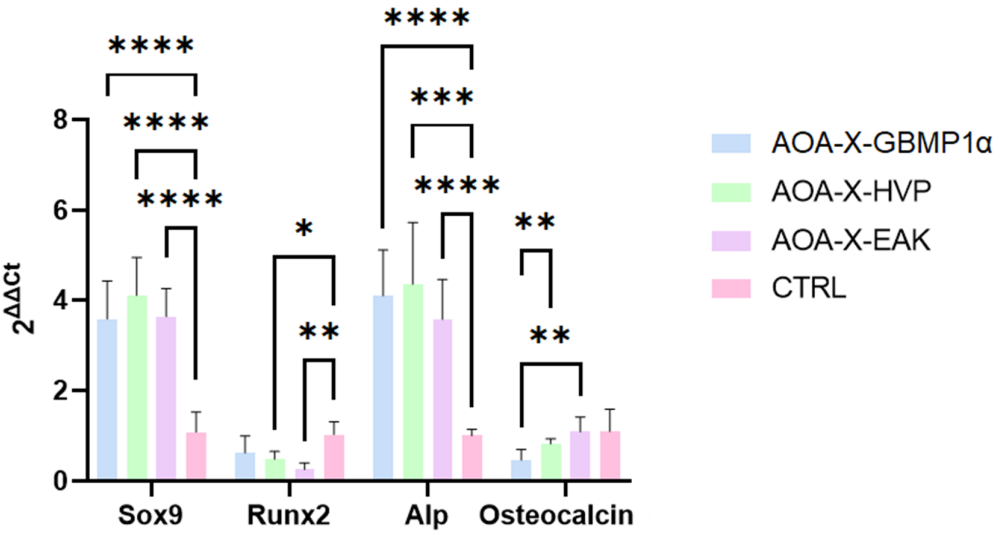

Figure 4.11 – *Gene expression at day 1 after HOB cells seeding. Scaffolds were functionalized with 10^{-4} M peptide concentration. Ctrl is untreated PEEK. Significance levels: * = 0.0330, ** = 0.0071 for RUNX2; 0.0094 and 0.0017 for osteocalcin, *** = 0.0004 for ALP, *** <0.0001*

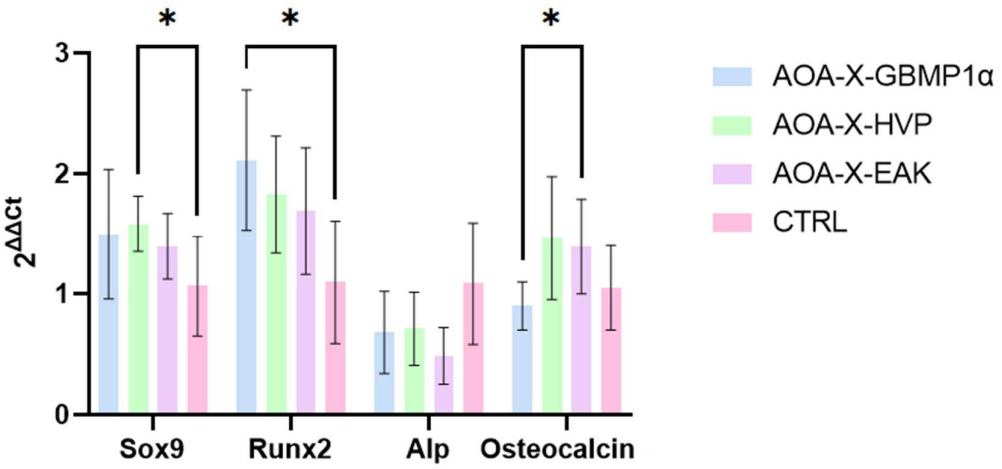

Figure 4.12 – *Gene expression at day 7 after HOB cells seeding. Scaffolds were functionalized with 10^{-4} M peptide concentration. Ctrl is untreated PEEK. Significance levels: * < 0.05*

We can see that the samples modulate differently at day 7 respect to day 1. At day 1, transcription factor SOX9 and early marker ALP are overexpressed with respect to the control in every functionalized scaffold, while the late marker osteocalcin and transcription factor RUNX2 are

underexpressed. At day 7, scaffolds functionalized with Aoa-x-HVP show an overexpression of SOX9, and scaffolds functionalized with Aoa-x-GBMP1α show an overexpression of RUNX2.

Chapter 5

Conclusions

Bone-tissue engineering is an interdisciplinary approach that is gaining more and more popularity nowadays for the treatment of bone defects. A fundamental phase of tissue engineering is the choice of an adequate biomaterial, able to be implanted in the human body with as low as possible negative consequences. Polyetheretherketone (PEEK) has been used as a bone substitute for its mechanical properties close to the human bone, as well as for its great biocompatibility, but it is also bioinert. Since biomaterials science for bone-tissue engineering has known in the last years a rise in popularity of bioactive biomaterials over bioinert ones, for the ability of the former to promote osteointegration, and the better survivability, PEEK implants have been functionalized in several ways, as literature relates.

In a previous work by Yakufu *et al*., PEEK functionalization with bioactive peptides was evaluated with XPS and WCA measures, that were able to detect the peptide and its ability to modify the substrate's surface. Furthermore, it was proven that functionalization enhances cell proliferation, calcium deposition and alkaline phosphatase activity [61].

In this work, PEEK was covalently biofunctionalized with bioactive peptide sequences, namely Aoa-x-HVP, Aoa-x-GBMP1α, and with a self-assembling peptide, Aoa-x-EAK. These biomolecules were synthesized, purified, and characterized in the Chemical Bioengineering lab of the Department of Industrial Engineering of Padova. Functionalized PEEK disks were analyzed through surface, mechanical, and biological tests. The main findings are reported below.

XPS results on samples with Aoa-x-HVP-F confirmed the peptide presence by acknowledging that the electronic band of fluorine is present on functionalized surface. However, fluorine was detected even in the control sample, where it should be absent. Moreover, the increase of atomic ratio values from the control to the functionalized surfaces is very low: this is probably due to the hydrophobicity of PEEK, that does not allow a wide contact between surface and solution. The peptide concentration 10^{-5} M has a quantity of fluorine equal to the control, but a nitrogen quantity that is almost double, thus probably a different quantification technique should be tested. Further analyses can be realized using different functionalization techniques, for example a peptide with N_3-phenylalanine instead of F-phenylalanine.

WCA results established qualitatively that functionalization induces superficial modification on the samples, in accordance with Yakufu *et al*. study. Samples with GBMP1α, which is a hydrophobic peptide, have a higher contact angle, while the more hydrophilic HVP and EAK have a smaller WCA than the control.

AFM measurements showed that surface functionalization has the effect of increasing stiffness at the interface, because peptides organize themselves to build a composite system with strong inter-chain interactions, thus raising the Young modulus value for all analyzed surfaces, particularly for PEEK functionalized with HVP and GBMP1α. Furthermore, the untreated PEEK surface has low adhesion force because there is low interaction between the cantilever tip and the sample. Peptide presence on the surface allows the formation of weak bonds, mostly intermolecular forces, and this translates into higher adhesion force values. Among the peptides analyzed, EAK seems to have the highest value of adhesion force with the tip.

Live and Dead assay showed negligible levels of cytotoxicity in our scaffolds, and an enhanced cell viability in functionalized scaffolds compared to untreated PEEK, especially for HVP and GBMP1α-treated ones. Moreover, it is evident that cells tend to accumulate to patterned surface's cavities.

The SEM results show the bioactive peptides' influence on cell morphology: on the samples containing the peptides the cells are elongated and multilayered while on the PEEK surface they are round-shape. Moreover, PEEK + HVP substrate is preferred by the cells, as it has a greater number of osteoblasts than the other scaffolds.

AlamarBlue™ assay established that the best concentration of peptide solution for osteoblast proliferation is 10^{-4} M. Further analyses confirmed that functionalized scaffolds are able to promote cell proliferation at 1 and 21 days after cell seeding.

Alizarin Red S assay confirmed that only functionalization with the self-assembling peptide EAK is able to promote calcium deposition.

Finally, qPCR test revealed that every functionalized scaffold is able to increase, at day 1, the expression of alkaline phosphatase and transcription factor SOX9, while at day 7 only HVP-functionalized scaffolds increase SOX9 expression, and only GBMP1α-functionalized scaffolds increase RUNX2 expression. No scaffold was able to significantly increase the expression of osteocalcin, at any day. Therefore, further analyses with more time points are needed to evaluate the late markers' expression.

Cell proliferation and ALP activity results confirm the findings of Yakufu *et al*.

In the next future, the samples could be analyzed with different peptide combinations, and in vivo tests should be performed.

6 Bibliography and Sitography

[1] Langer and Vacanti, "Tissue engineering," *Science,* 1993.

[2] U. Kneser, D. Schaefer, E. Polykandriotis and R. Horch., "Tissue engineering of bone: the reconstructive surgeon's point of view," *J. Cell. Mol. Med.,* vol. 10, no. 1, pp. 7-19, 2006.

[3] B. Ratner and G. Zhang, "A History of Biomaterials," *Biomaterials Science (Fourth Edition),* pp. 21-34, 2020.

[4] D. Williams, The Williams Dictionary of Biomaterials, p. 42.

[5] S. Dorozhkin and M. Epple, "Biological and medical significance of calcium phosphates," Angewandte Chemie International Edition, 2002.

[6] B. R. G. Castner, "Biomedical surface science: Foundations to frontiers," *Surface Science,* pp. 28-60, March 2002.

[7] L. Hench, "Bioactive materials: The potential for tissue regeneration," *Journal of Biomedical Materials Research,* 1998.

[8] M. Navarro, A. Michiardi, O. Castano and J. Planell, "Biomaterials in orthopaedics," *Journal of the Royal Society Interface,* 2008.

[9] J. Goddard and J. Hotchkiss, "Polymer surface modification for the attachment of bioactive compounds," *Progress in Polymer Science,* pp. 698-725, 2007.

[10] X. Tang, S. K. Thankappan, P. Lee, S. E. Fard, M. D. Harmon, K. Tran and X. Yu, "Polymeric Biomaterials in Tissue Engineering and Regenerative Medicine.," *Natural and Synthetic Biomedical Polymers,* pp. 351-371, 2014.

[11] L. S. Nair and C. T. Laurencin, "Biodegradable polymers as biomaterials," *Progress in Polymer Science,* vol. 32, no. 8-9, pp. 762-798, August–September 2007.

[12] J. Venugopal, M. P. Prabhakaran, Y. Zhang, S. Low, A. T. Choon and S. Ramakrishna, "Biomimetic hydroxyapatite-containing composite nanofibrous substrates for bone tissue

engineering," *Philosophical Transactions: Mathematical, Physical and Engineering Sciences,* pp. 2065-208., April 2010.

[13] J. Gleeson, N. Plunkett and F. O'Brien, "Addition of hydroxyapatite improves stiffness, interconnectivity and osteogenic potential of a highly porous collagen-based scaffold for bone tissue regeneration," *European Cells and Materials,* pp. 218-230, 2010.

[14] P. Wutticharoenmongkol, N. Sanchavanakit, P. Pavasant and P. Supaphol, "Preparation and Characterization of Novel Bone Scaffolds Based on Electrospun Polycaprolactone Fibers Filled with Nanoparticles," *Macromolecular Bioscience,* pp. 70-77, 2006.

[15] S. Kurtz, Synthesis and Processing of PEEK for Surgical Implants.

[16] J. Martínez, M. Farré-Lladós, J. Cano-Batalla and J. Cabratosa-Termes, "Polyetheretherketone (PEEK) as a medical and dental material. A literature review," *Medical Research Archives,* vol. 5, May 2017.

[17] [Online]. Available: 18. https://www.nbcnews.com/science/science-news/medical-first-3-d-printed-skull-successfully-implanted-woman-n65576.

[18] S. Kurtz and J. Devine, "PEEK biomaterials in trauma, orthopedic, and spinal implants," pp. 4845-4869., 2007.

[19] O. Searle and R. Pfeiffer, "Victrex poly(ethersulfone) (PES) and Victrex poly(etheretherketone) (PEEK)," *Polymer Engineering and Science,* pp. 474-476, 1985.

[20] T. Sasuga and M. Hagiwara, "Radiation deterioration of several aromatic polymers under oxidative conditions," *Polymer,* pp. 1915-1921, 1987.

[21] P. Raea, E. Browna and E. Orlerb, "The mechanical properties of poly(ether-ether-ketone) (PEEK) with emphasis on the large compressive strain response," *Polymer,* pp. 598-615., 2007.

[22] T. Conrad, D. Jaekel, S. Kurtz and R. Roeder, "Effects of the mold temperature on the mechanical properties and crystallinity of hydroxyapatite whisker-reinforced polyetheretherketone scaffolds," *Journal of Biomedical Materials Research Part B: Applied Biomaterials,* pp. 576-583, 2013.

[23] I. Panayotov, V. Orti, F. Cuisinier and J. Yachouh, "Polyetheretherketone (PEEK) for medical applications," *Journal of Materials Science: Materials in Medicine,* vol. 27, no. 118, 2016.

[24] N. Inagaki, S. Tasaka, T. Horiuchi and R. Suyama, "Surface Modification of Poly(aryl ether ether ketone) Film by Remote Oxygen Plasma," *Journal of Applied Polymer Science,* vol. 68, no. 2, pp. 271-279, 1998.

[25] O. Noiset, Y.-J. Schneider and J. Marchand–Brynaert, "Surface modification of poly(aryl ether ether ketone) (PEEK) film by covalent coupling of amines and amino acids through a spacer arm," *Journal of Polymer Science Part A: Polymer Chemistry,* vol. 35, no. 17, pp. 3779-3790, 1997.

[26] M. Becker, S. Lorenz, D. Strand, C.-F. Vahl and M. Gabriel, "Covalent Grafting of the RGD-Peptide onto Polyetheretherketone Surfaces via Schiff Base Formation," *The Scientific World Journal,* pp. 1-5, 2013.

[27] R. Harting, M. Barth, T. Bührke, R. S. Pfefferle and S. Petersen, "Functionalization of polyethetherketone for application in dentistry and orthopedics," *BioNanoMaterials,* 2017.

[28] S. Berretta, R. Davies, Y. Shyng, Y. Wang and O. Ghita, "Fused Deposition Modelling of high temperature polymers: exploring CNT PEEK composites," *Polymer Testing,* pp. 251-262, 2017.

[29] M. Rinaldi, T. Ghidini, F. Cecchini, A. Brandao and F. Nanni, "Additive layer manufacturing of poly (ether ether ketone) via FDM," *Composites part B: Engineering,* pp. 162-172, 2018.

[30] M. Schmidt, D. Pohle and T. Rechtenwald, "Selective laser sintering of PEEK," *CIRP Annals,* pp. 205-208., 2007.

[31] P. Wang, B. Zou, H. Xiao, S. Ding and C. Huang, "Effects of printing parameters of fused deposition modeling on mechanical properties, surface quality, and microstructure of PEEK," *Journal of Material Processing Technology,* pp. 62-74., 2019.

[32] C. Mas-Moruno, "Surface funtionalization of biomaterials for bone tissue regeneration and repair," in *Peptides and Proteins as Biomaterials for Tissue Regeneration and Repair*, 2018, pp. 73-100.

[33] K. C. Dee, T. T. Andersen and R. Bizios, "Design and function of novel osteoblast-adhesive peptides," *Journal of Biomedical Materials Research,* vol. 40, pp. 371-377, 1998.

[34] M. Dettin, M. T. Conconi and R. Gambaretto, "Effect of synthetic peptides on osteoblast adhesion," *Biomaterials,* vol. 26, pp. 4507-4515, 2005.

[35] I. Schvartz, D. Seger and S. Shaltiel, "Vitronectin," *The International Journal of Biochemistry & Cell Biology,* vol. 31, pp. 539-544, 1999.

[36] P. Brun, A. Zamuner, L. Cassari, G. D'Auria, L. Falcigno, S. Franchi, G. Contini, M. Marsotto, C. Battocchio, G. Iucci and M. Dettin, "Chitosan Covalently Functionalized with Peptides Mapped on Vitronectin and BMP-2 for Bone Tissue Engineering," *Nanomaterials (Basel),* vol. 11, p. 2784, November 2021.

[37] S. Zhang, C. Lockshin, A. Herbert, E. Winter and A. Rich, "Zuotin, a putative Z-DNA binding protein in Saccharomyces cerevisiae," *The EMBO Journal ,* vol. 11, no. 10, pp. 3787-3796, 1992.

[38] S. Zhang, T. Holmes, C. Lockshin and A. Rich, "Spontaneous assembly of a self-complementary oligopeptide to form a stable macroscopic membrane," *Proceedings of the National Academy of Sciences USA,* vol. 90, pp. 3334-3338, April 1993.

[39] S. Zhang, "Emerging biological materials through molecular self-assembly," *Biotechnology Advances ,* vol. 20, p. 321 – 339, 2002.

[40] S. Petersen, "Biofunctionalization," *BioNanoMaterials,* vol. 18, no. 1-2, 2017.

[41] Y. Su, I. Cockerill, Y. Zheng, L. Tang, Y.-X. Qin and D. Zhua, "Biofunctionalization of metallic implants by calcium phosphate coatings," *Bioactive Materials,* vol. 4, pp. 196-206, 2019.

[42] R. Bahulekar, N. R. Ayyangar and S. Ponrathnam, "Polyethyleneimine in immobilization of biocatalysts," *Enzyme and Microbial Technology,* vol. 13, no. 11, pp. 858-868, 1991.

[43] H. C. Kolb, M. G. Finn and K. B. Sharpless, "Click Chemistry: Diverse Chemical Function from a Few Good Reactions," *Angewandte Chemie (International ed. in English) ,* vol. 40, no. 11, pp. 2004-2021, 2001.

[44] G. Thumshirn, U. Hersel, S. L. Goodman and H. Kessler, "Multimeric Cyclic RGD Peptides as Potential Tools for Tumor Targeting: Solid-Phase Peptide Synthesis and Chemoselective Oxime Ligation," *Chemistry - A European Journal,* vol. 9, no. 12, pp. 2717-2725, 2003.

[45] X. Meng and K. J. Edgar, "“Click” reactions in polysaccharide modification," *Progress in Polymer Science,* vol. 53, pp. 52-85, 2016.

[46] J. M. Gilmore, R. A. Scheck, A. P. Esser-Kahn, N. S. Joshi and M. B. Francis, "N-terminal protein modification through a biomimetic transamination reaction," *Angewandte Chemie (International ed. in English),* vol. 45, no. 32, pp. 5307-5311, 2006.

[47] R. B. Merrifield, "Solid Phase Peptide Synthesis. I. The Synthesis of a Tetrapeptide," *Journal of the American Chemical Society,* vol. 85, no. 14, p. 2149–2154, 1963.

[48] L. A. Carpino and G. Y. Han, "9-Fluorenylmethoxycarbonyl function, a new base-sensitive amino-protecting group," *Journal of the American Chemical Society,* vol. 92, no. 19, p. 5748–5749, 1970.

[49] L. A. Carpino and G. Y. Han, "9-Fluorenylmethoxycarbonyl amino-protecting group," *The Journal of Organic Chemistry,* vol. 37, no. 22, p. 3404–3409, 1972.

[50] G. Chen, M. Fan, Y. Liu, B. Sun, M. Liu, J. Wu, N. Li and M. Guo, "Advances in MS Based Strategies for Probing Ligand-Target Interactions: Focus on Soft Ionization Mass Spectrometric Techniques," *Frontiers in chemistry,* vol. 7, no. 703, 2019.

[51] G. Mezö, I. Szabó, I. Kertész, R. Hegedüs, E. Orbán, U. Leurs, S. Bösze, G. Halmos and M. Manea, "Efficient synthesis of an (aminooxy) acetylated-somatostatin derivative using (aminooxy)acetic acid as a ‘carbonyl capture’ reagent," *Journal of Peptide Science,* vol. 17, no. 1, pp. 39-46, 2010.

[52] S. Al-Nasiry, N. Geusens, M. Hanssens, C. Luyten and R. Pijnenborg, "The use of Alamar Blue assay for quantitative analysis of viability, migration and invasion of choriocarcinoma cells," *Human Reproduction,* vol. 22, no. 5, p. 1304–1309, 2007.

[53] A. Ligasová and K. Koberna, "DNA Dyes—Highly Sensitive Reporters of Cell Quantification: Comparison with Other Cell Quantification Methods," *Molecules ,* vol. 26, no. 18, p. 5515, 2021.

[54] D. J. Lee, H. C. Tseng, S. W. Wong, Z. Wang, M. Deng and C.-C. Ko, "Dopaminergic effects on in vitro osteogenesis," *Bone Research,* vol. 3, no. 15020, 2015.

[55] R. Nørgaard, M. Kassem and S. I. S. Rattan, "Heat Shock–Induced Enhancement of Osteoblastic Differentiation of hTERT-Immortalized Mesenchymal Stem Cells," *Annals of the New York Academy of Sciences,* no. 1067, pp. 443-447, 2006 .

[56] J. Nam, J. Johnson, J. J. Lannutti and S. Agarwal, "Modulation of embryonic mesenchymal progenitor cell differentiation via control over pure mechanical modulus in electrospun nanofibers," *Acta Biomaterialia,* vol. 7, pp. 1516-1524, 2011.

[57] A. Horii, X. Wang, F. Gelain and S. Zhang, "Biological Designer Self-Assembling Peptide Nanofiber Scaffolds Significantly Enhance Osteoblast Proliferation, Differentiation and 3-D Migration," *Plos One,* vol. 2, no. 2, p. e190, 2007.

[58] J. Domke, S. Dannöhl, W. J. Parak, O. Müller, W. K. Aicher and M. Radmacher, "Substrate dependent differences in morphology and elasticity of living osteoblasts investigated by atomic force microscopy," *Colloids and Surfaces B: Biointerfaces,* vol. 19, no. 4, pp. 367-379, 2000.

[59] E. Takai, K. D. Costa, A. Shaheen, C. T. Hung and X. E. Guo, "Osteoblast Elastic Modulus Measured by Atomic Force Microscopy Is Substrate Dependent," *Annals of Biomedical Engineering,* vol. 33, no. 7, p. 963–971, 2005.

[60] H. H. Fang, K.-Y. Chan and L.-C. Xu, "Quantification of bacterial adhesion forces using atomic force microscopy (AFM)," *Journal of Microbiological Methods,* vol. 40, p. 89–97, 2000.

[61] M. Yakufu, Z. Wang, Y. Wangb, Z. Jiaob, M. Guob, J. Liu and P. Zhang, "Covalently functionalized poly(etheretherketone) implants with osteogenic growth peptide (OGP) to improve osteogenesis activity," *RSC Advances,* vol. 10, pp. 9777-9785, 2020.

Ringraziamenti

Ringrazio innanzitutto la Professoressa Monica Dettin per avermi dato l'opportunità di prendere parte a questo progetto e per avermi seguita con costanza durante tutta la durata del tirocinio.

Ringrazio Leonardo, Annj, le colleghe Elena Z., Elena L. e Doina per avermi sempre aiutata quando ne avevo bisogno ed avermi insegnato l'esperienza del laboratorio e le sue responsabilità.

Ringrazio il mio ragazzo per essermi stato vicino nei periodi felici e in quelli tristi, per costituire sempre un rifugio sicuro dalle mie preoccupazioni.

Ringrazio la mia famiglia per aver supportato economicamente i miei studi per tutti questi anni.

Ringrazio Elisa, Caterina, Laura, Ago, Pol, Francesca, Eniana, Ambra, Nicolò, Gianluca, Stefano, Ilenia, Letizia, Maddy, Luisa, Benedetta e Federico per essere degli ottimi amici e amiche con cui è sempre piacevole stare in compagnia.

Ringrazio i/le compagni/e di corso, nonché amici e amiche, Ilaria, Olimpia, Valerio, Manuela e Martina, perché oltre all'amicizia hanno offerto anche un grande aiuto per lo studio e gli esami in questi anni universitari.

Infine ringrazio me stessa, per essere stata in grado di terminare questo percorso universitario dopo numerose difficoltà e dopo aver attraversato periodi molto bui, e di non aver dato troppo peso ai fallimenti, sfruttando le mie capacità fino in fondo.